

UNIVERSITY OF CALGARY

Density Prediction for Mixtures of Heavy Oil and Solvents

by

FATEMEH SARYAZDI

A THESIS

SUBMITTED TO THE FACULTY OF GRADUATE STUDIES
IN PARTIAL FULFILMENT OF THE REQUIREMENTS FOR THE
DEGREE OF MASTER OF SCIENCE

DEPARTMENT OF CHEMICAL AND PETROLEUM ENGINEERING
CALGARY, ALBERTA

August, 2012

© FATEMEH SARYAZDI 2012

UNIVERSITY OF CALGARY
FACULTY OF GRADUATE STUDIES

The undersigned certify that they have read, and recommend to the Faculty of Graduate Studies for acceptance, a thesis entitled “Density Prediction for Mixtures of Heavy Oil and Solvents” submitted by FATEMEH SARYAZDI in partial fulfillment of the requirements of the degree of MASTER OF SCIENCE IN ENGINEERING.

Supervisor, Dr. HARVEY W. YARRANTON

Dr. WILLIAM Y. SVRCEK

Dr. ZHANGXING CHEN

Dr. LAURENCE R. LINES

Date

Abstract

The design of solvent-based and solvent-assisted heavy oil and bitumen recovery processes requires the accurate prediction of the physical properties of heavy oil mixed with solvents. In particular, density is a critical parameter for gravity drainage and gravity separation based processes. It has proven challenging to accurately predict the density of these mixtures, particularly when the solvent is a dissolved gas. The objective of this thesis is to develop a straightforward method to predict the density of heavy oils or bitumens diluted with liquid solvents and dissolved gases.

Most mixtures of heavy oil and solvents are well below their critical point, and therefore liquid phase density prediction methods are appropriate. Excess volume based mixing rules were investigated with a binary interaction parameter used to relate the excess volume to the composition of the mixture. The mixing rules were tested on literature data for binary mixtures of hydrocarbons. The binary interaction parameters were found to correlate to the normalized difference in the molar volumes of the binary pairs.

To apply these mixing rules to a liquid containing a dissolved gas, the effective liquid density of the dissolved gas is required. However, while effective liquid densities have been used to estimate petroleum densities, values have only been developed for a very limited range of conditions. Nor have these values been rigorously tested. In this thesis, the effective liquid densities of light n-alkanes were determined by linearly extrapolating the molar volumes of higher n-alkane (C_7 and up) versus their molecular weight. The extrapolated molar volumes were converted to the mass density and correlated to temperature and pressure.

The correlation was validated on density data on *n*-alkane binary mixtures from the literature and from this thesis. Densities were measured with an Anton Paar density meter from room temperature to 175°C and from 10 to 40 MPa for ethane, propane, and *n*-butane as the dissolved gas and *n*-decane, toluene, and cyclooctane as the heavier liquid component. The effective liquid densities applied with regular solution mixing rules (zero excess volume) predicted the densities of these mixtures with an average absolute relative deviation (AARD) less than 1%.

Finally, the mixing rules and effective densities were tested on diluted bitumens. Densities were measured from room temperature to 175°C and from 0.1 to 10 MPa for bitumen/propane (this project), and bitumen/ethane, bitumen/ *n*-butane, and bitumen/*n*-heptane (as part of another project, Motahhari, 2012). The regular solution mixing rules (zero excess volume) predicted the mixture densities with an AARD less than 1%. The AARD was reduced to less than 0.15% with fitted excess volume mixing rules. The binary interaction parameters were correlated to the normalized molar volume difference with a quadratic expression. The AARD with the correlated parameters was less than 0.4%.

Overall, the excess volume mixing rules with the correlated interaction parameters predict the density of diluted bitumens to almost within experimental error as long as the mixture is subcritical and the component densities are known at the conditions of interest. The proposed method is suitable for hand calculations and could be implemented in a simulator with an appropriate database of component densities.

Acknowledgement

First of all, I am deeply indebted to my supervisor, Dr. Harvey W. Yarranton for his support, encouragement and constant guidance during my Master's degree program. It was an honor for me to be a member of his research group.

I also would like to express my deepest gratitude to our PVT lab manager Florian Schoeggel for his teaching and technical support he provided during experimental work.

I am also thankful to Elaine Baydak and Hamed reza Motahhari for their assistance and great help during my master's thesis.

I am thankful to the Department of Chemical and Petroleum Engineering, Asphaltene and Emulsion Research Group, Faculty of Graduate Studies at the University of Calgary for their assistance, NSERC, Shell Energy Ltd., Schlumberger-DBR, Petrobras for their financial support throughout my Masters Program.

Finally, from the deepest of my heart, I would like to thank my husband for his constant support and encouragement. I am really grateful for his caring and understanding.

Dedication

I dedicated this Dissertation to:

My Parents and My Husband

Table of Contents

University of Calgary.....	II
Abstract	III
Acknowledgement	V
Dedication	VI
Table of Contents.....	VII
List of Tables	IX
List of Figures and Illustrations.....	XI
List of Symbols, Abbreviation and Nomenclature	XIV
CHAPTER ONE: INTRODUCTION.....	1
1.1 OBJECTIVES	3
1.2 ORGANIZATION OF THESIS	4
CHAPTER TWO: LITERATURE REVIEW	5
2.1 DENSITY OF HYDROCARBON LIQUID MIXTURES.....	5
2.1.1 General Behavior of Liquid Mixtures	5
2.1.1.1 Partial Molar Volume	6
2.1.1.2 Excess Molar Volumes	8
2.1.2 Behaviour of Liquid-Liquid Hydrocarbon Mixtures	8
2.1.3 Behaviour of Liquid Hydrocarbons with Dissolved Gas	12
2.2 MODELING THE DENSITY OF LIQUID HYDROCARBON MIXTURES	14
2.2.1 Mixing Rule	14
2.2.2 Density Correlations.....	15
2.2.3 Corresponding States	23
2.2.4 Equation of State (EOS)	28
2.3 MODELING THE DENSITY OF LIQUID WITH DISSOLVED GAS.....	35
2.4 HEAVY OIL CHEMISTRY	37
2.4.1 Definition and Classification	37
2.4.2 Heavy Oil Composition.....	39
2.5 DENSITY OF BITUMEN AND MIXTURES WITH SOLVENT.....	44
2.5.1 Density of Heavy Oil and Bitumen.....	44
2.5.1.1 Measurement of Heavy Oil and Bitumen Density	44
2.5.1.2 Effect of the Temperature on Heavy Oil and Bitumen Density.....	44
2.5.1.3 Effect of Pressure on Heavy Oil and Bitumen Density	46

2.5.2 Density of Heavy Oil and Solvent Mixtures	46
2.5.3 Density Modeling for Mixtures of Heavy Oil and Solvents.....	49
2.6 SUMMARY	53
CHAPTER THREE: EXPERIMENTAL METHODS	54
3.1 MATERIALS	54
3.2 APPARATUS DESCRIPTION	55
3.2.1 Anton Paar Density Meter	55
3.2.2 Quizix Pump	57
3.2.3 Back Pressure Regulator (BPR).....	57
3.2.4 Air Bath Temperature Control.....	57
3.3 APPARATUS CALIBRATION	58
3.4 SAMPLE PREPARATION.....	60
3.5 EXPERIMENTAL PROCEDURE	63
3.6 APPARATUS CLEAN-UP.....	64
CHAPTER FOUR: RESULT AND DISCUSSION	65
4.1 DENSITY OF MIXTURES OF LIQUID HYDROCARBONS	65
4.2 DENSITY OF MIXTURES WITH GAS DISSOLVED IN A HYDROCARBON LIQUID	73
4.2.1 New Effective Density Correlation for Light n-Alkanes	76
4.2.2 Validation of New Effective Density Correlation	78
4.3 BITUMEN DENSITY CORRELATION.....	92
4.4 DILUTED BITUMEN DENSITY	94
CHAPTER FIVE: CONCLUSION AND RECOMMENDATION	102
5.1 SUMMARY	102
5.2 CONCLUSIONS.....	102
5.3 RECOMMENDATIONS.....	103
REFERENCES	105
APPENDIX A – PURE HYDROCARBON MIXTURES DENSITY DATA	115
APPENDIX B – DEAD BITUMENS DENSITY DATA	129
APPENDIX C – ADDITIONAL DENSITY DATA.....	132
APPENDIX D - ERROR ANALYSIS	133

List of Tables

Table 2-1. Tait Correlation for <i>n</i> -alkanes (Dymond and Malhotra, 1987).....	19
Table 2-2. Comparison of Requirements and range of applicability of methods studied by Rea <i>et. al.</i> (1973)	26
Table 2-3. Absolute average deviation of saturated liquid density predictions, temperature between 323.10 and 437.10 K.....	33
Table 2-4. UNITAR Classification of oil by physical properties at 15.6°C (Gray, 1994)	37
Table 2-5. Comparison of conventional crude and heavy oil (Briggs, <i>et al.</i> , 1988).38	
Table 4-1. Pure hydrocarbon mixtures for which density was measured by Chevalier <i>et al.</i> (1990).	67
Table 4-2. β_{ij} values for different types of pure hydrocarbon mixtures	68
Table 4-3. The fitting parameters of the new effective density correlation.	78
Table 4-4. Summary of the pure hydrocarbon mixtures and their composition, and temperature and pressure range for which density data collected.	80
Table 4-5. AAD, AARD, MAD, and MARD of pure hydrocarbon mixtures.	89
Table 4-6. Comparison between the effective liquid density of dissolved gas components with their API liquid density value at standard condition.	91
Table 4-7. Fitted parameters for Bitumens A and B.....	94
Table 4-8. The composition, temperatures, and pressures of the diluted bitumens for which density data were collected.	94
Table 4-9. The composition, temperatures, and pressures of the diluted bitumens for which density data were collected.	98
Table A-1. Measured densities for mixtures of 6 wt% ethane and 94 wt% <i>n</i> -decane.....	115
Table A-2. Measured densities for mixtures of 12.5 wt% ethane and 87.5 wt% <i>n</i> -decane.....	116
Table A-3. Measured densities for mixtures of 6 wt% propane and 94 wt% <i>n</i> -decane.....	117
Table A-4. Measured densities for mixtures of 12.5 wt% propane and 87.5 wt% <i>n</i> -decane.....	118
Table A-5. Measured densities for mixtures of 25 wt% propane and 75 wt% <i>n</i> -decane.....	119
Table A-6. Measured densities for mixtures of 6 wt% propane and 94 wt% Toluene.....	120
Table A-7. Measured densities for mixtures of 12.5 wt% propane and 87.5 wt% Toluene.....	121
Table A-8. Measured densities for mixtures of 25 wt% propane and 75 wt%	

Toluene.....	122
Table A-9. Measured densities for mixtures of 6 wt% propane and 94 wt% Cyclooctane.....	123
Table A-10. Measured densities for mixtures of 12.5 wt% propane and 87.5 wt% Cyclooctane.....	124
Table A-11. Measured densities for mixtures of 25 wt% propane and 75 wt% Cyclooctane.....	125
Table A-12. Measured densities for mixtures of 6 wt% <i>n</i> -butane and 94 wt% <i>n</i> -decane.....	126
Table A-13. Measured densities for mixtures of 12.5 wt% <i>n</i> -butane and 87.5 wt% <i>n</i> -decane.....	127
Table A-14. Measured densities for mixtures of 25 wt% <i>n</i> -butane and 75 wt% <i>n</i> -decane.....	128
Table B-1. Measured densities for dead bitumen A.....	129
Table B-2. Measured densities for dead bitumen B.....	131
Table C-1. Measured densities of <i>n</i> -decane diluted Heavy Oil at 23 °C. (Kumar, 2012).....	132
Table C-2. Measured densities of toluene diluted Bitumen A Maltene. (Sanchez, 2012).....	132
Table D-1. Composition accuracy of pure hydrocarbon mixtures.....	134
Table D-2. Error Analysis of Pure Hydrocarbon Mixtures.....	136
Table D-3. Error Analysis of Pure Diluted Bitumen.....	138

List of Figures and Illustrations

Figure 2–1. The slope of the plot of volume vs. Molar fraction is partial molar volume. Line I and II show the slope of the plot in two specific compositions. For line I the slope is positive and for line II the slope is negative.....	7
Figure 2–2. Excess molar volumes for <i>n</i> -hexane (x) and <i>n</i> -alkanes (1-x) at 298.15 K. (data adapted from Goates <i>et al.</i> , (1981)).....	8
Figure 2–3. Excess molar volumes for cyclohexane (x) with <i>n</i> -alkanes (1-x) at 298.15 K. (data adapted from Goates <i>et al.</i> , (1979)).....	9
Figure 2–4. Maximum values of excess molar volume, v^E , of binary mixtures versus the carbon number (n) of the <i>n</i> -alkane component at 298.15 K. (data adapted from Alonso <i>et al.</i> , (1983)).....	10
Figure 2–5. Excess molar volume of equimolar mixtures of 1,1-dimethylpropyl ether + <i>n</i> -alkane vs. <i>n</i> -alkane carbon number. (data adapted from Witek <i>et al.</i> , 1997).....	11
Figure 2–6. Variation of the density with composition at 333.15 K versus different pressures. (data adapted from Canet <i>et al.</i> , (2002)).....	13
Figure 2–7. The process of dissolving a gas component in a liquid mixture.....	35
Figure 2–8. Effect of molecular structure on boiling point (Boduszynski, 1987)...	40
Figure 2–9. Schematic of SARA fractionation procedure.	41
Figure 2–10. Effect of solvent carbon number on insolubles (Speight, 2007).....	42
Figure 2–11. A hypothetical Asphaltene structure, A, B and C represent larger aromatic clusters (Strausz, <i>et al.</i> , 1992). Note the structure is larger than typical for an asphaltene monomer and represents an amalgamated aggregate.....	43
Figure 2–12. The effect of temperature on the density of some Western Canadian crudes.....	45
Figure 2–13. Effect of pressure on density of CH ₄ -saturated bitumen, adopted from Mehrotra and Svrcek, (1985).....	47
Figure 2–14. Effect of temperature on the density of mixtures of athabasca bitumen with propane (Badamchi-zadeh <i>et al.</i> , 2009).....	48
Figure 3–1. Schematic of the density measurement apparatus.....	55
Figure 3–2. Comparison between literature data and experimental data for <i>n</i> -butane density at 75°C.....	59
Figure 3–3. Comparison between literature data and experimental data for <i>n</i> -decane density at 75°C.....	60
Figure 3–4. Charging the transfer cylinder for the compressed gas.	61
Figure 3–5. Charging from transfer cylinder to the sample cylinder.	62
Figure 4–1. Measured and fitted density of mixtures of <i>n</i> -hexane + <i>n</i> -heptane.....	69
Figure 4–2. Measured and fitted density of mixtures of <i>n</i> -hexane + <i>n</i> -hexadecane.....	70

Figure 4–3. Measured and fitted density of mixtures of cyclohexane + <i>n</i> -hexadecane.	70
Figure 4–4. The relationship between binary interaction parameters in the excess volume mixing rule and the normalized molecular weight difference.	71
Figure 4–5. The relationship between binary interaction parameters in the excess volume mixing rule and the normalized specific volume difference.	72
Figure 4–6. <i>n</i> -Alkane molar volumes versus molecular weight at 80°C and 10 MPa.	73
Figure 4–7. Effective liquid density of lower <i>n</i> -alkanes at 80°C and different pressures.	74
Figure 4–8. Comparison of extrapolated <i>n</i> -alkane molar volumes from Tharanivasan <i>et al.</i> (2011) with experimentally derived molar volume of methane at 80°C and 10 MPa.	75
Figure 4–9. Comparison of extrapolated <i>n</i> -alkane molar volumes using only higher <i>n</i> -alkanes with experimentally derived molar volume of methane at 80°C and 10 MPa.	76
Figure 4–10. New effective density of lower <i>n</i> -alkane series at 80°C and different pressures.	77
Figure 4–11. Measured and predicted densities for mixtures of 6 wt% propane and 94 wt% <i>n</i> -decane.	81
Figure 4–12. Measured and predicted densities for mixtures of 12.5 wt% propane and 87.5 wt% <i>n</i> -decane.	81
Figure 4–13. Measured and predicted densities for mixtures of 25 wt% propane and 75 wt% <i>n</i> -decane.	82
Figure 4–14. Reduced temperature and pressure at which the effective density correlation gives more than 3% error in mixture densities (to right of each point).	83
Figure 4–15. Predicted versus measured density for mixtures of <i>n</i> -butane and <i>n</i> -decane.	84
Figure 4–16. Predicted versus measured density for mixtures of propane and <i>n</i> -decane.	85
Figure 4–17. Predicted versus measured density for mixtures of ethane and <i>n</i> -decane.	85
Figure 4–18. Predicted versus measured density for mixtures of ethane and <i>n</i> -tetradecane (Kariznovi <i>et al.</i> , 2012).	86
Figure 4–19. Predicted versus measured density for mixtures of ethane and <i>n</i> -octadecane (Nourizadeh <i>et al.</i> , 2012)	86
Figure 4–20. Predicted versus measured density for mixtures of methane and <i>n</i> -decane (data from NIST database, 2008).	87

Figure 4–21. Predicted versus measured density for mixtures of methane and <i>n</i> -tetradecane (Nourizadeh <i>et al.</i> , 2012).....	87
Figure 4–22. Predicted versus measured density for mixtures of methane and <i>n</i> -octadecane (Kariznovi <i>et al.</i> , 2012).....	88
Figure 4–23. Predicted versus measured density for mixtures of propane and toluene.....	90
Figure 4–24. Predicted versus measured density for mixtures of propane and cyclooctane.....	90
Figure 4–25. Predicted versus measured density for mixtures of methane (C ₁) and toluene: a) regular solution mixing rule; b) excess volume mixing rule with $\beta_{ij} = -0.006$	91
Figure 4–26. Measured and correlated density of Bitumen A.	93
Figure 4–27. Measured and correlated density of Bitumen B.....	93
Figure 4–28. Calculated versus measured density for <i>n</i> -heptane (C ₇) diluted Bitumen A: a) regular solution mixing rule; b) excess volume mixing rule with $\beta_{ij} = +0.022$	96
Figure 4–29. Calculated versus measured density for <i>n</i> -butane (C ₄) diluted Bitumen B: a) regular solution mixing rule; b) excess volume mixing rule with $\beta_{ij} = +0.013$	97
Figure 4–30. Calculated versus measured density for propane (C ₃) diluted Bitumen A: a) regular solution mixing rule; b) excess volume mixing rule with $\beta_{ij} = +0.040$	97
Figure 4–31. Calculated versus measured density for ethane (C ₂) diluted Bitumen A: a) regular solution mixing rule; b) excess volume mixing rule with $\beta_{ij} = -0.001$	98
Figure 4–32. Comparison of binary interaction parameters for diluted bitumens and pure hydrocarbon mixtures.....	101
Figure 4–33. Density of bitumen diluted with <i>n</i> -alkanes at: a) 50°C and 2.5 MPa; b) 100°C and 10 MPa. Equation 4-13 was used to determine the β_{ij} for the excess volume mixing rule.....	101

List of Symbols, Abbreviation and Nomenclature

Abbreviation

APR	Advanced Peng-Robinson
ARC	Alberta Research Council
BPR	Back Pressure Regulator
CN	Carbon Number
EoS	Equation of State
HC	Hydrocarbon
MW	Molecular Weight
PR	Peng-Robinson
SRK	Soave-Redlich-Kwong
SG	Specific Gravity
SF	Shrinkage factor
Wt%	Weight Percent

List of Symbols

a	Attractive constant in Equation of State
b	Repulsive constant in Equation of State
c	Volume translation
c_n	Characteristic carbon number
Z_{RA}	Racket compressibility factor
\tilde{V}	Mixture pseudo-volume
m	Mass fraction
x	Mole fraction
P	Pressure
T	Temperature
v	Molar volume
R	Universal gas constant
Z	Compressibility
n	Number of moles

Greek Symbols

ρ	Density
ω	Acentric factor

β	Compressibility
β_{ij}	Binary interaction parameter between two component i and j
φ	Volume fraction

Subscripts

<i>ave</i>	Average
<i>C</i>	Critical
<i>I</i>	Component i
<i>J</i>	Component j
<i>mix</i>	Mixture
<i>N</i>	Normalized
<i>R</i>	Reduced
<i>S</i>	Saturated
<i>0</i>	Reference

Superscripts

<i>E</i>	Excess
----------	--------

CHAPTER ONE: INTRODUCTION

As the supply of conventional oil resources shrinks, unconventional hydrocarbon feedstocks, such as bitumen and heavy oils, have been recognized as alternate energy sources (Sarkar, 1984). However, primary recovery techniques have had limited success for heavy oils and bitumens due to the high viscosity of the oil. In Canada, steam based methods are often applied to reduce the oil viscosity and improve recovery (Kokal and Sayegh, 1990). Unfortunately, these methods require significant amounts of natural gas, which is costly, and water, which is in limited supply. For example, almost 34 m³ of natural gas and 0.2 m³ of groundwater are required to produce one barrel of bitumen (Canada's Oil Sand Report, 2007). Solvent or solvent-assisted recovery methods are alternatives that may reduce the energy and water requirements for these processes.

Solvent based recovery processes such as VAPEX (Vapor Extraction) and ES-SAGD (Enhanced Solvent – Steam Assisted Gravity Drainage) involve gravity drainage and therefore depend strongly on the density of the solvent diluted heavy oil (or bitumen). Many surface processes involve the dilution of bitumen with solvent. For example, heavy oil is diluted for oil-water separation where the density contrast between the oil and water is critical for effective separation. Heavy oils are also diluted to reduce their viscosity for pipeline transportation and to modify properties during refining. Hence, the density of heavy oil and solvent liquid mixtures is a critical property for the design and operation of both reservoir and surface processes (Audonnet and Padua, 2004).

While some data are available for the density of bitumens and dissolved gases, there are significant gaps. Ward and Clark (1950) were the first, to present experimental density data for Athabasca bitumen. Jacob et al. (1980) measured the viscosity for dead Athabasca bitumen and bitumen saturated with CO₂, CH₄, and N₂ over a wide

range of pressures and temperatures. Mehrotra and Svrcek (1985) published data sets for the viscosity, density and gas solubility for N_2 , CO , CH_4 , CO_2 , and C_2H_6 in a number of dead and live bitumens. Yarranton et al. (2008) and Badamchi-Zadeh et al. (2009) measured the density of mixtures of propane and Athabasca bitumen and also propane/ CO_2 and Athabasca bitumen. However, to date, there has not been a systematic investigation of the density of mixtures of heavy oil and dissolved gases that include the n-alkane series up to butane.

Nor has there been a systematic study on the prediction of density for these mixtures. Marra et al. (1988) reviewed a variety of approaches for predicting the density of hydrocarbon mixtures including regular solution mixing rules, partial molar or excess volumes, corresponding states principle, and the equations of state. In case of diluted bitumen mixtures, Mehrotra and Svrcek modeled the density of Alberta bitumen saturated with CO_2 and C_2H_6 by applying and Peng-Robinson equation of state. Kokal and Sayegh (1990) and Loria *et al.*, (2009) also applied modified Peng-Robinson equation of state to predict the gas-saturated bitumen density. In general, although a cubic equation-of-state is a useful tool for predicting phase behavior such as saturation pressures, it does not provide accurate density predictions for mixtures over a wide range of conditions.

This thesis focuses on regular solution and excess volume mixing rules which are applied to the component densities. With a regular solution, the volumes of the components are additive. With a non-regular solution, the volumes are not additive and the deviation can be expressed as an excess volume. A significant challenge with this approach is how to handle mixtures with dissolved gases. In this case, the pure gas component has a gas density while its density when part of a liquid mixture is more like that of a liquid. One approach to this problem is to use “effective” liquid densities for the dissolved gas. The effective liquid density is the hypothetical density of a gas component when it is part of the liquid mixture.

Tharanivasan *et al.* (2011) developed a correlation for calculating effective density of light n-alkane series. They applied pure liquid hydrocarbon molar volume data from NIST (National Institute of Standard and Technology) database to estimate the effective liquid molar volumes (and densities) of the gaseous n-alkanes. However, Tharanivasan's correlation is inaccurate at pressures lower than 10 MPa and must be modified to apply to the lower pressures of interest to heavy oil reservoir and surface applications.

1.1 Objectives

The purpose of this research is to measure and model the density mixtures of bitumen with different solvents and particularly dissolved gases. One objective is to evaluate regular solution and excess volume mixing rules for the density of diluted bitumens. A second objective is to develop a correlation to predict the effective liquid density of dissolved light n-alkane gases. Density data for pure hydrocarbon mixtures and for diluted bitumens are collected to test the mixing rules and the proposed correlation. For pure hydrocarbon systems, the tests are performed on densities measured for binary mixtures with components of different size and from different chemical families. For the diluted bitumen, the tests are performed on densities measured with liquid and dissolved gas diluents. The specific objectives are to:

1. Measure the density of mixtures of pure hydrocarbons including: n-decane with ethane, propane, and n-butane; toluene with propane; and cyclooctane with propane.
2. Develop a correlation for the effective liquid densities of light n-alkanes based on extrapolated n-alkane molar volumes.
3. Test the proposed correlation on the data for the pure hydrocarbon systems.
4. Measure the density of mixtures of bitumen with ethane, propane, n-butane, and n-heptane.

5. Model the density of diluted bitumen using the effective density correlation and test both regular solution and excess volume mixing rules.
6. Determine excess volumes for non-regular mixtures and generalize if required

1.2 Organization of Thesis

This thesis is organized into five chapters as outlined below.

Chapter 2 presents a review of the data and modeling for mixtures of pure hydrocarbons. The models include the regular solution mixing rule, partial and excess molar volumes, corresponding states, and equations of state. Heavy oil chemistry and the density of diluted heavy oil are also reviewed.

Chapter 3 presents the chemicals and materials used in the experiments; a description of the apparatus and calibration techniques, sample preparation procedures both for pure hydrocarbon mixtures and diluted bitumen mixtures, and the density measurement procedure.

Chapter 4 examines density data for liquid/liquid pure hydrocarbon mixtures from the literature and tests both regular solution and excess volume mixing rules on these data. Then, the effective density correlation developed by Tharanivasan is evaluated and a modified correlation is presented. The density is tested on the data collected in this thesis for liquid hydrocarbon mixtures with dissolved gases. Finally, the mixing rules and effective density correlation are applied to the data collected for the diluted bitumen.

Chapter 5 summarizes the major finding of this thesis and provides recommendations for future work.

CHAPTER TWO: LITERATURE REVIEW

In this chapter, the density of hydrocarbon mixtures is examined and the different approaches taken for modeling these mixtures are presented. Finally, heavy oil chemistry is briefly reviewed and the modeling of diluted heavy oil density is discussed.

2.1 Density of Hydrocarbon Liquid Mixtures

2.1.1 General Behavior of Liquid Mixtures

The simplest liquid mixtures are ideal solutions. An ideal solution is a mixture in which the intermolecular forces between like neighbours and between unlike neighbours are the same. Formally, an ideal solution is a solution for which each component obeys Raoult's law:

$$p_i = x_i p_i^* \quad \text{Equation 2-1}$$

where p_i is the vapour pressure of the component i as part of the solution, x_i is the composition and p_i^* is the vapour pressure of the pure substance i at the same temperature.

Another requirement for an ideal solution is that there is no volume change and or enthalpy change upon mixing. In this case, the volume and mass are both additive parameters and the density can be calculated as follows

$$\rho_{mix} = \frac{\sum m_j}{\sum V_j} = \sum \phi_j \rho_j = \frac{1}{\sum w_j / \rho_j} \quad \text{Equation 2-2}$$

where m_j is component mass, V_j is component volume, and ϕ_j is the component volume fraction.

A liquid mixture where the volumes are additive is termed a regular solution. Regular solutions are not necessarily ideal although ideal solutions are regular. If the composition of a regular hydrocarbon mixture is known, the density of the components can be determined based on density data or correlations and the mixture density estimated with Equation 2-2. This method is only valid for regular solutions and is difficult to apply to petroleum where the fluid composition is ill-defined.

In contrast to regular solutions, where volumes are strictly additive and mixing is always complete, the volume of a non-regular solution is not the simple sum of the volumes of the component pure liquids and solubility is not guaranteed over the whole composition range. Two analytical methods to determine the specific volume (or density) of a liquid mixture are partial molar volumes and excess molar volumes.

2.1.1.1 Partial Molar Volume

The partial molar volume is the contribution that a component of a mixture makes to the overall volume of the solution and is defined as follows:

$$\bar{V}_j = \left(\frac{\partial V}{\partial n_j} \right)_{T,P,n_{i \neq j}} \quad \text{Equation 2-3}$$

where \bar{V}_j is the partial molar volume of the component j , V is the volume of the mixture, and n is the moles of component j . The partial molar volume can be thought of as the slope of the plot of the total volume versus a changing amount of the component j when the temperature, pressure, and moles of the other components are all held constant, Figure 2-1.

Once the partial molar volumes of the components of a mixture are known, the specific volume of the mixture, v_{mix} , is given by:

$$v_{mix} = \sum x_j \bar{v}_j \quad \text{Equation 2-4}$$

where x_j is the molar fraction of each component. The density of the mixture is given by:

$$\rho_{mix} = \frac{MW_{mix}}{v_{mix}} \quad \text{Equation 2-5}$$

where ρ_{mix} is the mass density of the mixture and MW_{mix} is molecular weight.

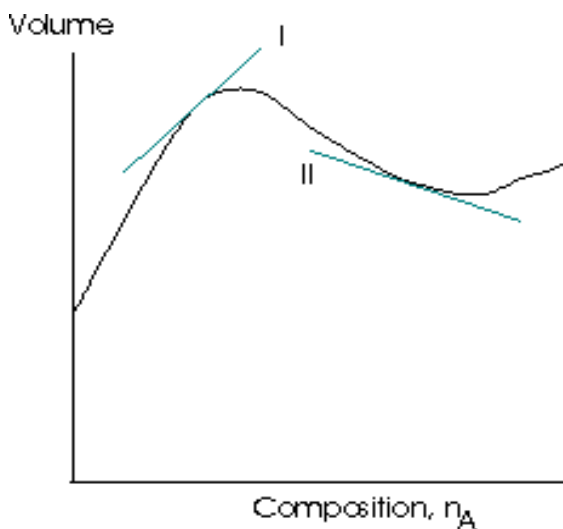


Figure 2–1. Mixture volume versus molar composition for a hypothetical binary mixture. The slope is the partial molar volume which can be positive (Line I) or negative (Line II).

The use of partial volumes to predict mixture properties is not common, since partial molar volume data are not easy to obtain. Many correlations derived based on this approach are for a mixture containing a specific gas, while in practice we may have a mixture of gases dissolved in the liquid. In addition, these correlations are mostly in graphical form and are not suitable for computer calculations. Since these methods are empirical in nature, there can be large errors when extrapolating beyond the range of variables used to develop the correlation (Kokal and Sayegh, 1990).

2.1.1.2 Excess Molar Volumes

The excess molar volume is the difference between the actual molar volume and the ideal molar volume of a mixture (Shana'a *et al.*, 1968):

$$v^E = v_{mix} - \sum_i x_i v_i^\circ \quad \text{Equation 2-6}$$

where v^E is the excess molar volume and v_i° is the molar volume of the pure component i at the same temperature and pressure as the mixture. The use of excess volume methods for hydrocarbon mixtures is discussed later.

2.1.2 Behaviour of Liquid-Liquid Hydrocarbon Mixtures

Hydrocarbons form nearly regular mixtures but there are small excess volumes of mixing as shown in Figure 2-2 and Figure 2-3. The excess volumes of hydrocarbon mixtures are typically less than $0.5 \text{ cm}^3/\text{mol}$ (approximately 0.3% of the molar volume of the mixture). Hence, the error from assuming ideal mixing is usually small and can be neglected in many practical applications.

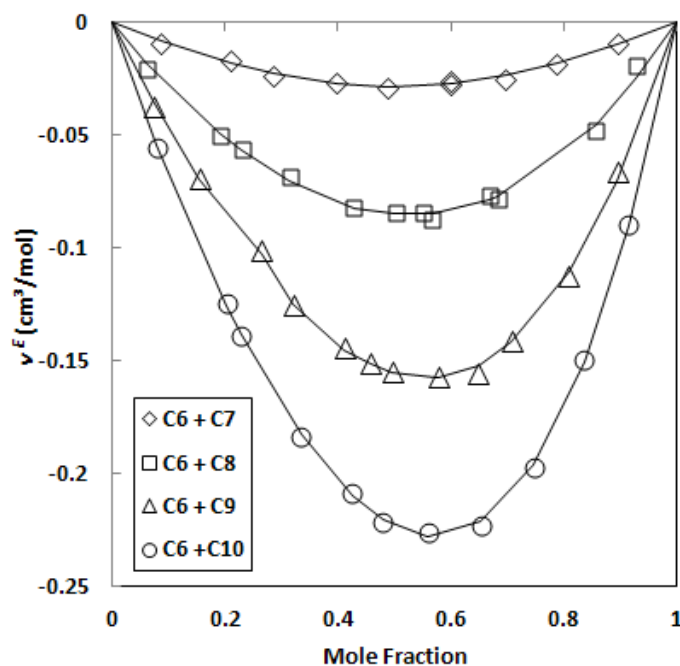


Figure 2–2. Excess molar volumes for n -hexane (x) and n -alkanes ($1-x$) at 298.15 K (adapted from Goates *et al.*, 1981)

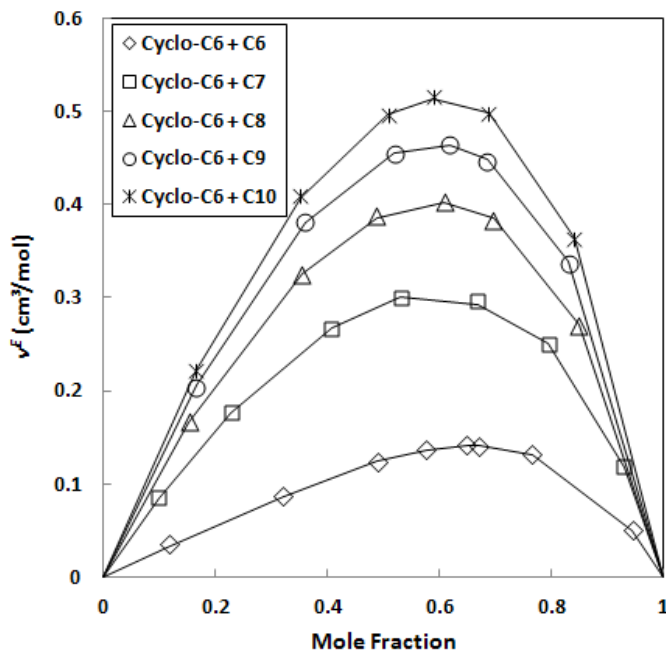


Figure 2–3. Excess molar volumes for cyclohexane (x) with *n*-alkanes (1-x) at 298.15 K. (adapted from Goates *et al.*, 1979)

There are two main contributors to the excess volume of hydrocarbon mixtures: differences in the size (or chain length) of the components and differences in their chemical family. There is a systematic increase in the magnitude of v^E as the size difference of similar hydrocarbons increases. For *n*-alkane mixtures, the excess volumes become more negative as the size difference between the components increase, Figure 2-2. It appears that similar molecules of different size pack more efficiently leading to a decrease in volume (increase in density).

For mixtures of cyclohexanes and *n*-alkanes, the excess volumes become more positive as the size difference increases, Figure 2-3. Gómez-Ibáñez and Liu (1961) showed that for binary mixtures of cyclohexane with *n*-hexane with *n*-dodecane, the excess volume was independent of the temperature. They also observed that the excess volume increased as the length of the paraffin increased. They showed that the excess volume was linearly related to $1/(CN+2)$ with a negative slope.

Alonso *et al.* (1983) measured the excess molar volume for five different aromatic + *n*-alkane mixtures including *p*-xylene + *n*-alkane, *o*-xylene + *n*-alkane, *m*-xylene + *n*-alkane, benzene + *n*-alkane, and toluene + *n*-alkane at 298.15 K. They plotted the maximum value of excess volume against the carbon number of the *n*-alkane component, Figure 2-4. Although some excess volumes were negative at low carbon numbers, in all cases the excess volumes became more positive as the size difference between the molecules increased. The methylated aromatics had lower excess mixing volumes with the *n*-alkanes than the unsubstituted aromatics. It appears that when unlike components are mixed together, the average distance between the molecules usually increases because the repulsive force between them is higher. The increase in distance (or volume) increases as the size difference of the molecules increases.

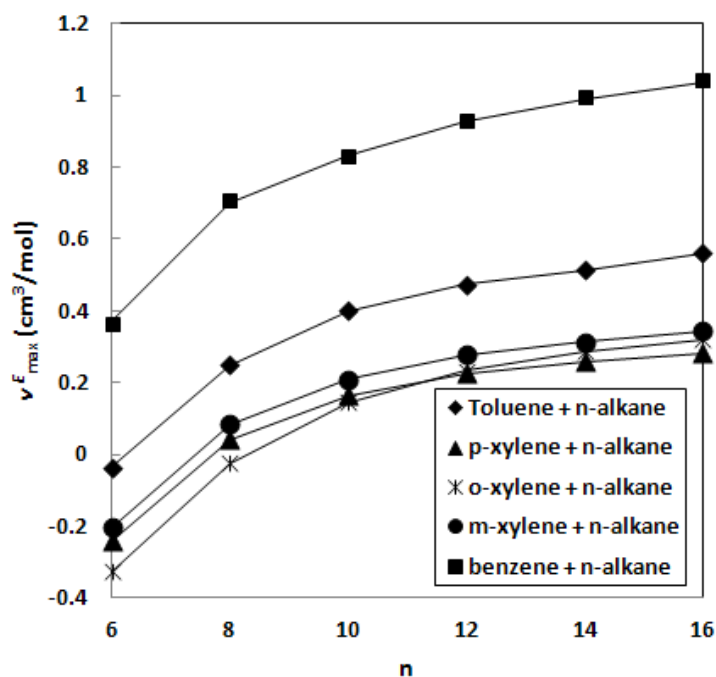


Figure 2-4. Maximum values of excess molar volume, v^E , of binary mixtures versus the carbon number (n) of the *n*-alkane component at 298.15 K. (data adapted from Alonso *et al.*, (1983).

Non-zero excess volumes are expected when a hydrocarbon is mixed with a non-hydrocarbon. For example, Witek, *et al.*, (1997) measured the excess molar volume for the binary mixtures of with 1,1-dimethylpropyl ether with benzene, cyclohexane, hexane, octane, decane, dodecane, tetradecane and hexadecane. The excess volumes increased with increasing n -alkane carbon number up to n -octane and then decreased at higher carbon numbers, Figure 2-5. It appears that both increases repulsion and packing play in a role in the excess volumes of these mixtures.

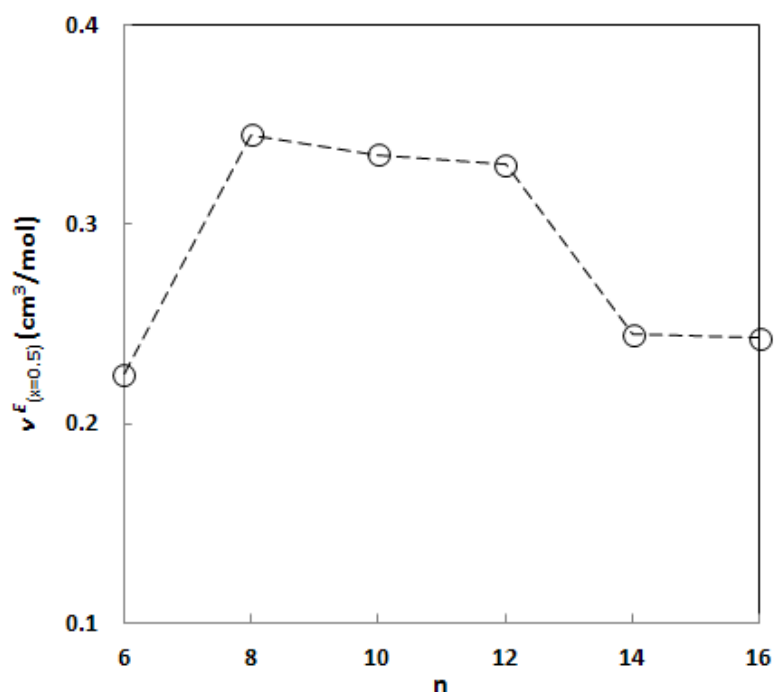


Figure 2–5. Excess molar volume of equimolar mixtures of 1,1-dimethylpropyl ether + n -alkane vs. n -alkane carbon number. (data adapted from Witek *et al.*, 1997)

Other data for binary hydrocarbon mixtures include: the excess molar volume for the binary mixtures of hexane, decane, hexadecane and squalane with benzene at 298.15 K (Lal *et al.*, 2000); densities of different pure hydrocarbon binary mixtures such as cyclohexane with n -hexane, n -heptane, n -octane, n -nonane, n -decane and

benzene and mixtures of *n*-hexane with *n*-heptane, *n*-octane, *n*-nonane, *n*-decane at different temperatures (Goates *et al.* 1977, 1979, 1981); densities of binary mixtures of *n*-alkanes (Hutching and Van Hook, 1985; Schrodtr and Akel, 1989; Chevalier *et al.*, 1990; Cooper and Asfour, 1991; Oliveira and Wakeham, 1992; Wu and Asfour, 1994; Aucejo *et al.*, 1995). The observations from these datasets are consistent with those reported above.

2.1.3 Behaviour of Liquid Hydrocarbons with Dissolved Gas

Lee *et al.* (1966) presented density data for mixture of methane and *n*-decane. Knapstad *et al.* (1990) also measured the liquid density for this mixture at four different methane compositions in the temperature range 20-150°C and at pressures up to 40 MPa. Canet *et al.* (2002) compared the Knapstad *et al.* (1990) and Lee *et al.* (1966) data and observed a significant difference between their results, possibly because they were obtained at different conditions. To fill this gap in the data, they measured monophasic liquid densities for binary mixtures of methane with decane at high pressures (up to 140 MPa) and in the temperature range 293.15 to 373.15 K. They showed that for each composition the density increases with pressure, Figure 2-6, and decreases with temperature. The behaviour was the same as would be expected for a mixture of two liquid components. Audonnet and Pádua (2004) also measured the density of methane from 303 to 393 K and pressure up to 75 MPa. They correlated their results with the Tait equation, which will be explained in Section 2.2.2.

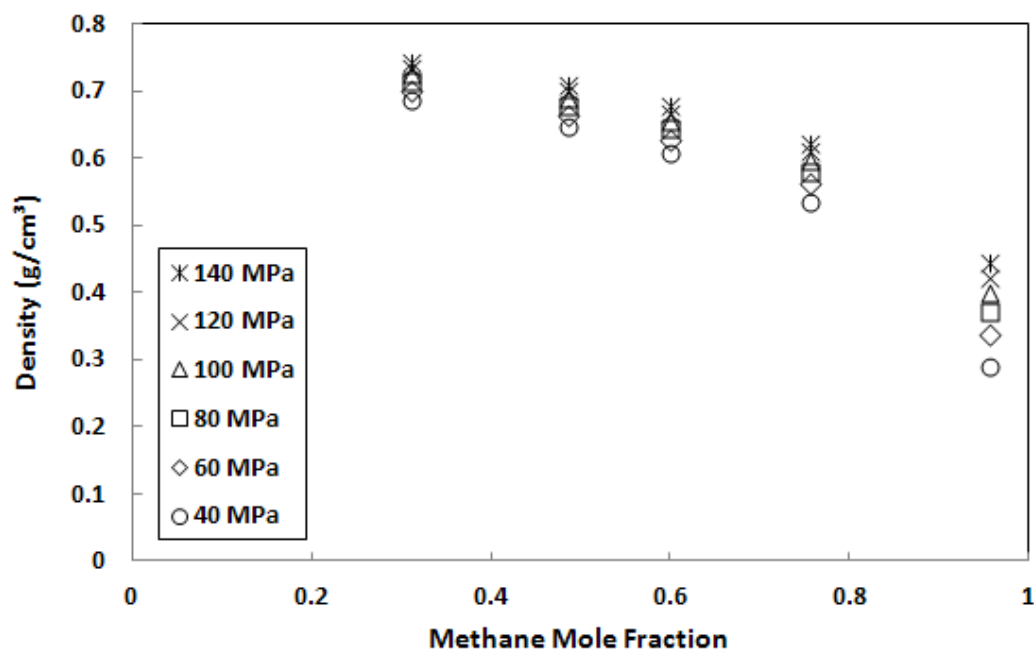


Figure 2–6. Variation of the density with composition at 333.15 K versus different pressures. (data adapted from Canet *et al.*, (2002))

Shana'a and Canfield (1968) presented saturated liquid density for light hydrocarbons such as methane, ethane, propane and their binary and ternary mixtures. The density were reported at -165°C over a wide range of compositions. They also studied the applicability of principle of congruence (Brønsted *et al.*, 1946) according to which the thermodynamic properties of a mixture of n -alkanes are determined by an average chain length n_{ave} :

$$n_{ave} = \sum_i n_i x_i \quad \text{Equation 2-7}$$

where n_i is the number of carbon atoms in a molecule of i th species, and x_i is the mole fraction of that species in the mixture. Their results for the methane-decane mixture did not show a good match with this principle suggesting that molecular packing could be a significant factor.

Aschcroft and Isa (1997) studied the effect of dissolved gases on the density of heavier hydrocarbons. They measured the density for mixtures of dissolved methane

and some other gas components such as air, nitrogen, oxygen, hydrogen and carbon dioxide with higher *n*-alkanes from heptane to hexadecane and also cyclohexane, methylcyclohexane and toluene. To study the effect of dissolved gas on the density of higher *n*-alkanes, they plotted the density difference between gas-saturated density and degassed density versus *n*-alkane chain length. Except for mixtures with carbon dioxide and methane, the density differences were rather small and decreased linearly with increasing *n*-alkane carbon number. For methane and carbon dioxide, the effect was much larger and carbon dioxide, in contrast to the other gases, caused an increase in density.

2.2 Modeling the Density of Liquid Hydrocarbon Mixtures

There are four main approaches to calculate the density of a liquid mixture: mixing rules, density correlations, corresponding states, and equations-of-state (EOS). Each method is presented below.

2.2.1 Mixing Rule

Mixing rules based on component densities were presented in Section 2.1.1. Typically, hydrocarbon liquid mixtures are assumed to be regular solutions or excess volume methods are used. Goates, *et al.*, (1977, 1979, 1981) calculated the excess molar volume for mixtures including *n*-alkane/*n*-alkane, cycloalkane/*n*-alkane, cycloalkane/aromatic binaries at temperatures 283.15, 298.15, and 313.15. They expressed the excess molar volume as a function of composition as follows:

$$V^E = x(1 - x) \sum_{j=0}^3 A_j (1 - 2x)^j \quad \text{Equation 2-8}$$

where x denotes the mole fraction, and A_j values were optimized to fit the experimental data. For *n*-alkane/*n*-alkane mixtures the summation upper limit in Equation 2-8 is 2. They presented the A_j values in tabular form. For cycloalkane/*n*-alkane mixtures, they obtained an excellent fit to Equation 2-8 for each mixture at

all three temperatures by expressing the first two coefficients in this equation as quadratic function of temperature T as follows:

$$A_0 = a_0 + b_0(T - 298.15) + c_0(T - 298.15)^2 \quad \text{Equation 2-9a}$$

$$A_1 = a_1 + b_1(T - 298.15) + c_1(T - 298.15)^2 \quad \text{Equation 2-9b}$$

A_2 and A_3 were temperature independent. The coefficients $a_0, b_0, c_0, a_1, b_1, c_1, A_2, A_3$ were summarized in tabular form. In case of cycloalkane/aromatic mixtures they measured the excess volume for the mixture of cyclohexane/benzene at 298.15 K, and correlated the data with Equation 2-8, the absolute average deviation was less than $0.0007 \text{ cm}^3/\text{mol}^{-1}$.

Witek *et al.*, (1997) derived the excess molar volumes data for their mixtures from density experimental values using the following relation:

$$V_m^E = \frac{M_1X_1 + M_2X_2}{\rho_m} - \left(\frac{M_1X_1}{\rho_1} + \frac{M_2X_2}{\rho_2} \right) \quad \text{Equation 2-10}$$

where subscripts 1 and 2 denote the two components. Then they fitted Equation 2-8 to the data derived from Equation 2-10, and presented the best fit coefficients in tabular form. Lal *et al.* (2000) did the same for binary mixtures of hexane, decane, hexadecane and squalane with benzene at 298.15 K. They showed that for all mixtures the standard deviation in is less than $0.005 \text{ cm}^3 \cdot \text{mol}^{-1}$.

2.2.2 Density Correlations

An alternative to mixing rules applied to component densities is to treat the mixture as a single component fluid and apply a density correlation. In this case, the parameters of the correlation must be correlated to the component properties.

Dymond and Robertson (1982) presented density data for pure hydrocarbons such as octane, decane, and dodecane and their 50% binary mixtures at four different temperatures from 25°C to 100°C and pressures from atmospheric to 500 MPa. To calculate isothermal densities over the pressure range they applied secant bulk modulus K as a polynomial function of pressure as follows:

$$K = K_0 + ap + bp^2 + \dots \quad \text{Equation 2-11}$$

where K is defined as:

$$K = (p - p_0)\rho/(\rho - \rho_0) \quad \text{Equation 2-12}$$

and a , b , and K_0 are presented in tabular form for all single components and binary mixture. The corresponding density can then be calculated from:

$$\rho = \rho_0 K / (K - (\rho - \rho_0)) \quad \text{Equation 2-13}$$

where ρ_0 is the density at 101.325 KPa and 298.15 K.

The Tait equation is considered to be the most satisfactory of the equations investigated in reproducing liquid density measurements over a wide range of pressure (Dymond and Malhotra, 1987, 1988). The original equation of Tait (1888) was developed for the compressibility of fresh water and sea water. A modified version is used for a broader range of fluids and is given by:

$$\frac{\rho - \rho_0}{\rho} = C \log_{10} \left(\frac{B + P}{B + P_0} \right) \quad \text{Equation 2-14}$$

or in terms of volume:

$$\frac{v_0 - v}{v_0} = C \log_{10} \left(\frac{B + P}{B + P_0} \right) \quad \text{Equation 2-15}$$

where subscript 0 refers to 0.101 MPa, B and C are fitting parameters. Depending on the application, parameter C is either constant, has the same value for a series of compounds, or is a weak function of temperature. Parameter B is usually a linear or quadratic temperature dependent function.

Dymond and Malhotra (1987) applied Tait equation to correlate the density data from different sources (Dymond *et al.*, 1980, Dymond and Robertson, 1982, Kashiwagi and Makita, 1982, and Doolittle, 1964) on *n*-alkane from *n*-hexane up *n*-heptadecane with the *C* parameter as constant equal to 0.2000 and the *B* parameter as function of reduced temperature and pressure as follows:

$$B = 341.539 - 734.292T_r + 411.189T_r^2 - \frac{1}{(C_n - 6)} \quad \text{Equation 2-16}$$

C_n is the characteristic carbon number which is equal to actual number of carbon atoms in the case of *n*-alkanes.

The Tait equation was also extended to include the high pressure density data of binary and ternary mixtures of *n*-alkanes. The *C* parameter was held constant at 0.2000 and the *B* parameter was calculated from the one-fluid approximation with $C_{n,mix}$, the carbon number for the equivalent *n*-alkane, defined as follows:

$$C_{n,mix} = \sum_i x_i C_{ni} \quad \text{Equation 2-17}$$

The comparison between the densities predicted based on Tait equation and experimental values show that the correlation can fit all *n*-alkane data within an average absolute percentage deviation of 0.09%. Although this correlation was developed with the high-pressure density data on *n*-alkanes from *n*-hexane to *n*-heptadecane, it also correlates the high-pressure densities of lower *n*-alkane such as ethane, propane, and *n*-butane very satisfactorily. Table 2-2 presents the deviations of the Tait correlation for *n*-alkane high pressure densities.

Assael *et. al.* (1994) modified the version of the Tait correlation from Dymond and Malhotra (1987) based on new experimental density data for *n*-pentane, *n*-heptane, and *n*-octane at low temperatures. The new correlation is applicable for *n*-alkane from methane up to *n*-hexadecane in an extended pressure range of up to 500 MPa.

The overall average deviation of the calculated values from those of experimental measurements is $\pm 0.10\%$. They modified the parameter B as follows:

for C_2H_6 to $C_{16}H_{34}$,

$$B = 331.2083 - 719.86T_r + 401.61T_r^2 - D \quad \text{Equation 2-18}$$

where

$$\text{for } C_2H_6 \text{ to } C_7H_{16}, \quad D=0$$

$$\text{for } C_7H_{16} \text{ to } C_{16}H_{34}, \quad D = 0.8 (C_n - 7)$$

and for CH_4 ,

$$B = 175.8 - 314.57T_r + 134.3T_r^2 \quad \text{Equation 2-19}$$

There are two main advantages for the improved correlation compared with the old one (Dymond and Malhotra, 1987): 1) methane was included in the correlation; 2) the temperature and pressure range was extended. For n -alkane mixtures, they predicted the mixture density from the pure components densities, assuming there is no volume change upon mixing. The mixture density was therefore calculated by,

$$\rho_{mix} = \frac{\sum_i m_i}{\sum_i V_i} = \left(\sum_i \frac{w_i}{\rho_i} \right)^{-1} \quad \text{Equation 2-20}$$

Table 2-1. Tait Correlation for *n*-alkanes (Dymond and Malhotra, 1987)

Compound	No. of points	Temp. range, T_R	Max. press (MPa)	Max. % dev.	Av. abs. % dev.
Ethane	50	0.33–0.49	32.1	0.18	0.08
Propane	50	0.24–0.38	31.5	0.11	0.05
<i>n</i> -Butane	62	0.33–0.59	32.2	0.23	0.14
<i>n</i> -Hexane	8	0.59–0.64	144.5	0.21	0.11
	28	0.44–0.59	126.8	0.21	0.09
	72	0.59–0.66	111.8	0.22	0.09
<i>n</i> -Heptane	14	0.56–0.59	150.0	0.24	0.10
	71	0.55–0.65	111.6	0.24	0.11
	47	0.51–0.68	117.7	0.09	0.04
<i>n</i> -Octane	13	0.52–0.61	152.2	0.15	0.06
	78	0.52–0.61	111.4	0.12	0.05
	47	0.53–0.69	117.7	0.14	0.07
<i>n</i> -Nonane	21	0.51–0.63	150.0	0.19	0.08
	91	0.51–0.71	140.0	0.19	0.08
	48	0.51–0.66	117.7	0.27	0.12
<i>n</i> -Decane	75	0.48–0.56	111.1	0.09	0.04
	8	0.48–0.60	150.5	0.33	0.16
	109	0.48–0.58	490.1	0.27	0.10
<i>n</i> -Undecane	21	0.48–0.58	150.0	0.15	0.07
<i>n</i> -Dodecane	67	0.45–0.53	111.2	0.22	0.13
	31	0.45–0.57	441.9	0.24	0.10
	91	0.45–0.54	416.9	0.18	0.09
	24	0.46–0.60	117.7	0.31	0.14
<i>n</i> -Tridecane	28	0.45–0.63	150.0	0.19	0.06
<i>n</i> -Tetradecane	113	0.43–0.52	366.8	0.12	0.05
<i>n</i> -Hexadecane	17	0.42–0.52	154.2	0.18	0.08
	89	0.42–0.50	290.2	0.29	0.13
<i>n</i> -Heptadecane	21	0.44–0.65	150.0	0.34	0.11

Cibulka and Hnědkovský (1996) presented the Tait equation parameters in a tabular form in temperature and pressure range within the liquid state. They also compared the results from their fits with those from Assael *et al.* (1994) and showed that the deviations are either within or close to the experimental error and are mostly negative at lower temperature and pressure and positive at higher pressure.

Aalto, *et al.* (1996) applied the Hankinson-Thomson correlation (Hankinson and Thomson, 1979) to calculate saturate liquid densities and the Chang-Zhao equation (Chang and Zhao, 1990) to calculate the density in the compressed liquid region. The Hankinson-Thomson correlation is given by:

$$\frac{v_s}{v^*} = V_R^{(0)} [1 - \omega_{SRK} V_R^{(\delta)}] \quad \text{Equation 2-21}$$

$$V_R^{(0)} = 1 + a(1 - T_r)^{1/3} + b(1 - T_r)^{2/3} + c(1 - T_r) + d(1 - T_r)^{4/3} \quad \text{Equation 2-22}$$

$$V_R^{(\delta)} = (e + fT_r + gT_r^2 + hT_r^3)/(T_r - 1.00001) \quad \text{Equation 2-23}$$

where v_s is the molar volume of the saturated liquid, v^* is a characteristic molar volume, which is required for each pure compound, $V_R^{(\delta)}$ is a spherical model function, and $V_R^{(0)}$ represents the deviation from spherical molecule behavior.

The Chang-Zhao equation is given by:

$$v = v_s \frac{A + C^{(D-T_r)^B} (P_r - P_{s,r})}{A + C(P_r - P_{s,r})} \quad \text{Equation 2-24}$$

where P_r is reduced pressure and $P_{s,r}$ is reduced pressure of saturated vapor. C and D are constants and A and B are modified as following equations:

$$A = a_0 + a_1 T_r + a_2 T_r^3 + a_3 T_r^6 + a_4 / T_r \quad \text{Equation 2-25}$$

$$B = b_0 + b_1 \omega_{SRK} \quad \text{Equation 2-26}$$

where a and b values are fitting parameters presented in tabular form, and T_r is reduced temperature.

Aalto, *et al.* (1996) applied their correlation to a database containing 4426 density points for 29 pure alkanes and alkenes to fit their model. They compared their results with those from the two correlations they applied in their work and it was found that their model was the most accurate of the three models. In the second part of their work, they tried to apply their correlation to mixtures. They considered the mixture as a hypothetical pure fluid having the parameter values calculated by mixing rules. They tried 75 combinations of the mixing rules applying 4223 density data point for 49 binary and ternary hydrocarbon systems. The new model was compared to the original HBT correlation (Thomson, *et al.*, 1982), and based on the comparison it was found that the new model was more accurate than HBT and could be applied at higher temperatures near the critical point.

Recently Estrada *et al.* (2006) measured the atmospheric liquid densities of *n*-pentane, *n*-hexane, *n*-heptane and their binary mixtures. Their measured values agree with published densities within an average absolute percentage value of 0.1. They combined the Tait equation with principle of congruence to predict liquid densities at high pressure. The average percentage deviation of Tait equation from experimental values is 0.15%. They also correlated the atmospheric liquid densities of *n*-alkane. The final form of their correlation which depends on temperature and the carbon number is as follows:

$$\rho_0 = (1 - 4.8203 \cdot 10^{-4}T - 2.72932 \cdot 10^{-12}T^{3.5}) - \frac{1}{(0.55240422 + 7.775 \cdot 10^{-5}T^{1.5})n^{-0.87}} \quad \text{Equation 2-27}$$

where T is the temperature, and n is average chain length. Combining the new correlation with Tait equation results in a correlation extrapolating density within the experimental error at high pressures, and also capable of predicting the correct liquid density behavior for *n*-alkane mixtures using a molar fraction average of the carbon number of the pure components of the mixtures.

Another method to calculate the density of any pure compound or mixture at any temperature or pressure is applying Colstad equation (Robinson, 1983). This equation is based upon critical condition of pure components, and is divided into two regions, saturation condition and elevated pressures. Mixing rules are also proposed when the properties of mixtures are concerned. Density at saturation conditions corresponding to a given temperature can be calculated from:

$$v_s = v^* v_R^{(0)} (1 - \omega v_R^\delta) \quad \text{Equation 2-28}$$

where v_s is the molar volume at saturation conditions, v^* is characteristic volume (tabulated for pure components), ω is acentric factor, and $v_R^{(0)}$ and v_R^δ are reduced temperature dependent functions.

At pressures above saturated, density is given by:

$$v = v_s \left[1 - C \ln \left\{ \frac{B + P}{B + P_s} \right\} \right] \quad \text{Equation 2-29}$$

where v is the molar volume, P_s is the vapor pressure at the saturated temperature, B is a function of reduced temperature and acentric factor, and C is an acentric factor dependent function.

The proposed mixing rules for the mixtures are as follows:

$$T_{cm} = \sum_i \sum_j \frac{x_i x_j v_i^* T_{cij}}{v_m^*} \quad \text{Equation 2-30}$$

$$v_m^* = 1/4 \left\{ \left(\sum_i x_i v_i^* \right) + 3 \left(\sum_i x_i v_i^{*2/3} \right) \left(\sum_i x_i v_i^{*1/3} \right) \right\} \quad \text{Equation 2-31}$$

$$\omega_m = \sum_i x_i \omega_i \quad \text{Equation 2-32}$$

The overall correlation accuracy is reported as following: for pure compounds the average absolute error is 0.37%, and for mixtures it is 1.41%.

2.2.3 Corresponding States

The principle of corresponding states holds that fluid properties, such as density, are the same for most fluids when plotted in reduced coordinates. A reduced property for a fluid is a given property divided by its value at the critical point of the fluid. For example, the reduced density at a given reduced temperature and pressure is expected to be the same for most fluids, particularly dispersion force dominated fluids such as hydrocarbons.

The graphical Lu Chart method (Lu, 1959) is one of the recommended correlations in predicting the compressed liquid densities. This correlation is based on the following approach, suggested by Watson (1943):

$$\rho_1/\rho_R = K_1/K_R \quad \text{Equation 2-33}$$

where ρ_1 and ρ_R are the desired density and the density at reference condition, respectively., and K_I and K_R are corresponding correlating parameters. The K factors are given in graphical form as function of reduced pressure and reduced temperature. This correlation is valid for a reduced temperature range of 0.5 to 1.0, and reduced pressure range from saturation to 30.0.

Rea *et al.*, 1973 presented the correlating parameters for Lu Chart, K factors, as a set of generalized polynomial in terms T_r and P_r . The final form of the equation is as follows:

$$K = A_0 + A_1 T_r + A_2 T_r^2 + A_3 T_r^3 \quad \text{Equation 2-34}$$

where A_i is given by

$$A_i = B_{0,i} + B_{1,i} P_r + B_{2,i} P_r^2 + B_{3,i} P_r^3 + B_{4,i} P_r^4 \quad \text{Equation 2-35}$$

The values of $B_{j,i}$ coefficients are presented in tabular form.

One of the alternative analytical methods for graphical Lu Chart method is the generalized equation developed by Yen and Wood (1966) for pure hydrocarbons. The equation is explicitly relating reduced density to reduced temperature and reduced pressure. For pure hydrocarbons, usually one corresponding state equation is applied for saturated liquids and another one for compressed liquids. Francis (1959) fitted the following equation to the experimental data of saturated pure liquids with a good accuracy:

$$\rho = A - BT - \frac{C}{E - T} \quad \text{Equation 2-36}$$

where A , B , C , and E are specific coefficients, and T is temperature.

However, Eq. 2-36 is not applicable for temperatures near the critical region. Martin (1959) improved the correlation near the critical region with the following four parameter expression:

$$\rho_{rs} = 1 + A(1 - T_r)^{1/3} + B(1 - T_r)^{2/3} + C(1 - T_r) + D(1 - T_r)^{4/3} \quad \text{Equation 2-37}$$

where ρ_{rs} is the reduced saturated liquid density (ρ/ρ_c where ρ_c is the critical density) and A , B , C , and D are fluid specific constants. Yen and Wood (1966) found the fourth term in Equation 2-37 to have little effect on its accuracy. Literature data for sixty-two pure compounds was fitted satisfactorily with the following three parameter equation:

$$\rho_{rs} = 1 + A(1 - T_r)^{1/3} + B(1 - T_r)^{2/3} + D(1 - T_r)^{4/3} \quad \text{Equation 2-38}$$

The coefficients A , B , and D are presented either in tabular form or as generalized function of the critical compressibility, $Z_c = P_c v_c / RT_c$, where P_c , T_c , and v_c are the critical pressure temperature and volume respectively, and R is the universal gas constant.

The undersaturated (compressed) liquid density increases with an increase in pressure and can be correlated as follows:

$$\rho_r = \rho_{rs} + (\Delta\rho_r)_{27} + \delta_{Z_c} \quad \text{Equation 2-39}$$

where the sum of the $(\Delta\rho_r)_{27}$ and δ_{Z_c} is the isothermal pressure effect. The term $(\Delta\rho_r)_{27}$ is the increase in reduced density for a pure liquid from the vapour pressure to a given pressure for compound with Z_c equal to 0.27. The term δ_{Z_c} is zero for $Z_c=0.27$ and is a non-zero correction for the isothermal pressure effect on density for compounds with other Z_c values. $(\Delta\rho_r)_{27}$ has been calculated as a function of reduced temperature and pressure ΔP_r and T_r and then fitted to the following equation:

$$\Delta(\rho_r)_{27} = E_{27} + F_{27} \ln \Delta P_r + G_{27} e^{H_{27} \Delta P_r} \quad \text{Equation 2-40}$$

where E_{27} , F_{27} , G_{27} , and H_{27} are all defined as function of reduced temperature.

For compounds of the other selected Z_c values 0.29, 0.25, 0.23, it is necessary to calculate δ_{Z_c} values. The δ_{Z_c} values have been calculated as function of ΔP_r and T_r and then fitted to the following equation:

$$\delta_{Z_c} = I + J \ln \Delta P_r + K e^{L \Delta P_r} \quad \text{Equation 2-41}$$

where I , J , K are all defined as function of reduced temperature.

Another alternative analytical method for Lu Chart method is a generalized correlation presented by Chueh and Prausnitz (1969), as follow:

$$\log \rho = \log \rho_s + \frac{1}{9} \log [1.0 + 9\beta_s (P - P_s)] \quad \text{Equation 2-42}$$

where β_s is the compressibility at saturation given as a function of T_r and ω . The accuracy of the correlation for liquid densities at elevated pressure depends strongly on the value of the saturated liquid density applied (Rea *et al.*, 1973). The Racket equation (1970) is an easy and accurate method to predict the saturated liquid densities over the entire temperature range up to critical temperature (Spencer and Danner, 1972). This equation is given by:

$$\frac{1}{\rho_s} = \left(\frac{RT_c}{MP_c} \right) Z_{RA}^{[1.0+(1.0-T_r)^{\frac{2}{7}}]} \quad \text{Equation 2-43}$$

where Z_{RA} is a specific constant for each compound. If no Z_{RA} is available, Z_c can be used with some loss in accuracy.

Rea *et al.* (1973) compared the above three corresponding states methods and presented their range of applicability, Table 2-1. The applicable temperature range extends to the critical point, except for the Lu Chart method. However, the pressure range is smaller than that of industrial interest. Also, the overall fit to experimental density data for *n*-alkanes is at best 0.6% and the difference can exceed 10%. Dymond and Malhotra (1987) recommend the Tait equation over the corresponding state methods.

Table 2-2. Comparison of Requirements and range of applicability of methods studied by Rea *et al.* (1973)

	Lu Chart	Yen and Woods	Chueh and Prausnitz
Input	T_c, P_c, ρ_{ref}	$T_c, P_c, Z_c, V_c, Z_{RA}$	T_c, V_c, ω, Z_{RA}
T range, T_r	0.50-0.76	0.3-1.0	0.4-0.98
P range, P_r	Sat.-3.0	0.2-60	Sat.-60

Since the corresponding states correlations were specifically developed for pure liquid substances, mixing rules must be applied for mixtures (Kokal, *et al.*, 1990). For mixtures, the critical properties can be determined using the Prausnitz and Gunn method (1971), as follows:

$$T'_c = \sum_{i=1}^N x_i T_{ci} \quad \text{Equation 2-44a}$$

$$V'_c = \sum_{i=1}^N x_i V_{ci} \quad \text{Equation 2-44b}$$

$$Z'_c = \sum_{i=1}^N x_i Z_{ci} \quad \text{Equation 2-44c}$$

$$P'_c = Z'_c RT'_c / V'_c \quad \text{Equation 2-44d}$$

The reduced saturated liquid density is calculated from equation 2-38 using the critical temperature of the mixture. Then the reduced liquid density at the given temperature and pressure is calculated from equation 2-39 again using the critical properties of the mixture. Yen and Woods (1966) evaluated the corresponding states method against data from fifteen binary mixtures, one ternary mixture, and one quinary mixture at both saturation and compressed liquid conditions. They showed that, for the total one hundred fifty nine points, the average deviation was 2.8%.

Since no binary interaction parameters are included in Equations 2-44a to 2-44d; the mixing rules cannot truly reflect mixture properties (Reid *et al.* 1987). For cases where gas mixture density is also required, there can be a discontinuity near the critical region of the mixture (Kokal, *et al.*, 1990). Another disadvantage of this method is that most of the equations were developed without the consideration of non-hydrocarbons such as CO₂ (Marra *et al.* 1988).

2.2.4 Equation of State (EOS)

The simplest equation of state is the ideal gas law:

$$P = RT/v \quad \text{Equation 2-45}$$

where P is pressure, R , is the universal gas constant and T is temperature. However, as its name implies, the ideal gas law can only describe the behaviour of an ideal gas. The real gas law is given by:

$$P = ZRT/v \quad \text{Equation 2-46}$$

where Z is the compressibility factor. The real gas law can describe the behaviour of a non-ideal gas but not a liquid. To describe both gas and liquid behaviour, equations of state generally consist of two terms representing the repulsion and attraction forces. Van der Waals (1873) proposed the first general equation of state as follows:

$$P = \frac{RT}{v-b} - \frac{a}{v^2} \quad \text{Equation 2-47}$$

where a is the attraction parameter and b is the repulsion parameter (or excluded volume).

The van der Waals equation shows two crucial improvements comparing with the ideal gas law. First, the prediction of liquid behaviour is more accurate because at high pressure the volume reaches a limiting value, the excluded volume:

$$\lim_{P \rightarrow \infty} v(P) = b \quad \text{Equation 2-48}$$

Second, the prediction of non-ideal gas behaviour is improved. The term $RT/(v-b)$ approximates ideal behaviour and the term a/v^2 accounts for non-ideal behaviour.

Peng Robinson Equation of State

After the introduction of the van der Waals equation of state (EOS), many other cubic EOS correlations were developed from the Redlich-Kwong EOS (1949) to the

Peng-Robinson EOS (1976). Most petroleum engineering applications rely on the Peng-Robinson EOS or a modified Peng-Robinson EOS. The Peng and Robinson (1976) equation of state (PR EOS) is a two-constant equation that resulted in improved vapour-liquid equilibrium description and also improved liquid density predictions. The PR EOS is given by:

$$P = \frac{RT}{v - b} - \frac{\alpha(T)}{v(v + b) + b(v - b)} \quad \text{Equation 2-49}$$

where,

$$a = 0.45724 \frac{R^2 T_c^2}{P_c} \quad \text{Equation 2-50a}$$

$$b = 0.07780 \frac{RT_c}{P_c} \quad \text{Equation 2-50b}$$

$$\alpha(T) = [1 + m(1 - \sqrt{T_r})]^2 \quad \text{Equation 2-50c}$$

$$m = 0.37464 + 1.54226w - 0.26992w^2 \quad \text{Equation 2-50d}$$

where T_c is critical temperature, P_c is critical pressure, T_r is reduced temperature and w is acentric factor. The PR EOS can also be expressed or in terms the Z factor ($Z = Pv/RT$) as follows:

$$\begin{aligned} Z^3 - (1 - B)Z^2 + (A - 3B^2 - 2B)Z \\ - (AB - B^2 - B^3) = 0 \end{aligned} \quad \text{Equation 2-51}$$

where,

$$A = \frac{aP}{R^2 T^2} \quad \text{Equation 2-52a}$$

$$B = \frac{bP}{RT} \quad \text{Equation 2-52b}$$

$$Z = \frac{PV}{RT} \quad \text{Equation 2-52c}$$

Although the PR EOS is in widespread application for the description of pure component vapour pressures and the vapour liquid equilibrium of mixtures, the predictions of volumetric properties like density, are relatively poor.

Volume Translation

The density predictions from an equation of state can be improved using a shift along the volume axis, which leaves the predicted phase equilibrium unchanged. The volume translation concept was first proposed by Martin (1979). In an independent study, Peneloux *et al.* (1982) introduced molar translation, c , to improve the accuracy of the Soave-Redlich-Kwong (1972) equation of state. The parameter c can be defined as follows:

$$c = v^{cal} - v^{exp}|_{T_r=0.7} \quad \text{Equation 2-53}$$

where v^{cal} is the saturated liquid volume as predicted by equation of state and $v^{exp}|_{T_r=0.7}$ is the experimental saturated liquid volume at a reduced temperature $T_r=0.7$. For pure hydrocarbon up to n -decane the following correlation was presented by Peneloux *et al.* (1982):

$$c = 0.40768 \left(\frac{R \cdot T_c}{P_c} \right) (0.29441 - Z_{RA}) \quad \text{Equation 2-54}$$

where T_c and P_c are the critical properties of the pure components and Z_{RA} is the Rackett compressibility factor.

Jhaveri and Youngren (1988) proposed volume shifts for light hydrocarbon for the Peng-Robinson equation of state. They defined a dimensionless shift parameter s , as follows:

$$s = c/b \quad \text{Equation 2-55}$$

where b is the co-volume in the EOS. For light hydrocarbons up to n -hexane, s is represented as a power function of the molecular weight (M_w) by the same authors,

$$s = 1 - \frac{d}{M_w^e} \quad \text{Equation 2-56}$$

d and e were also presented for n -alkanes.

Soreide (1989) presented two different temperature dependent correlations. The first is applicable to light components such as CO_2 , N_2 , CH_4 , C_2H_6 , and to some extent C_3H_8 at temperatures higher than critical temperature and is given by:

$$s = a_1 + a_2 \cdot T_r \quad \text{Equation 2-57}$$

The second is applicable to components such as C_3H_8 , $i\text{-C}_4\text{H}_{10}$, $n\text{-C}_4\text{H}_{10}$, $i\text{-C}_5\text{H}_{10}$, $n\text{-C}_5\text{H}_{10}$, $n\text{-C}_6\text{H}_{10}$, benzene and is given by:

$$s = |T_r - a_1|^{a_2} + a_3 + a_4 \cdot \omega + a_5^{[a_6 \cdot (T_r - 1)]} \quad \text{Equation 2-58}$$

Magoulas and Tassios (1990) presented another temperature-dependent expression for c as a function of critical parameters (T_c , P_c , Z_c) and acentric factor,

$$c = c_0 + (c_c - c_0)^{\beta(1-T_r)} \quad \text{Equation 2-59}$$

where,

$$c_0 = \frac{RT_c}{P_c} (k_0 + k_1 \cdot \omega + k_2 \cdot \omega^2 + k_3 \cdot \omega^3 + k_4 \cdot \omega^4) \quad \text{Equation 2-60}$$

$$\beta = l_0 + l_1 \cdot \omega \quad \text{Equation 2-61}$$

$$c_c = \frac{RT_c}{P_c} (Z_c^* - Z_c) \quad \text{Equation 2-62}$$

where Z_c^* is the critical compressibility factor calculated without volume translation. Its value is 0.3074 for the Peng-Robinson EOS. Z_c is also given by the expression proposed by Czerwiński *et al.* (1988) valid up to *n*-eicosane,

$$Z_c = 0.2890 - 0.0701\omega - 0.0207\omega^2 \quad \text{Equation 2-63}$$

Ungerer and Batut (1997) also suggested a new expression for the volume translation as a function of temperature and molecular weight:

$$c(T) = A.T + B \quad \text{Equation 2-64}$$

where

$$A = 0.023 - 0.00056.MW \quad \text{Equation 2-65a}$$

$$B = -34.5 + 0.4666.MW \quad \text{Equation 2-65b}$$

and A and B are expressed in $\text{cm}^3/\text{mol.K}$ and cm^3/mol , respectively.

After calculating volume translation term for mixture components, the pseudovolume for the mixture, \tilde{V} , is defined as follows:

$$\tilde{V} = V + \sum_{i=1}^P c_i n_i \quad \text{Equation 2-66}$$

Substitution of \tilde{V} for V in the EOS improves the predictions of volumetric properties.

de Sant'Ana *et al.* (1998) compared all the above correlations on the determination of the molar volume of pure hydrocarbon liquid densities (up to C₁₅). Table 2-3 and Table 2-4 describe the density prediction of different methods by showing the absolute average error. Table 2-3 shows the absolute average error for high pressure density prediction, while Table 2-4 shows the absolute average error for saturated liquid densities.

Table 2-3. Absolute average deviation of saturated liquid density predictions, temperature between 323.10 and 437.10 K.

component	Jhaveri and Youngren	Soreide	Magoulas and Tassios	Ungerer and Batut
	AAD(%)	AAD(%)	AAD(%)	AAD(%)
<i>n</i> -Hexane	4.17	1.92	1.69	5.77
<i>n</i> -Heptane	1.21	1.49	0.74	1.8
<i>n</i> -Nonane	2.39	4.48	1.13	0.72
<i>n</i> -Undecane	3.27	inapplicable	1.44	0.35
<i>n</i> -Dodecane	3.37	inapplicable	1.44	0.53
<i>n</i> -Tridecane	3.68	inapplicable	1.78	0.81
Cyclopentane	Inapplicable	inapplicable	1.31	5.76
Cyclohexane	Inapplicable	3.54	2.98	1.64
Ethylbenzene	0.44	inapplicable	1.87	1.05
Butylbenzene	0.76	inapplicable	1.96	0.55
Hexylbenzene	1.83	inapplicable	1.49	0.2
Methylcyclopentane	Inapplicable	inapplicable	1.97	1.55
Methylcyclohexane	1.03	inapplicable	2.17	2.77
Propylcyclopentane	Inapplicable	inapplicable	2.23	3.14
Propylcyclohexane	3.17	inapplicable	2.40	4.45
Butylcyclohexane	3.87	inapplicable	2.48	4.62
1-Methylnaphtalene	Inapplicable	inapplicable	3.92	1.36
2-methylnaphtalene	Inapplicable	inapplicable	3.27	1.81
Saturated liquid densities tested	2.43	2.86	2.02	2.16

The Jhaveri and Youngren (1988) method as well as Ungerer and Batut (1997) correlation provide very good predictions in the entire pressure-temperature domain investigated. However, a number of disadvantages must be considered when applying a specific volume translation method. The Jhaveri and Youngren (1988) as well as the Soreide (1989) correlations are only applicable for a limited number of hydrocarbons, which makes them inappropriate for reservoir fluid applications. Another issue with Jhaveri and Youngren (1988) correlation is that the volume translation is independent of temperature which restricts temperature extrapolation at high pressure. On the other hand, the method of Ungere and Batut (1997) can be easily applied since only the molecular weight of the components is needed. Therefore, only this method is recommended for reservoir fluid applications.

EOS are commonly applied to predict the phase behaviour of hydrocarbon mixtures, two factors restrict their practical application as a predictive tool. First, even the simplest cubic EOS has two or three adjustable parameters and requires the solution of a cubic equation. Second, the EOS must be tuned with real data from the system under consideration. Hence, one must know the answer or at least partial answer *a priori* to use an EOS. Typically, the saturation properties of the system, including density, are used as benchmarks and the EOS and volume translation parameters are adjusted to match these data. Once matched the the benchmarks, it is assumed that the EOS will provide accurate predictions at any other set of conditions. This is not necessarily true. Thus, from the practical point of view, one must know the answer before an EOS can be used (Marra *et al.* 1988).

Even with volume translation, the prediction of fluid properties from an equation of state are subject to error due to the inherent limitation on the accuracy of the equation of state and to the limitation in the characterization of the fluid. This characterization might be the most significant source of error when dealing with crude oil (Loria *et al.*, 2009).

2.3 Modeling the Density of Liquid with Dissolved Gas

The density of mixtures with dissolved gases can be modeled directly, although not necessarily accurately, with the equations of state or corresponding states methods. However, when mixture densities are modeled using mixing rules, a liquid mixture with a dissolved gas is a special case. The density of the gas dissolved in the liquid is not the same as the density of the pure gas, Figure 2-7. What then is the correct density to use in a regular solution mixing rule such as Equation 2-2. One solution is to determine the density of the gas in a hypothetical liquid state; that is, its effective density when part of a liquid mixture.

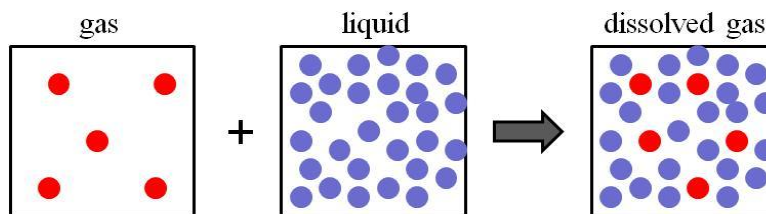


Figure 2–7. The process of dissolving a gas component in a liquid mixture

Standing and Katz (1942) presented an empirical correlation based on this method to determine the density of liquid hydrocarbon mixtures containing dissolved methane and ethane. Using compressibilities and thermal expansion coefficients, they extrapolated measured mixture densities to a reference condition of 101.325 kPa and 15.7°C. Then, they calculated the densities of methane and ethane from the mixture densities and a regular solution mixing rule. It was assumed that propane and any higher carbon number components behaved as regular solutions.

The method was originally designed to determine live oil densities. Since the solution gas composition is usually unknown, Standing and Katz (1942) developed an applicable correlation for calculating the density when only the oil API gravity, the gas gravity, and the solution GOR are known. The method is graphical and not suitable for computer modeling.

Tharanivasan *et.al.* (2011) developed empirical correlations to predict the effective density of the dissolved gas component in petroleum. His correlations were divided into two separate groups, one correlation for *n*-pentane and higher *n*-alkane and the other one for light *n*-alkane from methane up to *n*-butane and *i*-butane. The density data for the higher *n*-alkanes were fit at a given temperature using a pressure-dependent compressibility as follows:

$$\rho = \rho_o \exp\{\alpha_1 P + \alpha_2(1 - \exp(-\beta P))\} \quad \text{Equation 2-67}$$

where ρ_o is the density in kg/m³ at 101 kPa, α_1 is the compressibility at high pressure, and $\alpha_2 = \Delta\alpha/\beta$ where $\alpha_1 + \Delta\alpha$ is the compressibility at low pressure, β is the decay rate from the low to high pressure compressibility, and P is the pressure in kPa. The correlation parameters were then related to temperature as follows:

$$\rho_o = a_0 + b_0 T + c_0 T^2 \quad \text{Equation 2-68}$$

$$\alpha_2 = a_1 T^n \quad \text{Equation 2-69}$$

where a_0 , a_1 , b_0 , c_0 and n are fit parameters and T is temperature in K.

For methane, ethane, propane, *n*-butane, and *i*-butane the molar volume of the higher *n*-alkanes were plotted versus their molar mass and fit with a quadratic equation. The plot was extrapolated for lighter *n*-alkane to estimate the molar volume (and therefore density). The extrapolated densities were fit in the same procedure as for higher carbon number components with Equation 2-67 but the temperature dependent parameters were modified as follows:

$$\rho_o = a_0 + b_0 T + c_0 T^2 \quad \text{Equation 2-70a}$$

$$\alpha_1 = a_1 + b_1 T \quad \text{Equation 2-70b}$$

$$\alpha_2 = a_2 + b_2 T + c_2 T^2 \quad \text{Equation 2-70c}$$

The fit parameters for the light hydrocarbons were given in a tabular form.

2.4 Heavy Oil Chemistry

2.4.1 Definition and Classification

The word petroleum, which is derived from the Latin *petra* and *oleum*, literally means rock oil. The petroleum industry generally identifies petroleum (also called crude oil) by its geographic location (*e.g.* West Texas Intermediate, Brent, or Oman), API gravity (an oil industry measure of density) and sulfur content are commonly measured of the value of a crude oil. Crude oils are classified into different grades based on the physical properties, Table 2-5.

Table 2-4. UNITAR Classification of oil by physical properties at 15.6°C (Gray, 1994)

	Viscosity (mPa.s)	Density (Kg/m ³)	API Gravity(°API)
Conventional Oil	< 10 ²	< 934	>20
Heavy Oil	10 ² - 10 ⁵	934 – 1000	20 – 10
Bitumen	> 10 ²	> 1000	< ~ 10

Conventional petroleum is the part of petroleum which exists in the reservoir in the liquid state and is mobile enough to flow naturally from the reservoir into the well bore. Heavy oils have a much higher viscosity (and lower API gravity) than conventional petroleum, and usually cannot be produced with primary recovery techniques (Speight, 2007). Heavy oils also have higher asphaltene, sulfur, and metal contents compared to conventional oils and are more difficult to refine. Bitumens are even more viscous than heavy oils and are found in oil sand deposits (Speight, 2007). The largest heavy oil and bitumen resources are located in Canada, Venezuela, and the Soviet Union and include more than 90% of the world heavy oil

in place (Briggs, *et al.*, 1988). Table 2-6 compares typical heavy-oil properties with conventional oil.

Table 2-5. Comparison of conventional crude and heavy oil (Briggs, *et al.*, 1988).

Attribute	Athabasca	Cold Lake	Conventional crude, Alberta
Gravity, ° API	7 to 8	10 to 12	35
Hydrocarbon type, wt%			
Saturates	18 to 23	21	70 to 90
Aromatics	29	19	
Asphaltene	17	16	0.1 to 2
Resins	35	44	9 to 15
Sulfur, wt%	4.7	4.5	0.1 to 2
Vanadium, ppm	NR	250	1 to 5
Nickel, ppm	NR	100	1 to 5
Reservoir oil viscosity, cp	500,000	100,000	1

NR – not reported in this source

From a chemical point of view, petroleum is defined as a naturally occurring mixture of hydrocarbons, oxygen-, nitrogen-, and sulfur-containing compounds plus a trace amount of metal-containing compounds. The difference in physical properties between conventional crude oil and bitumen is a result of the variety of organic constituents and physical conditions that affect the petroleum formation. This variation in elemental composition and properties resulted in many attempts to characterize petroleum (Speight, 2007; Whitson, *et al.*, 2000; Riazi, 2005). Carbon number distribution, distillation curves, distillation residue properties and solubility class are all used for petroleum characterization (Ortiz, 2009).

2.4.2 Heavy Oil Composition

Boduszynski *et al.* (1987, 1988) developed analytical procedures for the detailed molecular characterization of heavy crude oils and petroleum residues. They related heteroatom (S, N, O, V, Ni, Fe) concentration, hydrogen deficiency (H/C atomic ratio), molecular weight distribution and also molecular chemical composition of heavy petroleums to their atmospheric equivalent boiling point. Figure 2–8 summarized some of their key observations. For a given homologous series of compounds, the boiling point increases with molecular weight. At any given molecular weight, the paraffins have the lowest boiling point. Compounds with aromatic rings or a functional group capable of hydrogen bonding have higher boiling point at a given molecular weight because the intermolecular attractive forces are larger. Figure 2-8 highlights the complexity of crude oils and the challenges in modeling their properties. In particular, density models or mixing rules must contend with a complex mixture of hydrocarbons and heteroatomic species.

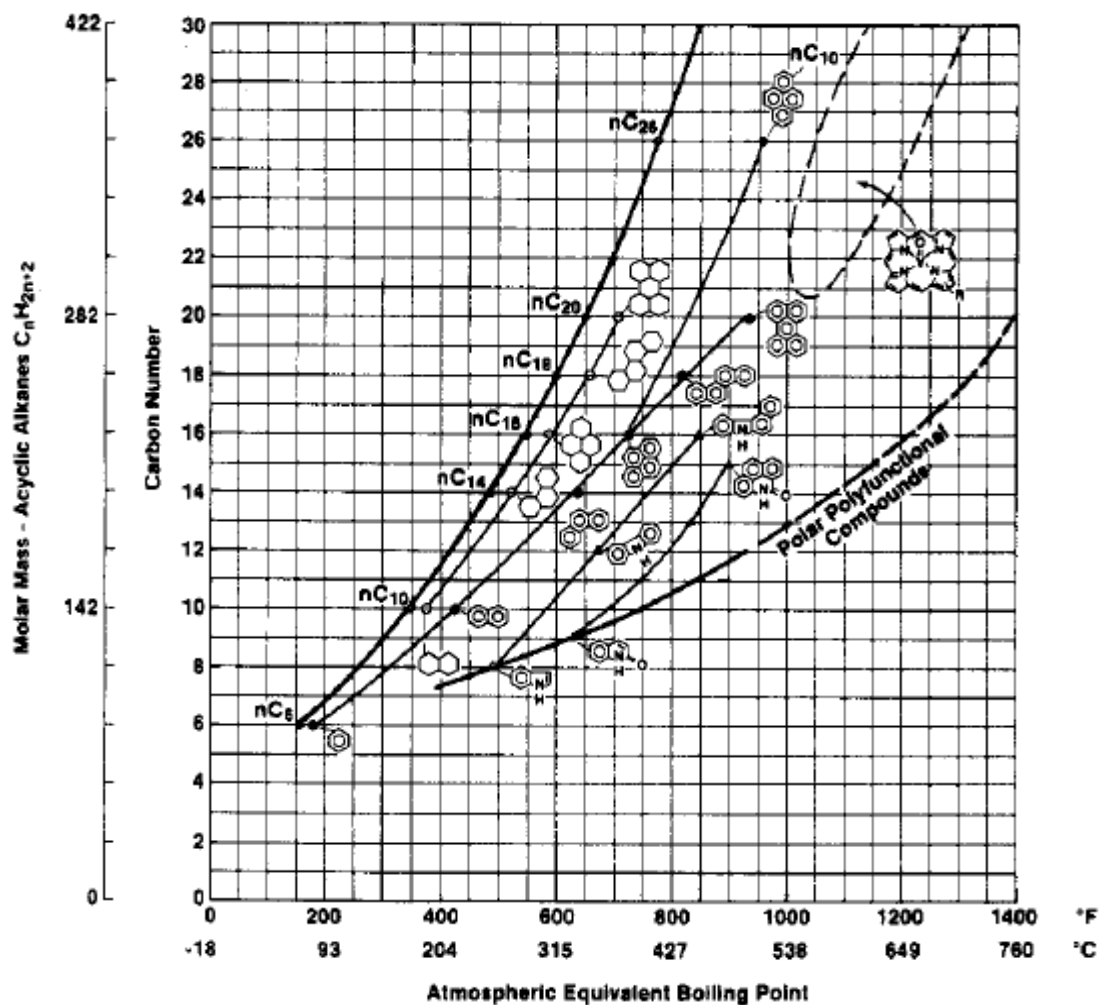


Figure 2-8. Effect of molecular structure on boiling point (Boduszynski, 1987)

Approximately 20 to 40 wt% of a heavy oil can be distilled and characterized into boiling fractions. Since the residue fraction is so large, heavy oil and bitumen is often divided into solubility and polarity classes instead. The most common method to obtain such classes is SARA fractionation, Figure 2-9, which provides four fractions: saturates (S), aromatics (A), resins (R), and asphaltene (A). Saturates consist of non-polar hydrocarbons such as *n*-paraffins, iso-paraffins, and naphthenes. Aromatics are the components which adsorb on silica gel and are made

up of species with benzene rings. They may have more than one benzene ring, and also contain attached saturated groups. Resins adsorb in clay and are soluble in the common organic solvents such as pentane and heptanes. They are also aromatic molecules but are larger, more polar, and more heteroatomic than the aromatics. Asphaltene are the materials which are insoluble in *n*-paraffins such as *n*-pentane and *n*-heptane but soluble in aromatic solvents such as toluene. Asphaltenes have some unique features and are discussed in more detail below.

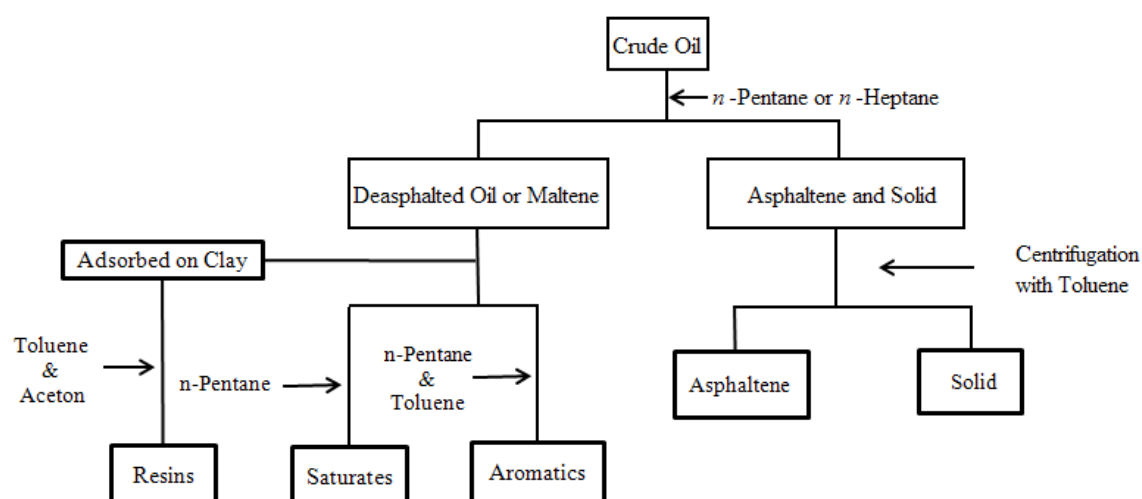


Figure 2–9. Schematic of SARA fractionation procedure.

Asphaltenes are dark brown to black friable solids that are precipitated from petroleum and bitumen by addition of a non-polar hydrocarbon (Speight, 2007). The classical definition is that asphaltenes are soluble in benzene and insoluble in low molecular weight *n*-alkane petroleum-derived solvent. The definition is imprecise because different solvents precipitate a different amount of asphaltenes, Figure 2-10, with slightly different properties. Therefore, asphaltenes must be defined by the procedure used to extract them from the bitumen.

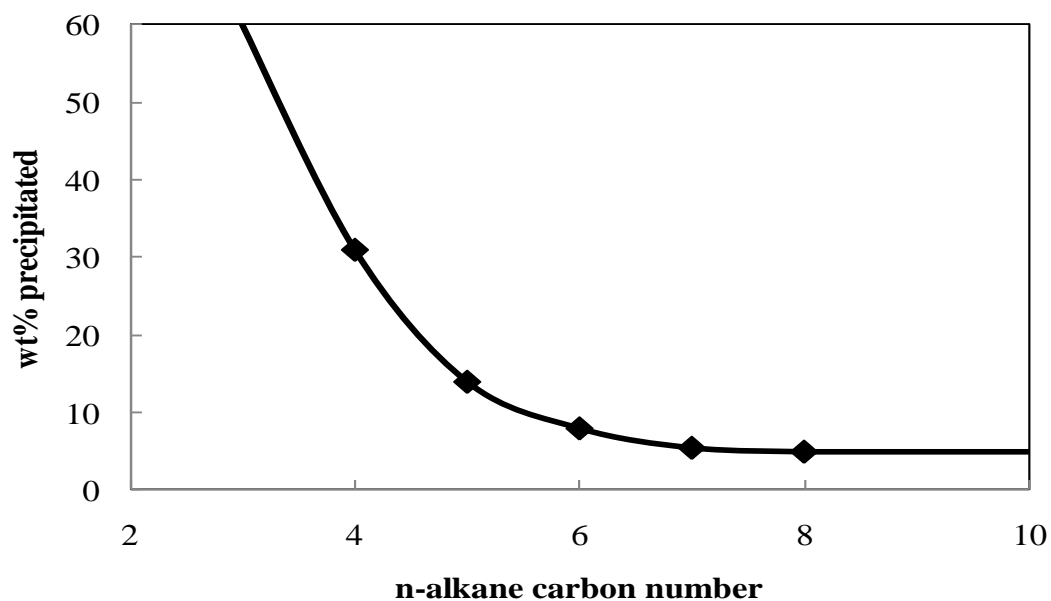


Figure 2–10. Effect of solvent carbon number on insolubles (Speight, 2007).

Nonetheless, asphaltenes obtained from different sources are similar. They are the most aromatic, polar, heteroatomic, and dense species in crude oils. Although determining the real structure of asphaltenes has proved to be difficult, they mostly consist of condensed aromatic nuclei that carry alkyl and alicyclic constituents with hetero-elements (such as nitrogen, oxygen, and sulfur), Figure 2-11. The proportion of asphaltenes in petroleum changes with origin, depth, API gravity of the crude oil, and the sulfur content of the crude oil (Kokal, *et al.*, 1995).

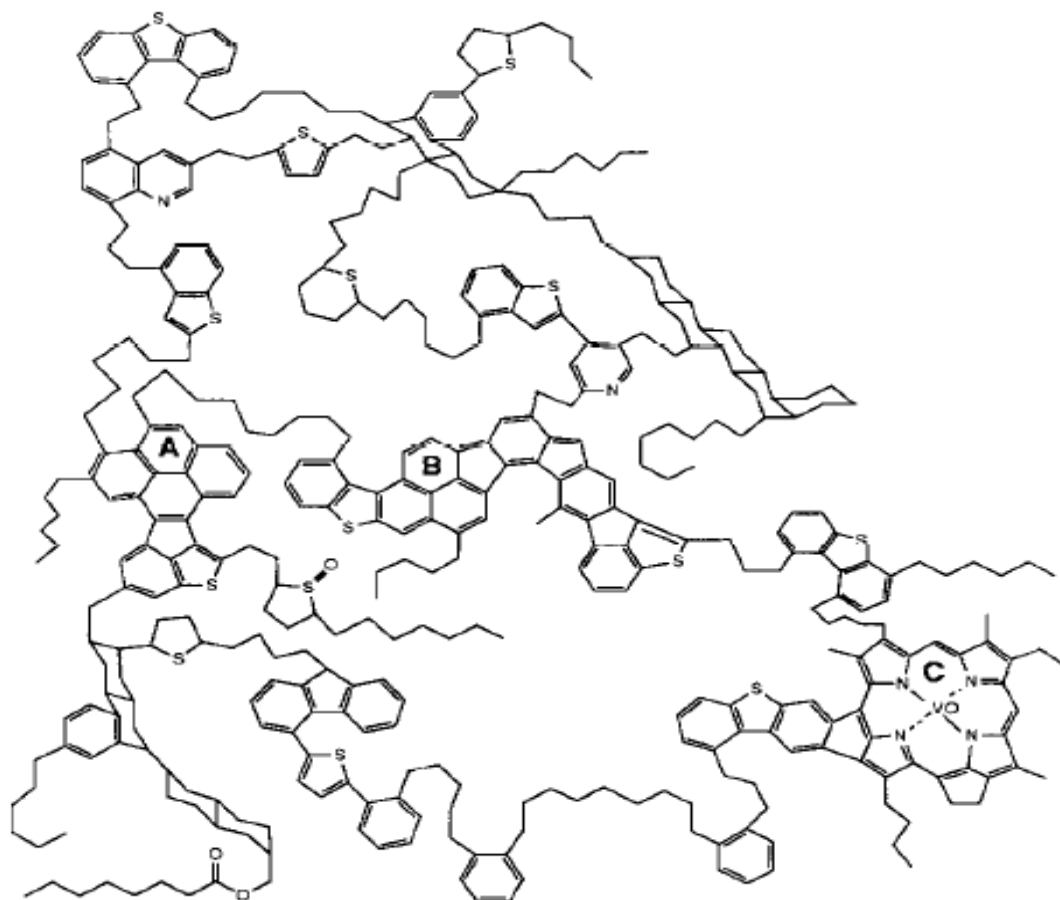


Figure 2–11. A hypothetical Asphaltene structure, A, B and C represent larger aromatic clusters (Strausz, *et al.*, 1992). Note the structure is larger than typical for an asphaltene monomer and represents an amalgamated aggregate.

Asphaltenes (or at least some of the asphaltenes) are known to self-associate, forming aggregates of 6-10 molecules (Speight, 2007; Yarranton *et al.*, 2000). Asphaltene self-association has been observed by different techniques including interfacial tension measurements, molar mass measurement which demonstrated that the asphaltene molar mass distribution is not constant. Asphaltene association depends on temperature and composition (Agrawala and Yarranton, 2001). This self-association mechanism is still debated and has been modeled as colloidal

aggregation or analogously to linear polymerization (Agrawala and Yarranton, 2001). It is not known what role, if any, aggregation plays in the density of mixtures including asphaltenes.

2.5 Density of Bitumen and Mixtures with Solvent

2.5.1 Density of Heavy Oil and Bitumen

2.5.1.1 Measurement of Heavy Oil and Bitumen Density

Several techniques are used to determine bitumen (or heavy oil) density such as pycnometers, displacement, digital density meters, and hydrometers which are described in ASTM D70, ASTM D71, ASTM 4052, and ASTM D1298, respectively (Speight, 2001). Since bitumen is highly viscous, sometimes dilution with a solvent is required to obtain a measurement. The densities of series of a bitumen/solvent mixture are determined using the desired method and the bitumen density is calculated from a mixing rule. An important point regarding this density determination is to assure that solution non-idealities are accounted for in calculation procedure; if this is not the case, some bias will be introduced into the determination (Helper and Hsi, 1989) Other problems which can interfere with the accurate bitumen density determination are:

- Residual solids or residual solvent may remain with the bitumen, if an extraction step is applied to isolate bitumen
- Light ends may be lost from bitumen during the isolation step

2.5.1.2 Effect of the Temperature on Heavy Oil and Bitumen Density

Figure 2-12 shows that the density for different Western Canadian crude oils decreases linearly with temperature. As reported by AOSTRA (1989) Bulkowsky and Prill studied the density variation of four Athabasca bitumen sample over the temperature range of 0 to 150°C and correlated their data as follows:

$$\rho = \rho_0 - 0.62T \quad \text{Equation 2-71}$$

where ρ and ρ_0 are the density kg/m^3 at the given temperature (T in $^{\circ}\text{C}$) and 0°C , respectively.

Gewers (1965) presented the densities of samples of Cold lake and Athabasca bitumens over the temperature range of 0 to 150°C . His data can be represented by the following equations:

$$\begin{aligned} \rho &= 1024 - 0.645T && 8.1^{\circ}\text{API Athabasca bitumen} \\ \rho &= 1009 - 0.634T && 10.4^{\circ}\text{API Cold Lake bitumen} \end{aligned}$$

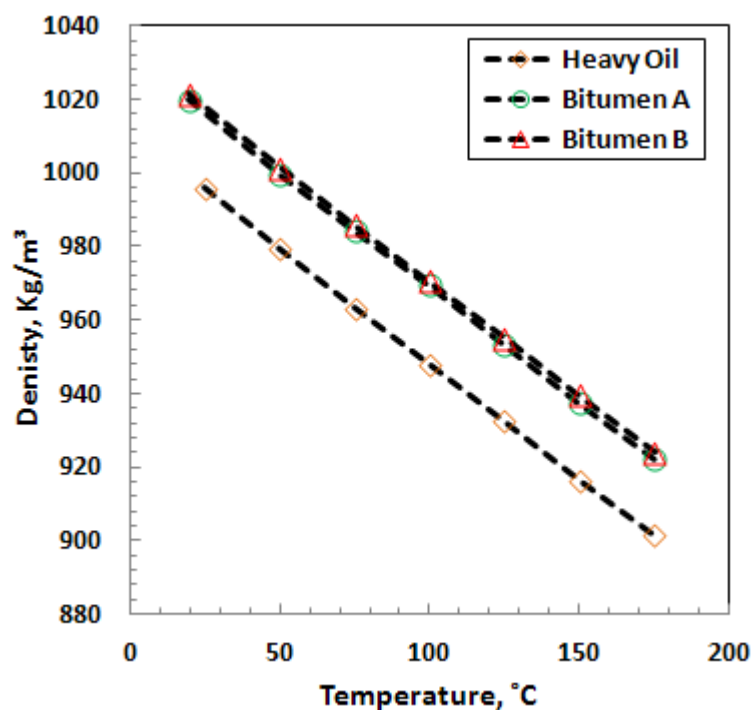


Figure 2-12. The effect of temperature on the density of some Western Canadian crudes (data from present work).

2.5.1.3 Effect of Pressure on Heavy Oil and Bitumen Density

The density of crude oil liquid phases increases exponentially with pressure although a linear approximation is often adequate. Density calculation for oil at pressures higher than saturation pressure is accomplished by applying the isothermal compressibility (McCain, 1990) as follows:

$$\rho = \rho_0 \exp[c_0(P - P_0)] \quad \text{Equation 2-72}$$

where ρ_0 is the density at the saturation pressure, P_0 and c_0 is the isothermal compressibility. ρ_0 and c_0 can be related to temperature as follows:

$$\rho_0 = a_1 - a_2T \quad \text{Equation 2-73}$$

$$c_0 = c_1 \exp(c_2T) \quad \text{Equation 2-74}$$

where a_1 , a_2 , c_1 , and c_2 are constants. Equations 2-71 to 2-74 can be used to fit and interpolate bitumen liquid density over any given temperature and pressure range.

2.5.2 Density of Heavy Oil and Solvent Mixtures

Mehrotra and Svrcek studied the density and viscosity of several bitumens saturated with dissolved gas including: Athabasca bitumen saturated with CO₂, CH₄, and N₂ (1982), Marguerite Lake bitumen saturated with CO₂, Athabasca bitumen saturated with CO, and C₂H₆ (1985), Peace River and Wabasca bitumen saturated with N₂, CO, CH₄, CO₂ and C₂H₆ (1985), and Cold Lake bitumen saturated with N₂, CH₄, CO₂, and C₂H₆ (1988). They observed that the density decreased with increasing temperature and pressure, Figure 2-13.

Since their experiments were performed at saturation conditions and not fixed composition, their data include several effects. Recall that the solubility of the dissolved gas decreases with increasing temperature but increases with increasing

pressure. Therefore, the mixture density in their experiments is expected to increase as the temperature increases but decrease as the pressure increases. However, the density of the bitumen itself is expected to change in the opposite direction; that is to decrease as temperature increases and increase as pressure increases. The overall changes in density are a combination of these effects.

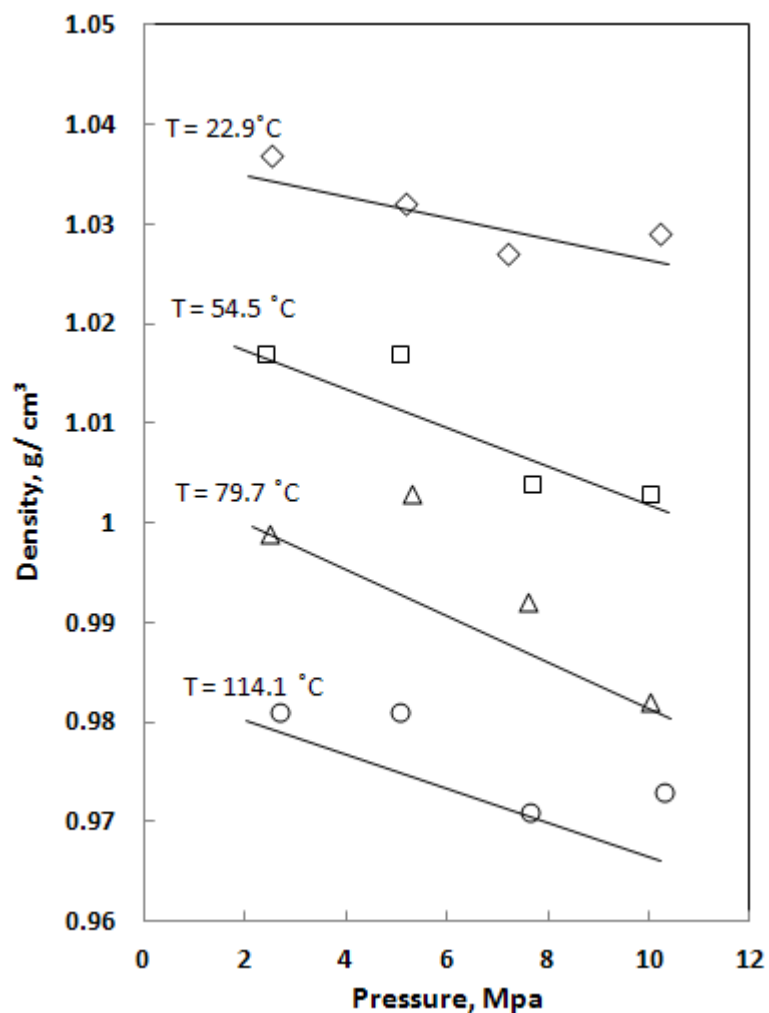


Figure 2–13. Effect of pressure on density of CH₄-saturated bitumen, adopted from Mehrotra and Svrcek, (1985)

Ashcroft *et al.*, (1992) measured the density of seven different crude oils diluted with toluene, cyclohexane, n-heptane, and seven other paraffinic solvents at

temperatures of 15°C and 25°C and atmospheric pressure. They presented the results in terms of plot of percentage relative excess volume or specific excess volume versus solvent mass fraction. Their results showed that the volumetric behavior of these mixtures were similar to the excess volume of binary mixtures of pure hydrocarbons, Figure 2-2 and 2-3. The maxima appear, at or close to, mass fraction equal to 0.5. For toluene and cyclohexane diluted bitumen, the excess volume was positive (expansion upon mixing), while for paraffinic diluted crude oil, the excess volume was negative. The shrinkage was greatest for the lowest-boiling point solvent.

Badamchi-zadeh *et al.*, (2009) studied the density of Athabasca bitumen saturated with propane, Figure 2-14. They observed that the density decreased linearly with temperature at each composition. They assumed no volume change upon mixing and predicted the densities within the accuracy of the measurement except at the highest propane content (25.5 wt%). Given the scatter in the data, it is not clear if the propane/bitumen mixtures form regular solutions or exhibit small excess volumes of mixing.

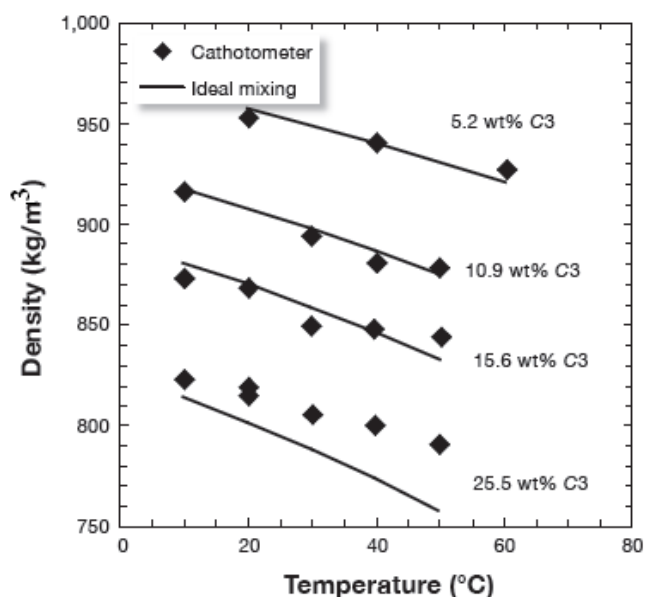


Figure 2–14. Effect of temperature on the density of mixtures of athabasca bitumen with propane (Badamchi-zadeh *et al.*, 2009)

2.5.3 Density Modeling for Mixtures of Heavy Oil and Solvents

Robinson (1983) modeled the density of diluted crude oils based on the Costald equation which permits inclusion of light end components in the mixture at high temperature and pressure. He compared his results for diluted crude oil at 15°C and 1.013 atm with those ones from API Standard 2450. The overall average deviation was 0.25%.

Erno *et al.*, (1994) measured the volume and density of heavy oil blended with condensates at 15°C and 50°C. They converted the volume to the shrinkage factor by applying the measured volumes of oil, condensate, and blend. They found observed shrinkage when a condensate was added to heavy oil. For blends up to 30% condensate, they fitted the shrinkage as follows:

$$SF = ax_c + bx_c^2 + cx_c^3 \quad \text{Equation 2-75}$$

where x_c is the condensate volume fraction, and a , b , and c are equal to 0.0249, $-3.31 \cdot 10^{-4}$, and $0.823 \cdot 10^{-6}$ respectively.

Marra *et al.* (1988) demonstrated that mixing rules can also be used to model the density of a mixture of crude oil and solvents. They applied the regular solution concept to develop a simple model for calculating the density of CO₂/crude oil mixtures with engineering accuracy. The mixture density is expressed as follows:

$$\rho_{SP} = \frac{m_s}{V_{SP}} = \frac{m_{HC} + m_{CO_2}}{\frac{m_{HC}}{\rho_{HCP}} + \frac{m_{CO_2}}{\rho_{CO_2P}}} \quad \text{Equation 2-76}$$

where ρ_{SP} is the pseudo-liquid density of the system containing CO₂, m_s is the mixture mass, V_{SP} is the pseudo-liquid volume of the system, m_{HC} is the hydrocarbon mass, m_{CO_2} is the CO₂ mass, ρ_{HCP} is the pseudo-liquid density of the hydrocarbon and ρ_{CO_2P} is the pseudo-liquid density of the CO₂. If mixture density

data are available, the apparent density of CO₂ can be calculated by rearranging Equation 2-76 as follows:

$$\rho_{CO_2P} = \frac{m_{CO_2}}{\frac{m_s}{\rho_{SP}} - \frac{m_{HC}}{\rho_{HCP}}} \quad \text{Equation 2-77}$$

The apparent liquid density of CO₂ can be plotted versus the pseudo-liquid system density. This plot can be further broken down based on the weight percent of CO₂ in the mixture. This shows that the apparent liquid density of CO₂ is a function of CO₂ concentration as well as pseudo-liquid system density. Since both apparent liquid density of CO₂ and pseudo-liquid system density both were unknown, the correlation requires a trial-and-error solution. To eliminate this trial-and-error solution, a third-order polynomial equation was developed as follows:

$$\rho_{SP} = a\rho_{HCP} + b \quad \text{Equation 2-78}$$

where

$$a = 0.9973 + 0.005134C_{CO_2} + 1.25C_{CO_2}^2 + 2.7 * 10^{-7}C_{CO_2}^3 \quad \text{Equation 2-79}$$

and

$$b = 0.1460 - 0.1843C_{CO_2} - 5.746 * 10^{-4}C_{CO_2}^2 + 1.07 * 10^{-5}C_{CO_2}^3 \quad \text{Equation 2-80}$$

With the correlation in this form, the density can be calculated directly at the appropriate reservoir pressure and temperature.

Most density modeling for bitumen/solvent systems has been done with cubic equations of state. Mehrotra *et al.* (1985) modeled the density of Alberta bitumen saturated with CO₂ and C₂H₆ using Peng-Robinson equation of state. They discussed different critical properties correlations including those proposed by

Cavet (1962), Bergman (1976), Kesler *et al.* (1976), Huang (1977), and Whitson (1980). They applied all the above correlations to estimate the critical properties of bitumen pseudo-components, and summarized the results separately for Athabasca and Peace River bitumens. The results show that for lighter pseudo-components, the predicted critical properties from each correlation are similar but for the heaviest pseudo-component the differences are significant. The predicted T_c , P_c and w were used in the Peng-Robinson EOS to predict density values. For the density data for gas-saturated bitumen the predicted densities were highly dependent on which properties correlation was applied. The predicted density values for CO₂-saturated bitumen were higher than the experimental data for Athabasca bitumen and lower for Peace River bitumen. The best prediction for Athabasca bitumen was with Lee-Kesler correlation, 3.6% deviation, and for Peace River was with Bergmann-Cavet correlation, 2.1%. The predicted densities of gas-saturated bitumen decreased linearly with temperature for all cases. Increasing the pressure also resulted in a slight reduction in density, contrary to the expected behavior.

Kokal and Sayegh (1990) modeled the density data for four different Alberta bitumens (Athabasca, Peace Rive, Wabasca, and Cold Lake) from Svrcek and Mehrotra (1982, 1984, 1985). They determined the volume translation parameter for pure components separately below the critical temperature (Equation 2-70) and above the critical temperature (Equation 2-82):

$$c = \bar{v} - \frac{RT_c}{P_c} Z_{RA}^{[1+(1-T_r)^{\frac{2}{7}}]} \quad \text{Equation 2-81}$$

$$c = \frac{RT_c}{P_c} (0.307 - Z_{RA}) \quad \text{Equation 2-82}$$

where c is the volume translation parameter, \bar{v} is the liquid molar volume calculated from EoS, R is the universal gas constant, T_c and P_c are the component critical temperature and pressure, and Z_{RA} is the Racket compressibility factor.

For mixtures, the c parameter is obtained from the following equation:

$$c = \sum x_i c_i \quad \text{Equation 2-83}$$

where c_i is the components volume translation parameter, and x_i is the component mole fraction in the mixture. For all systems, the average absolute error percent of the density predictions was less than 1%.

Loria *et al.*, (2009) develop a new tuning method for the volume translation parameters applied in the Peng-Robinson equation of state to predict gas-saturated bitumen densities from Strauzs and Lown (2003). The first step was to calculate the critical properties, acentric factor, specific gravity and molecular weight of each pseudo-component based on Lee-Kesler property correlations. Then, the liquid volume, $v_{i,actual}$, of each pseudo-component was calculated as follows.

$$v_{i,actual} = \frac{MW_i}{SG_i(\rho_{water}^{60^{\circ}F})} \quad \text{Equation 2-84}$$

Once the liquid volume of each pseudo-component is calculated, the volume translation for each component, c_i , was determined as follows:

$$c_i = v_{i,PR} - v_{i,actual} \quad \text{Equation 2-85}$$

where $v_{i,PR}$ is the calculated molar volume of the pseudo-component from the EOS without volume translation. The mixture molar volume is then given by:

$$v_{corrected} = v_{PR} + \sum_i c_i x_i \quad \text{Equation 2-86}$$

and the mixture density was calculated from the corrected molar volume and the average molecular weight. Note, Loria *et al.* (2009) set the binary interaction

parameters for all components to zero. The average absolute error in the calculated densities was 0.83%.

2.6 Summary

There is currently no generalized method to accurately predict the density of diluted heavy oils. The most comprehensive method is the equation of state. However, cubic equations of state (the most commonly used form of EOS) require volume translation to obtain accurate densities. Generalized volume translations are only accurate over a limited range of temperatures and pressures and are not usually very accurate for mixtures. Reasonably density predictions can be obtained if the volume translation is tuned to a particular dataset but the tuned translations are not likely to be accurate beyond the conditions used to tune them.

An alternative is to determine the density of hydrocarbon mixtures from correlations and mixing rules. However, these correlations are usually restricted to the liquid region and do not easily accommodate dissolved gases. This option is still appropriate for diluted heavy oils because, in practice, they are almost always far below their critical point and therefore well into the liquid phase region.

CHAPTER THREE: EXPERIMENTAL METHODS

This chapter describes the experimental methods used for measuring the density of mixtures of pure hydrocarbon liquids and bitumen diluted with a hydrocarbon liquid and with a dissolved hydrocarbon gas. The pure hydrocarbon mixtures include: propane and *n*-decane, propane and toluene, propane and cyclooctane, butane and *n*-decane and ethane and *n*-decane. The hydrocarbons used for the diluted bitumen mixtures are propane and *n*-heptane. The materials and apparatus are described and the experimental procedure is discussed.

3.1 Materials

Ethane 99% purity, propane 99.5% purity and *n*-butane 99.5% purity were purchased from PraxAir Canada Inc. Decane 99.7% purity, cyclo-octane purity $\geq 99\%$, and omnisolv high purity toluene 99.99% purity, were purchased from Fischer Scientific, Sigma-Aldrich, and VWR respectively. Technical grade acetone and toluene were applied for cleaning the apparatus and were supplied by VWR. Reverse osmosis water supplied by the University of Calgary water plant and Nitrogen 99.9% purity from PraxAir was used for apparatus calibration.

Two samples of bitumen from the same source (WC-B-B2 and WC-B-B3) were received from Shell Energy Canada. This bitumen was recovered from a steam assisted gravity process and was distilled by ARC (Alberta Research Counsel) to remove water and solids. For convenience WC-B-B2 and WC-B-B3 bitumen are denoted as Bitumen A and Bitumen B, respectively, throughout the thesis.

3.2 Apparatus Description

Figure 3-1 shows the schematic of the apparatus which consists of two transfer vessels connected on either side of an Anton Paar mPDS 2000V3 density meter. An air bath enclosed the apparatus and maintained a fixed temperature. The pressure was maintained and controlled by a Quizix Pump model Q5200. The main components of the apparatus are described below.

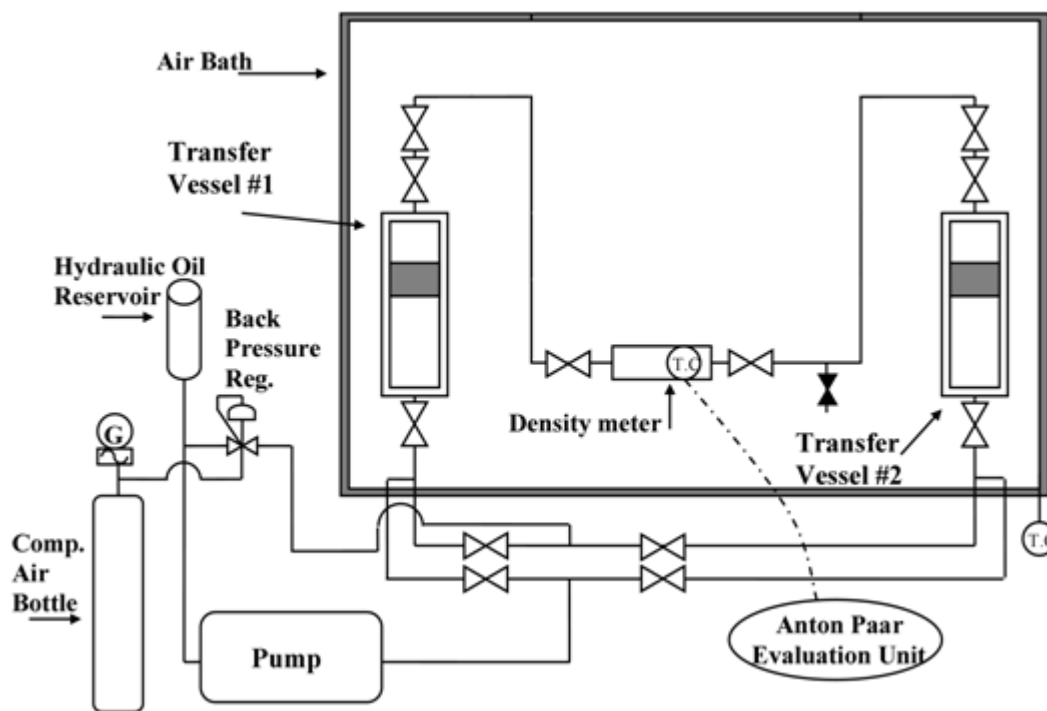


Figure 3–1. Schematic of the density measurement apparatus.

3.2.1 Anton Paar Density Meter

The in-line Anton Paar DMA HPM density meter cell has a built-in temperature sensor which was used to measure the equilibrium temperature. The cell is connected by an interface module to an Anton Paar mPDS 2000V3 evaluation unit displaying the meter oscillation period and the temperature. The oscillation period was measured with precision of ± 0.001 micro seconds and the temperature

measured with a precision of 0.01 C. Both are required to obtain an accurate density from the density meter.

The Anton Paar density meter is based on the measurement of the period of harmonic oscillation of a quartz U-tube. The sample fluid is injected into the U-tube and its density alters the oscillation period. The U-tube can be described as un-damped oscillation of a mass suspended from a spring (Lagourette et al., 1992). The period of oscillation for an oscillator with one degree of freedom is given by:

$$\Lambda = 2\pi\sqrt{\frac{E}{M}} \quad \text{Equation 3-1}$$

where Λ is the oscillation period, E is the elasticity constant of the spring, and M is the summation of U-tube mass and the sample fluid mass given by:

$$M = M_0 + \rho.V_0 \quad \text{Equation 3-2}$$

where M_0 is the U-tube mass, and V_0 and ρ are the volume and density of the fluid in the U-tube. Substituting Equation 3-2 into Equation 3-1 and rearranging gives:

$$\rho = \frac{E}{4\pi^2 V_0} \Lambda^2 - \frac{M_0}{V_0} \quad \text{Equation 3-3}$$

The above equation is simplified as follows:

$$\rho = D_A.\Lambda^2 - D_B \quad \text{Equation 3-4}$$

where D_A and D_B are pressure and temperature dependent constants They are determined at any given temperature and pressure from a calibration to two fluids of known densities. Once the constants are known, the density of the sample fluid can be determined. The calibration procedure is outlined in Section 3.3.

3.2.2 Quizix Pump

The Quizix SP-5200 pump system has three functions: 1) accurate volumetric injection for sample preparation, 2) sample mixing, 3) pressure control during the experiment. Sample preparation is described later. The process which creates the sample mixture ensures that the total composition is correct but does not ensure that the mixture is uniform throughout the total volume. The sample is mixed by flowing it through the density meter between the two sample cylinders with the pump in a volumetric flow mode. The mixture is considered uniform when a constant period/density is observed when the entire sample is displaced through it. The direction of flow through the meter is determined with the use of control valves which will allow the hydraulic fluid from the pump either into the sample cylinder or discharge to the back pressure regulator.

The final function of the pump is to provide an accurate stable pressure at which to take the readings once the fluid has equilibrated at temperature. To achieve constant pressure, the pump is set in a constant pressure mode and allowed to settle to a zero flow rate at the given temperature equilibrium.

3.2.3 Back Pressure Regulator (BPR)

The BPR has two main functions: 1) is to act as a safety relief valve to protect against over pressurization of the system during temperature increases, 2) to maintain a constant pressure for mixing ensuring that the fluid mixed in the apparatus is always above the mixture bubble pressure. The BPR back pressure is set by adjusting the pressure in the BPR air control cylinder.

3.2.4 Air Bath Temperature Control

The test fluid temperature is maintained using the air bath model POM-136B-1. It has self-tuning temperature controller that regulates the input power to the heating element of the air bath to maintain the temperature within $\pm 0.1^{\circ}\text{C}$. The air bath is equipped with a circulating fan to reduce temperature gradients inside the air bath.

For accuracy in experimental data the air bath temperature is adjusted to provide the equilibrium temperature based on the temperature readings from the Anton Paar meter's high accuracy temperature sensor. The precision of the sensor is ± 0.01 °C. Hence, the accuracy of the temperature is limited by consistency of the air bath control rather than the temperature sensor.

3.3 Apparatus Calibration

Apparatus calibration has three key factors which must be confirmed or adjusted for: temperature, pressure, and density. The first two factors are straightforward. First, the Anton Paar comes from the factory with a temperature certification. Second, the pressure is read from the pump pressure which was confirmed versus a lab calibration gauge.

The density is determined from the two unknown density meter constants (Equation 3-4) which must be calibrated. The density meter was calibrated to nitrogen and degassed reverse osmosis water for temperatures of 25, 50, 75, 125, and 175 °C and pressures of 10, 12.5, 15, 17.5, 20, 25, 30, 35, and 40 MPa. The densities of the calibration fluids were taken from the Anton Paar DMA HPM manual. The calibration constants were determined at each temperature and pressure and linearly interpolated versus the period squared for intermediate conditions. Note, the accuracy of the temperature control at 25°C was not sufficient for calibration purposes. Therefore, a linear extrapolation (with a correction factor based on measured *n*-decane densities at 18°C) was used to estimate the density meter constants for any measurements at temperatures below 50°C. The *n*-decane densities were compared with data from NIST (standard reference database, version 2008) for the correction.

The pure components density data were compared with literature values to verify the calibration. Figure 3-2 and 3-3 show the comparison between the literature density data and experimental values of propane and *n*-decane at various

temperatures, respectively. The AARD for propane is 0.17% and for *n*-decane is 0.12%. The AARD are within the error of the measurements. Note that the error in the measurements in this work is smaller than the symbols in Figures 3-2 and 3-3.

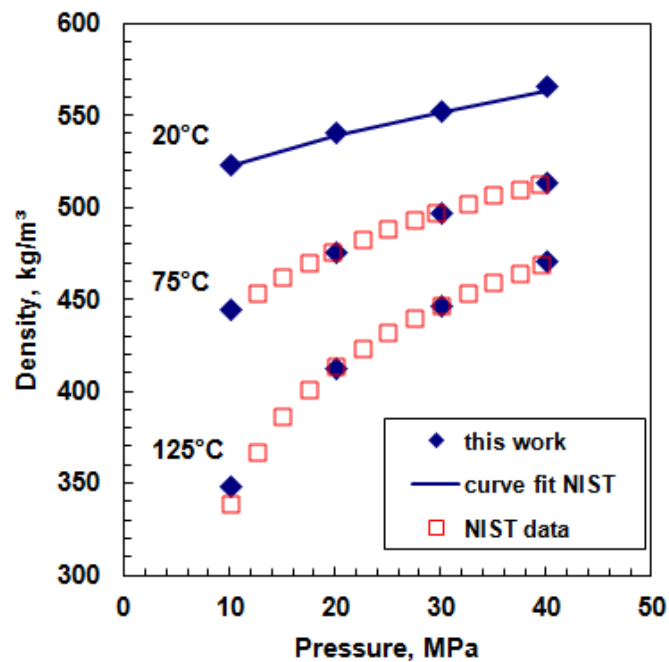


Figure 3–2. Comparison between experimental and literature data for propane density.

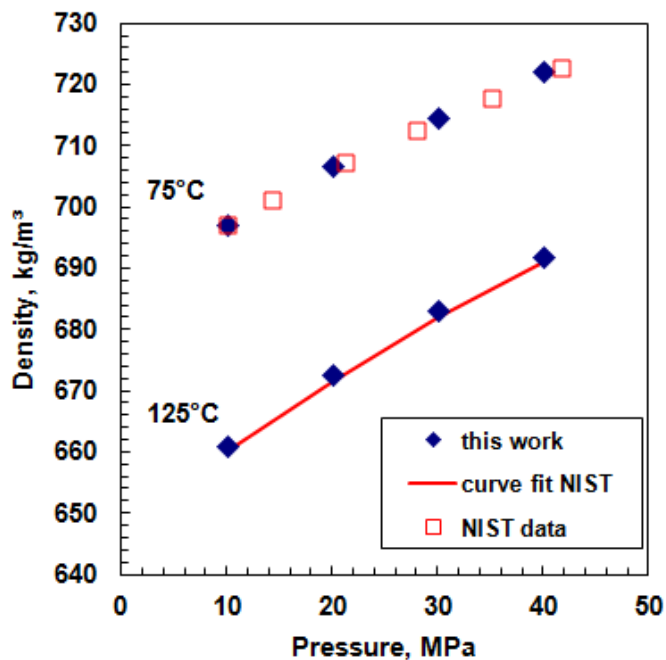


Figure 3–3. Comparison between experimental and literature data data for *n*-decane density.

3.4 Sample Preparation

Hydrocarbon Mixtures with Dissolved Gas

First, two transfer cylinders were prepared, each containing one of the solvents to be used in the experiment. The liquid solvent was poured into the first transfer vessel which was capped, and then vacuumed and pressurized to remove any air cap that may have been trapped. A second transfer vessel was connected to a bottle containing the gas to be dissolved in the liquid hydrocarbon, pressure tested, and purged. The gas was flowed into the transfer cylinder and then compressed to a liquid state, Figure 3-4.

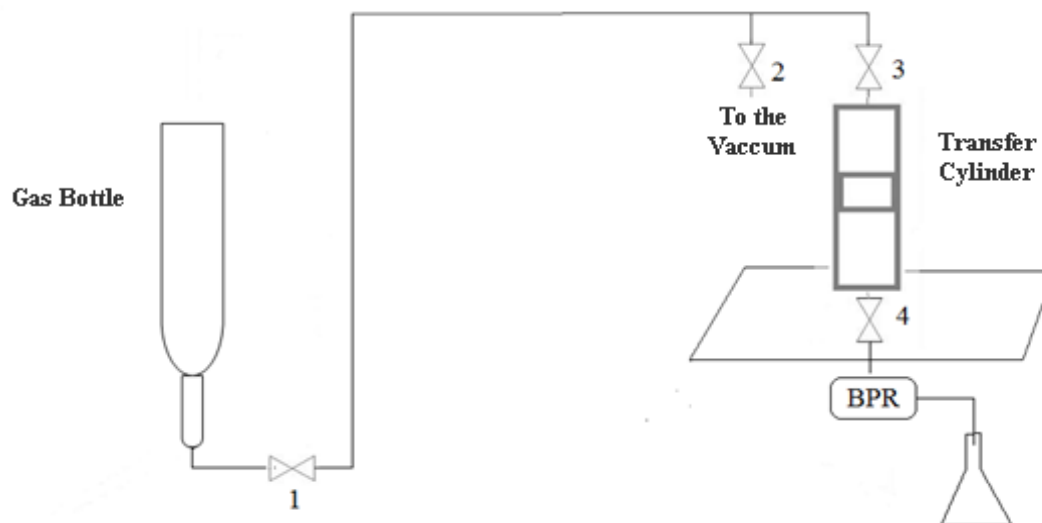


Figure 3–4. Charging the transfer cylinder for the compressed gas.

Next, the compressed gas was transferred into a third transfer cylinder (the sample cylinder). The transfer cylinder containing the compressed gas was connected to the sample cylinder which was pressure tested and purged. Then, the pump was used to displace a specified volume of compressed gas (in the liquid state) from the transfer cylinder to the sample cylinder, Figure 3-5. The compressed gas volume in the sample cylinder was determined from the pump displacement and verified from the volume of displaced hydraulic oil from the sample cylinder. The same procedure was used to transfer a specified volume of the liquid solvent to the sample cylinder. The mass of each solvent was determined from the volumes and densities of the components at the temperature and pressure of the displacements.

An important point regarding gas injection into the sample cylinder is the sample cylinder dead volume determination. While starting the compressed gas injection, for the first 3 to 3.5 cm³ of pump displacement no hydraulic oil transferred out. This volume is the sample cylinder dead volume which must be accounted for in

composition calculations. . The reported compositions are estimated to be accurate to within 0.30 wt% (see Appendix D for details).

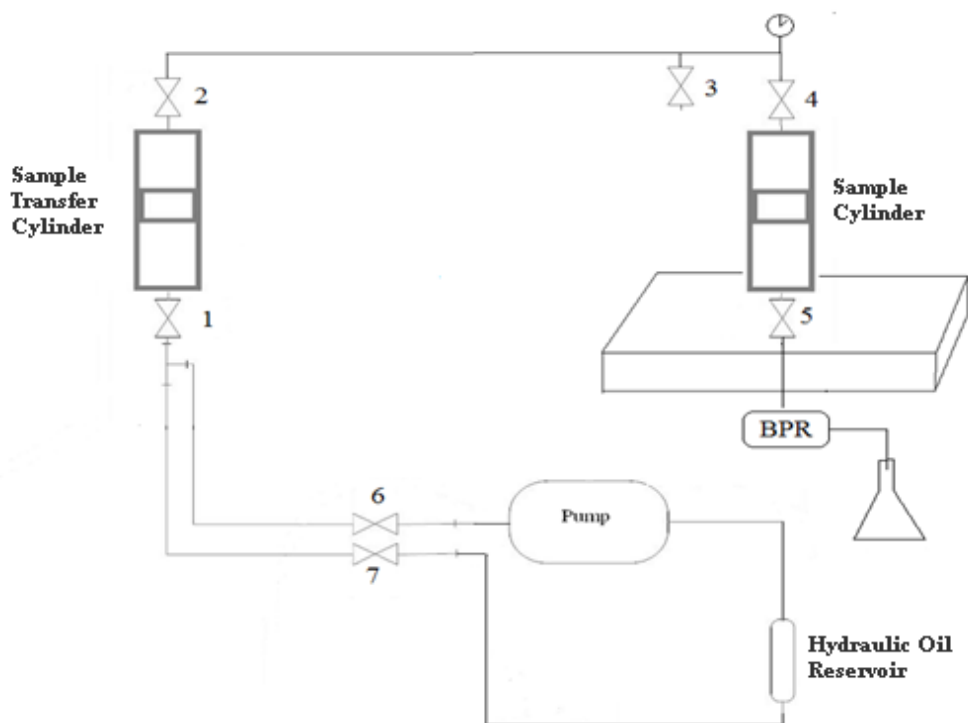


Figure 3–5. Charging from transfer cylinder to the sample cylinder.

Diluted Bitumens

Diluted bitumen samples were prepared using a contactor which consisted of a 600 cm³ horizontal 5 cm diameter cylinder equipped with a piston at each end and a perforated plate placed in the middle of the cylinder. Heating tape was used to control the temperature. Before each experiment, the contactor was cleaned and weighed. Compressed gas was displaced to the contactor as described previously. The contactor was reweighed to verify the mass of compressed gas in the sample vessel. The same procedure was used to inject the required volume of bitumen. The contactor was again weighed to determine the mass of bitumen. Then, the sample

was brought to 50°C and compressed to above its bubble point. The sample was displaced back and forth through the mixing plate in the contactor for approximately 8 hours per day. The pressure and volume were monitored overnight and the mixture was considered to be equilibrated when there was no longer any volume or pressure change, typically after one week of mixing. After the sample had equilibrated it was transferred to the transfer vessel used for the experiment. The reported compositions are estimated to be accurate to within 0.3 wt% (see Appendix D for details).

3.5 Experimental Procedure

The sample cylinder, containing the test fluid, was connected to the apparatus as shown in Figure 3-1. A second empty transfer cylinder was connected to the other end of the apparatus and the whole apparatus was pressure tested with compressed air to 40 MPa. The apparatus was depressurized and vacuumed. Then, the test fluid was displaced into the apparatus from the sample cylinder. Once the system was filled to a pressure greater than bubble pressure, the fluid was displaced back and forth through the apparatus from one vessel to the other one to obtain a uniform mixture. It usually took 4 passes through the equipment to create a uniform mixture where the density was uniform throughout the displacement.

To begin a density measurement, the air bath was set to the target temperature. When the temperature reading by Anton Paar temperature sensor was constant for one hour at the intended temperature, the pump was used to set the target pressure. Once the pressure was constant for 10 minutes, the oscillation period in the Anton Paar evaluation unit was recorded. Note: there was no flow through the density meter cell and therefore the fluid pressure inside the density meter was equal to the pump pressure. Then the conditions were set for the next measurement.

In this thesis, densities were measured at five temperatures from room temperature up to 175°C for each mixture and pure component for each mixture at 10, 20, 30,

and 40 MPa with a repeat measurement done at 50°C. The pure component density was compared with literature data available to verify the accuracy of the measurements, as noted previously. The pure component densities were repeatable to within ± 0.33 kg/m³, Appendix D based on a 90% confidence interval. Densities for diluted bitumens (six temperatures from room temperature up to 175°C and five pressures from atmospheric to 10 MPa) were measured by Hamed Motahhari as part of another project using the same procedures. These data are also used in this thesis. The diluted bitumen densities were repeatable to within ± 0.18 kg/m³, Appendix D.

3.6 Apparatus Clean-up

After taking the measurements for a sample fluid, the apparatus was cleaned before the next experiment. For the hydrocarbon mixtures, the apparatus was depressurized and the transfer vessels removed. The lines and density meter were flushed at room temperature with toluene, followed by acetone, and then dried. The transfer vessels were also washed with toluene and acetone, and then dried. For the diluted bitumens, the sample was displaced to one transfer vessel which was depressurized and emptied. The transfer vessel was filled with toluene, reconnected to the apparatus. The toluene was then displaced back and forth five times through the apparatus at room temperature over a time span of not less than half a day. The toluene wash was repeated approximately 5 times until the toluene was clear. A final wash was performed at 100°C for approximately one day including the time for heating and cooling.

CHAPTER FOUR: RESULT AND DISCUSSION

In this chapter, effective liquid densities are determined for *n*-alkanes and the regular solution and excess volume mixing rules are applied to diluted bitumens. First, the mixing rules are tested on density data for mixtures of pure liquid hydrocarbons. Then, the validity of the effective density correlation presented by Tharanivasan *et al.* (2011) is discussed and a modified correlation is presented. The new correlation is tested on density data for liquid hydrocarbon mixtures containing dissolved gas. Finally, the new correlation and the proposed mixing rules are tested on the density data collected for diluted bitumens.

4.1 Density of Mixtures of Liquid Hydrocarbons

Mixtures of liquid hydrocarbons were examined to test the excess volume based mixing rule that is the basis of the modeling in this thesis. Chevalier *et al.* (1990) presented a comprehensive dataset for the density of mixtures of liquid hydrocarbons including binary mixtures of *n*-alkane/*n*-alkane, *n*-alkane/branched, *n*-alkane/cyclic, *n*-alkane/aromatic, aromatic/cyclic, and aromatic/aromatic. Table 4-1 summarizes the systems for which density was measured. All the measurements were taken at 298.15 K and 101 kPa.

The densities of each binary system were fitted with an excess volume mixing rule of the following form:

$$\frac{1}{\rho_{mix}} = \frac{w_1}{\rho_1} + \frac{w_2}{\rho_2} - w_1 w_2 \left(\frac{1}{\rho_1} + \frac{1}{\rho_2} \right) \beta_{12} \quad \text{Equation 4-1}$$

where ρ_1 , ρ_2 , w_1 , and w_2 are the component densities and mass fractions, respectively, and β_{12} is the binary interaction coefficient between the two components. The last term in the equation is the excess volume. When β_{12} is zero,

the excess volume is zero and the binary pair forms a regular solution. The values of β_{12} used to fit the Chevalier *et al.* dataset are provided in Table 4-2.

Table 4-1. Pure hydrocarbon mixtures for which density was measured by Chevalier *et al.*(1990).

Binary Mixture Density		
alkane-alkane		
n-hexane + n-heptane	n-heptane + n-octane	n-octane + n-nonane
n-hexane + n-octane	n-heptane + n-nonane	n-octane + n-decane
n-hexane + n-nonane	n-heptane + n-decane	n-octane + n-dodecane
n-hexane + n-decane	n-heptane + n-dodecane	n-octane + n-tetradecane
n-hexane + n-dodecane	n-heptane + n-tetradecane	n-octane + n-hexadecane
n-hexane + n-tetradecane	n-heptane + n-hexadecane	
n-hexane + n-hexadecane		
n-nonane + n-decane	n-decane + n-dodecane	n-dodecane + n-tetradecane
n-nonane + n-dodecane	n-decane + n-tetradecane	n-dodecane + n-hexadecane
n-nonane + n-tetradecane	n-decane + n-hexadecane	
n-nonane + n-hexadecane		
n-tetradecane + n-hexadecane		
alkane-branched		
3-methylpentane + n-decane	2,3-dimethylpentane + n-tetradecane	isooctane + n-hexane
3-methylpentane + n-hexadecane	2,5-dimethylhexane + n-hexadecane	isooctane + n-decane
2-methylpentane + n-hexadecane	2,2-dimethylpentane + n-decane	isooctane + n-tetradecane
2-methylhexane + n-tetradecane	2,2-dimethylpentane + n-hexadecane	
	2,2-dimethylhexane + n-decane	
	2,2-dimethylhexane + n-hexadecane	
alkane + cyclic		
cyclohexane + n-hexadecane	methylcyclohexane + n-hexane	1,2-dimethylcyclohexane + n-hexane
	methylcyclohexane + n-decane	1,2,4-trimethylcyclohexane + n-hexane
	methylcyclohexane + n-hexadecane	
<i>cis</i> -1,2-dimethylcyclohexane + n-hexane		
<i>cis</i> -1,2-dimethylcyclohexane + n-hexadecane		
alkane + aromatic		
n-decane + toluene	n-hexane + o-xylene	n-hexane + p-xylene
n-tetradecane + toluene	n-decane + o-xylene	n-decane + p-xylene
	n-tetradecane + o-xylene	n-tetradecane + p-xylene
n-decane + benzene		
aromatic-aromatic		
benzene + o-xylene	benzene + p-xylene	o-xylene + p-xylene
toluene + o-xylene	toluene + p-xylene	
aromatic-cyclic		
benzene + cyclohexane	toluene + methylcyclohexane	o-xylene + cyclohexane
benzene + 1,2-dimethylcyclohexane		o-xylene + 1,2-dimethylcyclohexane

Table 4-2. β_{ij} values for different types of pure hydrocarbon mixtures

Mixture	β_{ij}	Mixture	β_{ij}
<i>n</i>-alkane + <i>n</i>-alkane		<i>n</i>-alkane + aromatic	
hexane + heptanes	0.0006	decane + benzene	-0.0150
hexane + octane	0.0014	hexane + o-xylene	0.0073
hexane + decane	0.0042	decane + o-xylene	-0.0019
hexane + dodecane	0.0024	tetradecane + o-xylene	-0.0034
hexane + tetradecane	0.0060	decane + toluene	-0.0061
hexane + hexadecane	0.0057	tetradecane + toluene	-0.0070
<i>n</i>-alkane + branched		<i>n</i>-alkane + cyclic	
hexane + isooctane	0.0009	hexadecane + cyclohexane	-0.0085
decane + isooctane	0.0025	hexane + methylcyclohexane	0.0030
tetradecane + isooctane	0.0046	decane + methylcyclohexane	-0.0017
decane + 3methylpentane	0.0037	hexadecane+ methylcyclohexane	-0.0021
hexadecane + 3methylpentane	0.0080	aromatic + branched	
tetradecane + 2methylhexane	0.0044	benzene + o-xylene	-0.0052
decane + 2,2dimethylpentane	0.0031	benzene + p-xylene	-0.0041
hexadecane + 2,2dimethylpentane	0.0069	toluene + o-xylene	-0.0009
decane + 2,2dimethylhexane	0.0008	toluene + p-xylene	-0.0002
hexadecane + 2,2dimethylhexane	0.0030	o-xylene + p-xylene	0.0003
cyclic + aromatic			
cyclohexane + benzene	-0.0131		
cyclohexane + o-xylene	-0.0103		
methylcyclohexane + toluene	-0.0067		

Not surprisingly, components of similar size in the same chemical family form nearly regular solutions. For example, the mixture of *n*-hexane and *n*-heptane can be fitted with a regular solution mixing rule ($\beta_{12} = \text{zero}$) with an absolute average deviation of only 0.01%, Figure 4-1. As the size difference between the molecules increases, the excess volume also increases. For example, a β_{12} of +0.0057 is required to fit the densities of mixtures of *n*-hexane and *n*-hexadecane, Figure 4-2. Mixtures of molecules of different chemical families also tend to have non-zero excess volumes. Figure 4-3 shows that, although the density of cyclohexane and *n*-hexadecane are similar, their mixtures do not form regular solutions and a β_{12} of -0.0085 is required to fit the data.

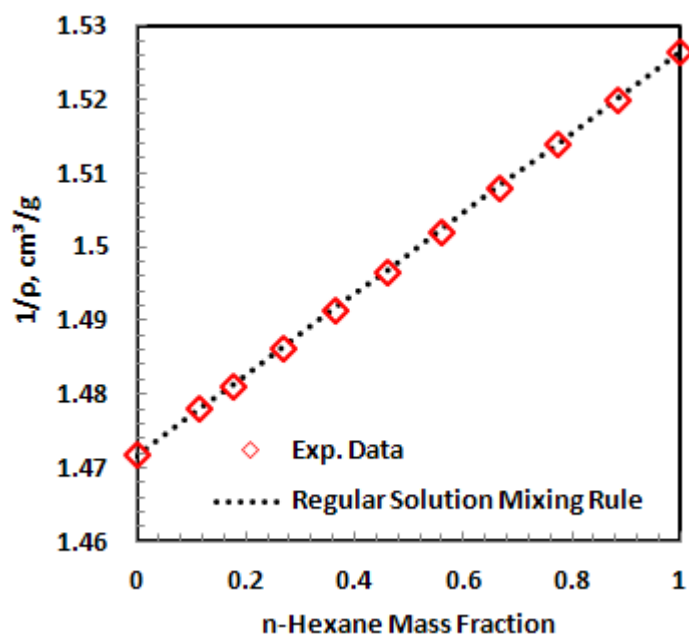


Figure 4–1. Measured and fitted density of mixtures of *n*-hexane + *n*-heptane (data adapted from Chevalier, *et al.*, (1990)).

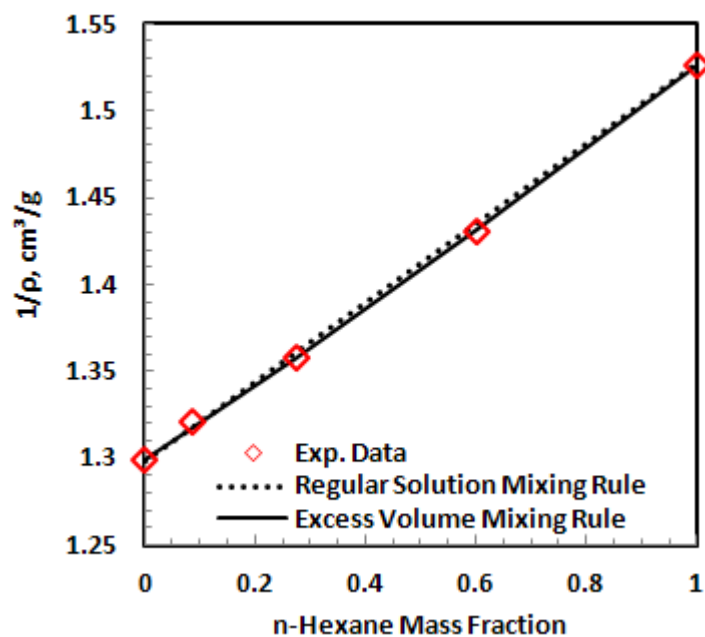


Figure 4–2. Measured and fitted density of mixtures of *n*-hexane + *n*-hexadecane (data adapted from Chevalier, *et al.*, (1990)).

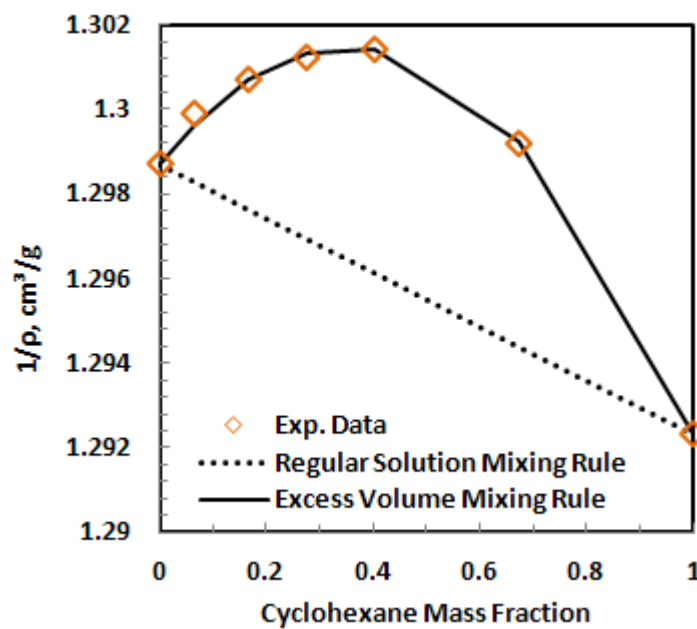


Figure 4–3. Measured and fitted density of mixtures of cyclohexane + *n*-hexadecane (data adapted from Chevalier, *et al.*, (1990)).

Figure 4-5 shows that a better correlation is observed when β_{12} values are plotted versus the normalized specific volume difference of the two components which is defined as:

$$\Delta v_N = \frac{2|v_1 - v_2|}{v_1 + v_2} \quad \text{Equation 4-3}$$

where v is the specific volume (the inverse of mass density). In this case, the β_{12} of mixtures of components from the same chemical family all increase linearly on the same trend line with increasing normalized specific volume difference. Interestingly, the β_{12} of mixtures of components from different chemical families all appear to group on another positive trend line. There is some scatter, particularly at lower values of normalized specific volume difference and therefore it is not clear how well the trends will extrapolate to diluted bitumen systems.

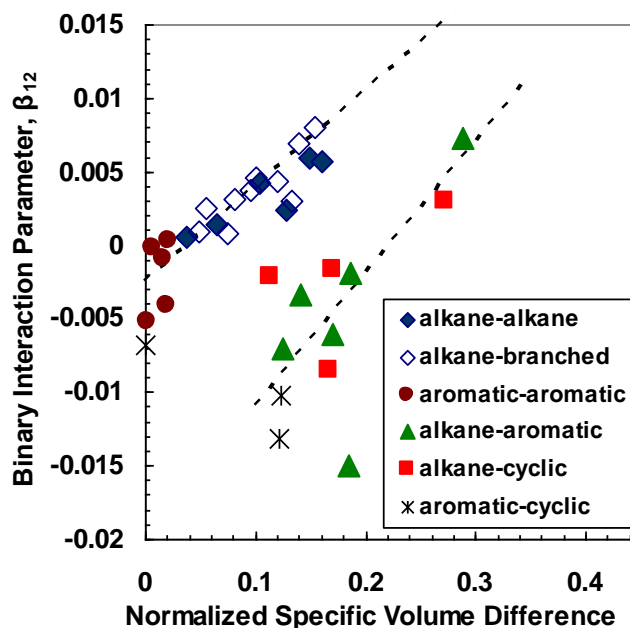


Figure 4–5. The relationship between binary interaction parameters in the excess volume mixing rule and the normalized specific volume difference.

4.2 Density of Mixtures with Gas Dissolved in a Hydrocarbon Liquid

It is proposed to calculate the density for mixtures containing a dissolved gas component using the same mixing rule as applied to liquid mixtures but with an effective liquid density for the gas. Tharanivasan *et al.* (2011) determined effective densities for *n*-alkanes at pressures above 10 MPa. They extrapolated the molar volumes of liquid *n*-alkanes plotted versus molecular weight to determine hypothetical or “effective” liquid molar volumes of lower *n*-alkanes that were gases in their pure state. The molar volume data were fitted with a quadratic equation at fixed temperatures and pressures, Figure 4-6.

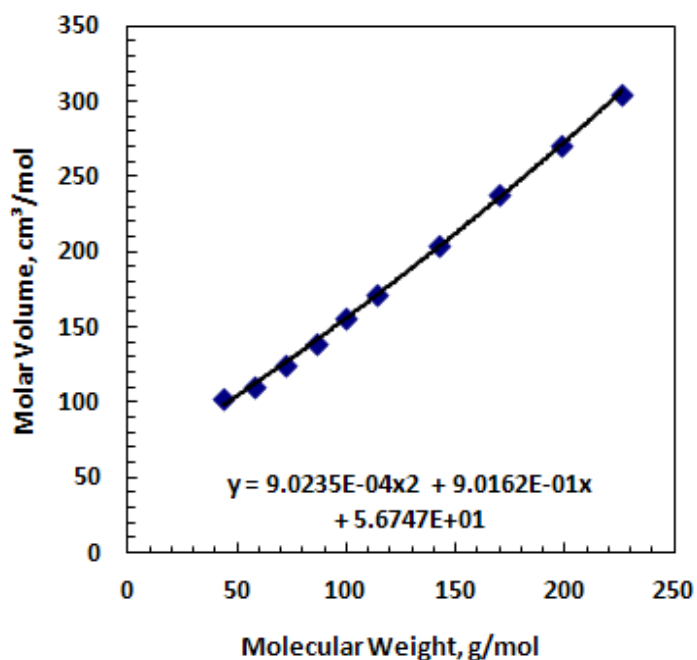


Figure 4–6. *n*-Alkane molar volumes versus molecular weight at 80°C and 10 MPa.

The effective molar volumes were converted to effective liquid densities ($\rho = MW/v$) and then plotted versus pressure at each fixed temperature, Figure 4-7. The hypothetical data for each component were fitted with an exponential function of temperature and pressure. Tharanivasan *et al.* (2011) used the effective densities to predict the density of a live conventional oil within experimental error. However,

there are two issues with Tharanivasan *et al.* correlation. First, the correlation underestimates densities at pressures lower than 10 MPa, Figure 4-7. Second, the correlation has not been rigorously tested on mixtures of hydrocarbons with dissolved gases.

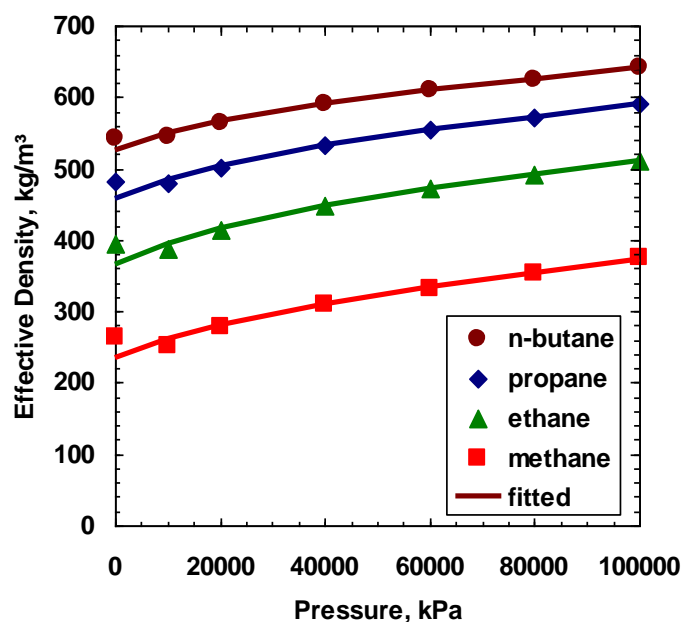


Figure 4–7. Effective liquid density of lower *n*-alkanes at 80°C and different pressures from Tharanivasan *et al.*, 2011.

The Tharanivasan *et al.* correlation was tested on the density of mixtures of methane and *n*-decane (NIST standard reference database, version 2008). As will be discussed later, these mixtures are nearly regular solutions. The effective liquid density for methane was calculated from the regular solution mixing rule and compared with the value predicted from Tharanivasan *et al.* (2011). Figure 4-8 shows that the back-calculated methane density falls below the extrapolated curve.

Examining Figure 4-8, it appears that the molar volumes of the lightest liquid n -alkanes are skewed to higher values because these n -alkanes are approaching their critical points. When the molar volumes of only the higher n -alkanes are considered, Figure 4-9, the molar volume trend is linear and extrapolates almost exactly to the experimentally derived effective density of methane. Therefore, the correlation was redeveloped using on the molar volumes of the higher liquid n -alkanes whose molar volumes were linearly related to their molecular weight.

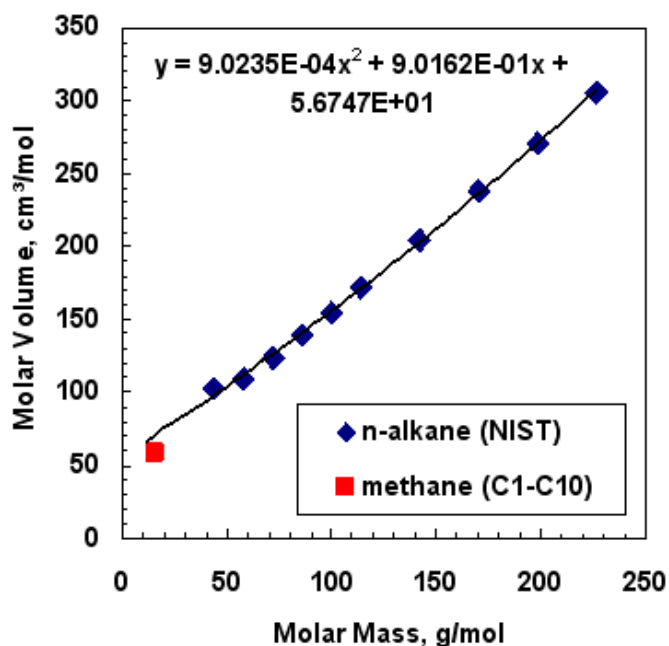


Figure 4–8. Comparison of extrapolated n -alkane molar volumes from Tharanivasan *et al.* (2011) with experimentally derived molar volume of methane at 80°C and 10 MPa.

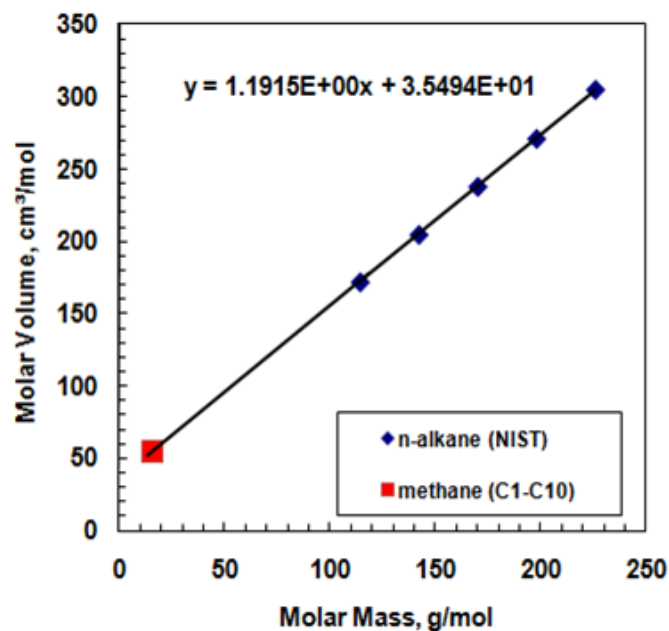


Figure 4–9. Comparison of extrapolated *n*-alkane molar volumes using only higher *n*-alkanes with experimentally derived molar volume of methane at 80°C and 10 MPa.

4.2.1 New Effective Density Correlation for Light *n*-Alkanes

To develop the new effective density correlation, the higher *n*-alkane molar volumes at fixed temperatures and pressures were extrapolated linearly to determine new effective molar volumes for the lighter *n*-alkanes. The effective molar volumes were converted to density and plotted versus pressure at fixed temperatures, Figure 4-10. The effective densities all followed linear trends versus pressure and were fitted as follows:

$$\rho = A + BP \quad \text{Equation 4-4}$$

where *A* and *B* are temperature dependent constants, defined as follows:

$$A = a_1 + a_2T \quad \text{Equation 4-5}$$

$$B = b_1 + b_2T \quad \text{Equation 4-6}$$

where a_1 , a_2 , b_1 , and b_2 are fitting parameters. The values for the parameters are provided in Table 4-3. The linear effective density equations are recommended for n -heptane and lower carbon number hydrocarbons. For n -alkanes higher than n -heptane, the Tharanivasan *et al.* (2011) correlation based on measured densities, Equation 2-67, is recommended. Note, the new correlation now matches the effective densities at all pressures including below 10 MPa. Also, all of the proposed correlations are only valid in the liquid region and will be inaccurate near the critical point.

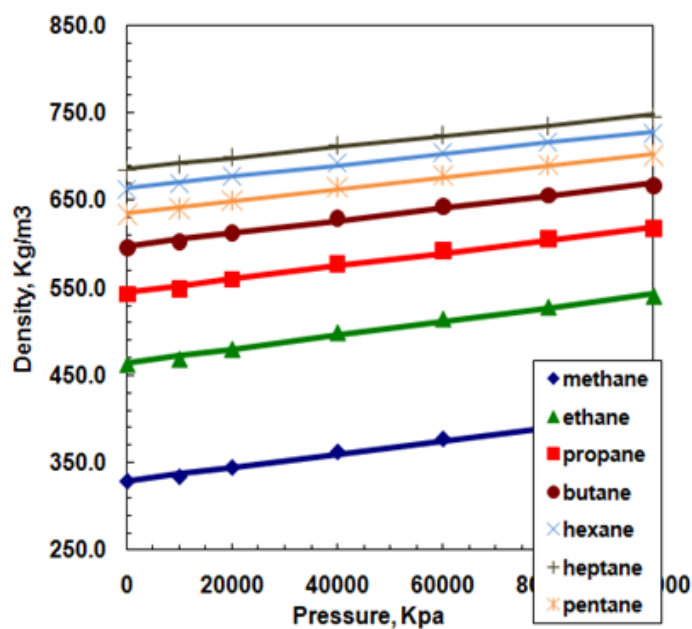


Figure 4–10. New effective density of lower n -alkane series at 80°C and different pressures.

Table 4-3. The fitting parameters of the new effective density correlation.

Component	a₁	a₂	b₁	b₂
	kg/m³	kg/m³K	kPa⁻¹	kPa⁻¹.K⁻¹
Methane	532.157	-0.69737	0.0004261	1.1426E-06
Ethane	704.9	-0.82749	0.0002144	2.0115E-06
propane	793.847	-0.85489	5.309E-05	2.4404E-06
<i>n</i> -butane	846.443	-0.85024	-5.45E-05	2.6479E-06
<i>n</i> -pentane	878.006	-0.82817	-9.23E-05	2.6481E-06
<i>n</i> -hexane	901.512	-0.80985	-0.000142	2.6846E-06
<i>n</i> -heptane	918.603	-0.791551	-0.000177	2.6919E-06

4.2.2 Validation of New Effective Density Correlation

The new correlation was validated against density data collected for three types of hydrocarbon mixtures: *n*-alkane/*n*-alkane, *n*-alkane/aromatic, and *n*-alkane/cyclic. Table 4-4 summarizes the mixtures, composition, and conditions for which density data were obtained. The data for methane/*n*-decane and methane/toluene were obtained from the NIST database (NIST standard reference database, version 2008) and the data for methane/*n*-tetradecane, methane/*n*-octadecane, ethane/*n*-tetradecane, and ethane/*n*-octadecane are obtained from Nourizadeh *et al.*, (2012) and Kariznovi *et al.*, (2012) work, respectively. The rest of the data were measured in this work and are tabulated in Appendix A.

The mixtures of propane and *n*-decane are presented as an example to illustrate the performance of the new correlation. The densities of these mixtures are shown at different temperatures and pressures at compositions of 6, 12.5, and 25 wt% in Figures 4-11 to 4-13, respectively. The mixture densities were predicted using the regular solution mixing rule and the effective densities from the new correlation (dashed lines on all figures). The predicted densities are generally within 1% of the

measured values except at conditions where the mixture is approaching its critical point; that is, at high temperature, low pressure, and high dissolved gas content. The good agreement with the data indicates that mixtures of propane and *n*-decane do form regular or nearly regular solutions and that the effective densities are accurate at least for mixtures of *n*-alkanes. However, it is necessary to develop a criterion related to the proximity to the critical point to identify where the correlation breaks down.

Table 4-4. Summary of the pure hydrocarbon mixtures and their composition, and temperature and pressure range for which density data collected.

Mixture	Composition (wt%)	Temperature Range (°C)	Pressure Range (MPa)	Source
methane/ <i>n</i> -decane	4.6, 10.1, 20.8 4.9, 9.7, 14.5, 26, 71.8	38 – 171 20 – 100	Up to 70 Up to 140	Lee <i>et al.</i> , (1966) Canet <i>et al.</i> , (2002)
methane/ <i>n</i> -tetradecane	0.7 – 4.4	22 – 175	Saturation Pressure	Nourizadeh <i>et al.</i> , (2012)
methane/ <i>n</i> -octadecane	0.5 – 3.4	50 – 175	Saturation Pressure	Kariznovi <i>et al.</i> , (2012)
ethane/ <i>n</i> -tetradecane	1.7 – 52	50 – 150	Saturation Pressure	Kariznovi <i>et al.</i> , (2012)
ethane/ <i>n</i> -octadecane	1.2 – 39	50 – 150	Saturation Pressure	Nourizadeh <i>et al.</i> , (2012)
ethane/ <i>n</i> -decane	6, 12.5	20 – 175	10 – 40	this work
propane/ <i>n</i> -decane	6, 12.5, 25	20 – 175	10 – 40	this work
<i>n</i> -butane/ <i>n</i> -decane	6, 12.5, 25	20 – 175	10 – 40	this work
methane/toluene	5.5, 9.3, 14.8, 23.7, 76.8	20 – 100	Up to 140	Baylaucq <i>et al.</i> , (2003)
propane/ toluene	6, 12.5, 25	20 – 175	10 – 40	this work
propane/cyclooctane	6, 12.5, 25	20 – 175	10 – 40	this work

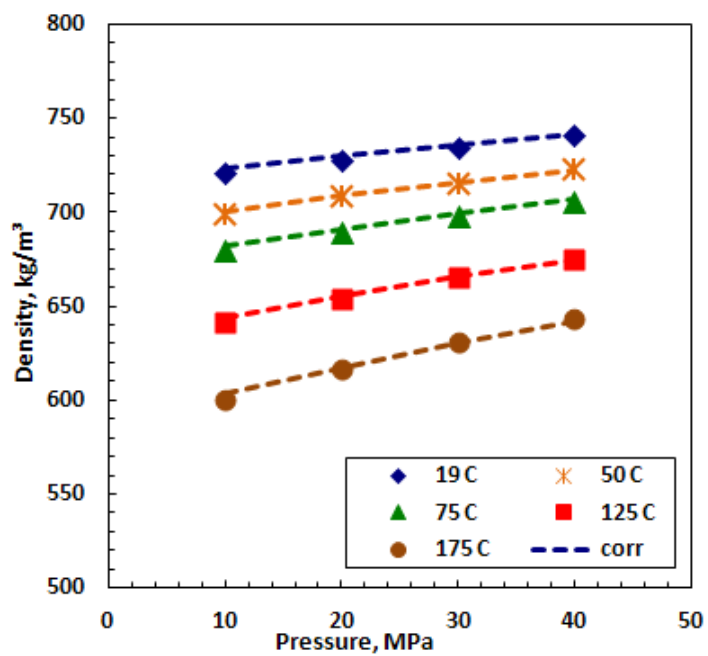


Figure 4–11. Measured and predicted densities for mixtures of 6 wt% propane and 94 wt% *n*-decane.

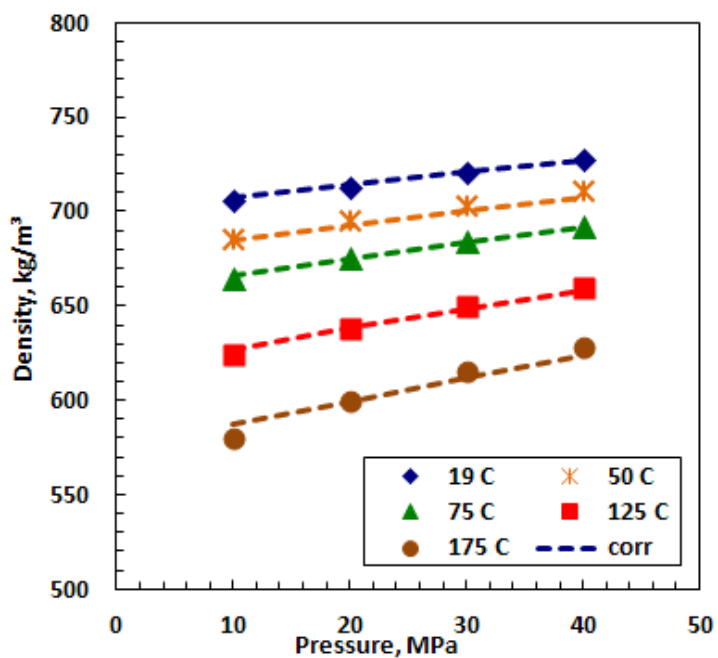


Figure 4–12. Measured and predicted densities for mixtures of 12.5 wt% propane and 87.5 wt% *n*-decane.

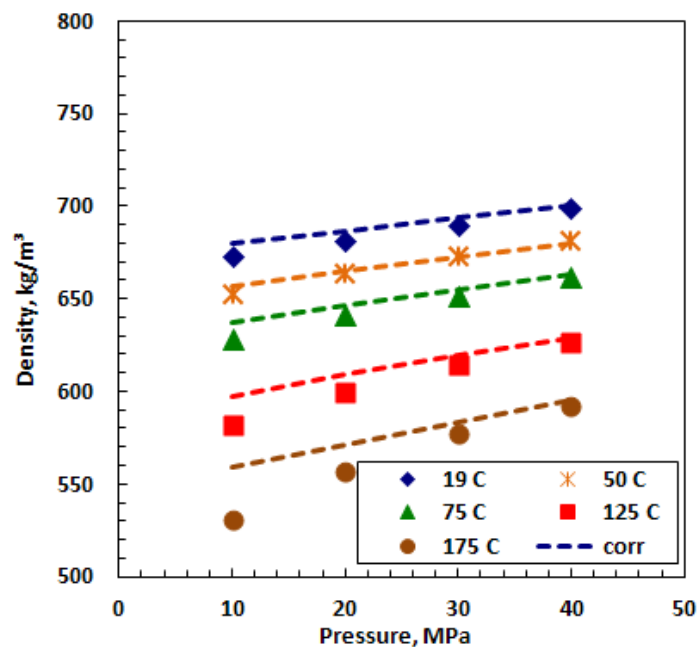


Figure 4–13. Measured and predicted densities for mixtures of 25 wt% propane and 75 wt% *n*-decane.

To develop a criterion to define the range of validity of the correlation, the limiting pressure and temperature were identified at which the error in the calculated mixture density exceeded 1%. The critical point of the mixture was determined using the Advanced Peng Robinson Equation of State in VMGSimTM software (Virtual Material Group Ltd.) with the default interaction parameters. The limiting temperature and pressure were converted to reduced coordinates and then the reduced limiting temperatures and pressures for all the binary mixtures measured in this work were plotted, Figure 4-14. Each symbol represents the boundary between accuracy less than 1% (to the right) or better than 1% (to the left). Most of the boundary points cluster along a line and therefore the following criterion was defined for the valid range of the correlation:

$$T_r < 0.52 + 0.021P_r$$

Equation 4-7

Only the data for 12.5 wt% ethane in *n*-decane violated the criterion. Possible explanations are: a composition error in the data, the criterion does not apply to more extreme differences in component properties, the critical point of the mixture is calculated incorrectly, or excess volumes must be accounted for. Note that the critical temperatures of diluted bitumens are expected to be high except at very high dilutions and therefore the effective density correlation is expected to be valid for all conditions of interest to this work.

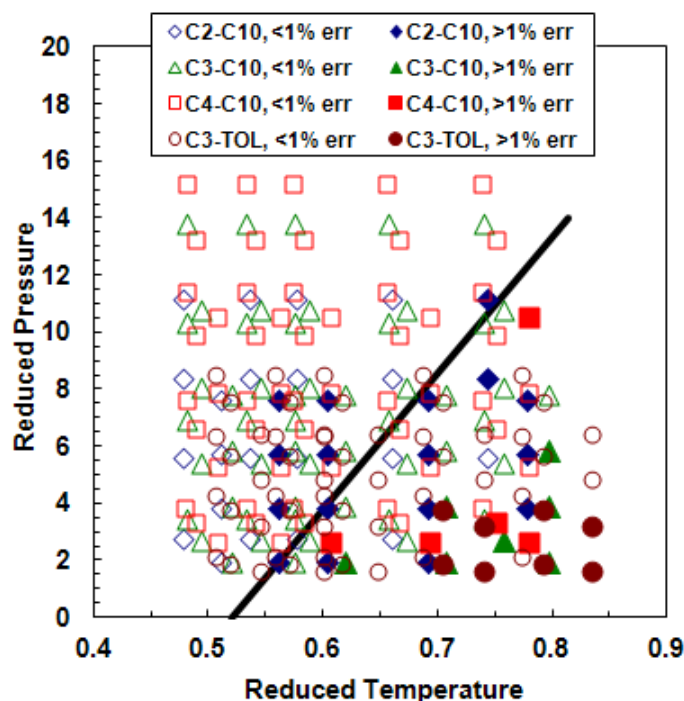


Figure 4–14. Reduced temperature and pressure at which the effective density correlation gives more than 1% error in mixture densities (to right of each point).

The criterion, Equation 4-7, was used to screen the data listed in Table 4-4. The accuracy of the correlation was then assessed against all of the screened data. Dispersion plots of the predicted density versus measured density for mixtures of butane/*n*-decane, propane/*n*-decane, ethane/*n*-decane, ethane/*n*-tetradecane, ethane/*n*-octadecane, methane/*n*-decane, methane/*n*-tetradecane, and methane/*n*-

octadecane are shown in Figures 4-15 to 4-22, respectively. The average absolute deviation (AAD), average absolute relative deviation (AARD), maximum absolute deviation (MAD), and maximum absolute relative deviation (MARD) for each case are summarized in Table 4-5. The predicted densities are generally in very good agreement with data with the highest deviations occurring when the fluid approaches the critical region and reaches the boundary where the correlation is no longer valid. There is no clear evidence of a systematic deviation at higher solvent contents that would be expected if there were excess volumes of mixing. There is some scatter in the ethane/*n*-decane and methane/*n*-decane mixture data which could obscure the excess mixing volumes. Nonetheless, based on the data available, it is concluded that these mixtures of *n*-alkanes form regular or nearly regular solutions.

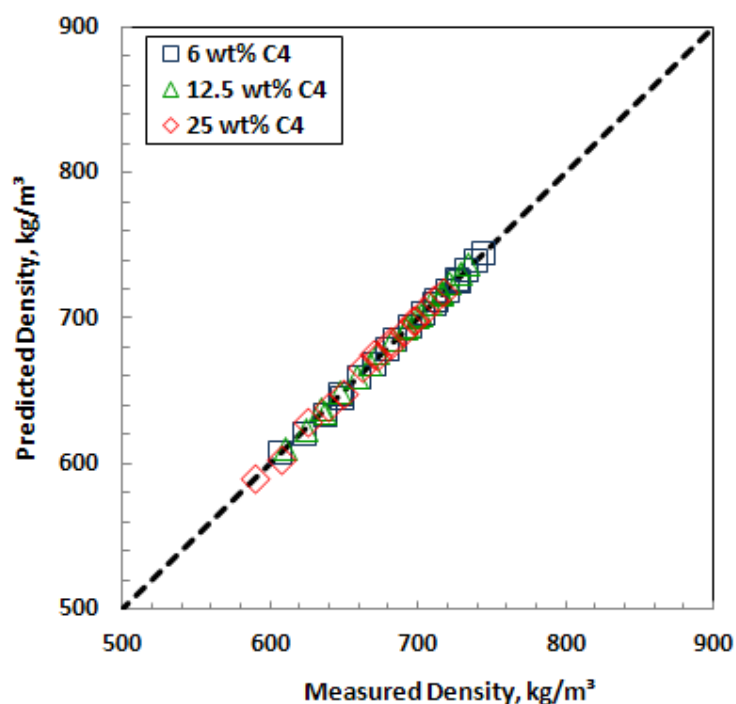


Figure 4–15. Predicted versus measured density for mixtures of *n*-butane and *n*-decane.

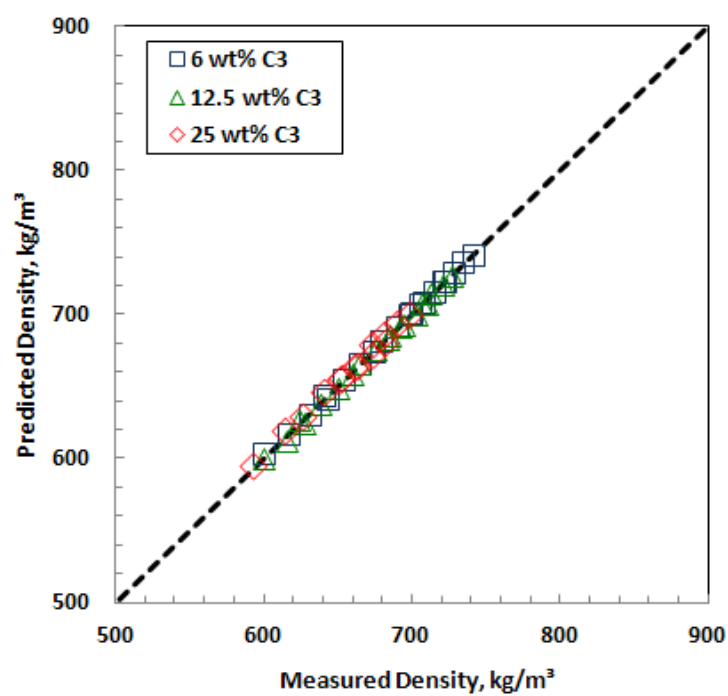


Figure 4–16. Predicted versus measured density for mixtures of propane and *n*-decane.

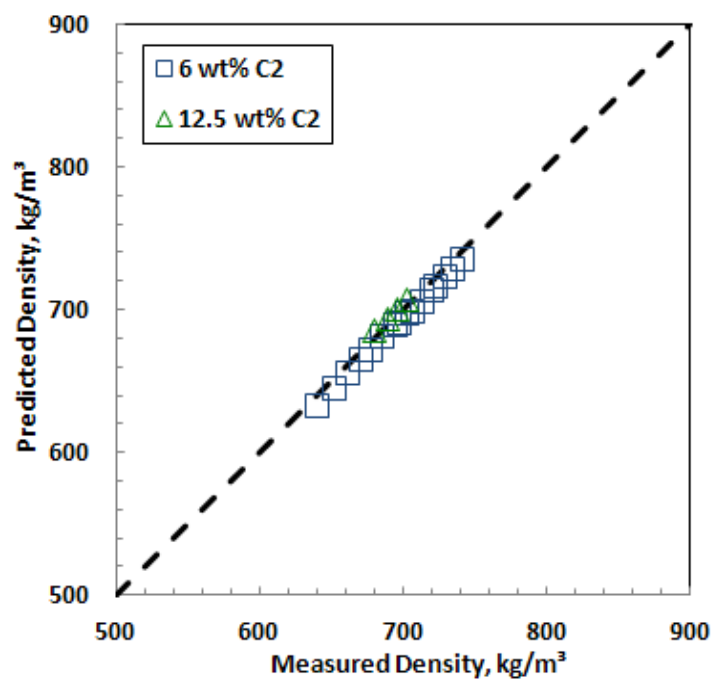


Figure 4–17. Predicted versus measured density for mixtures of ethane and *n*-decane.

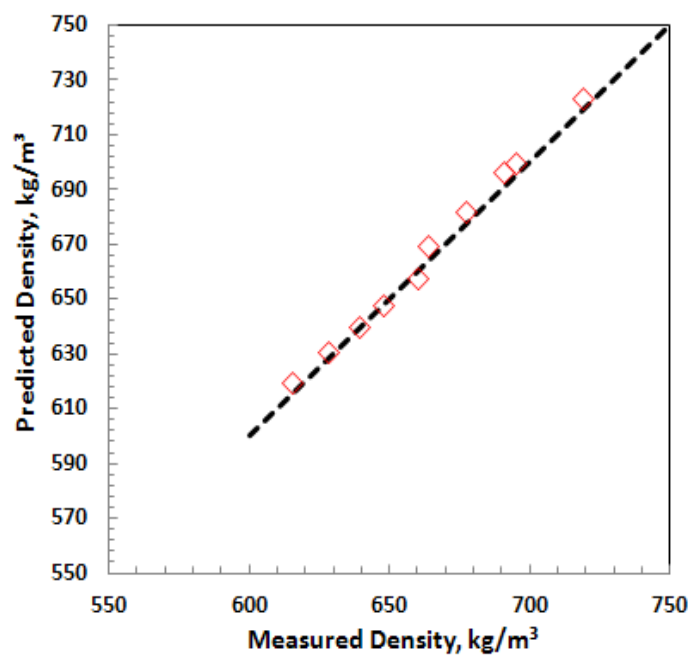


Figure 4–18. Predicted versus measured density for mixtures of ethane and *n*-tetradecane (Kariznovi *et al.*, 2012).

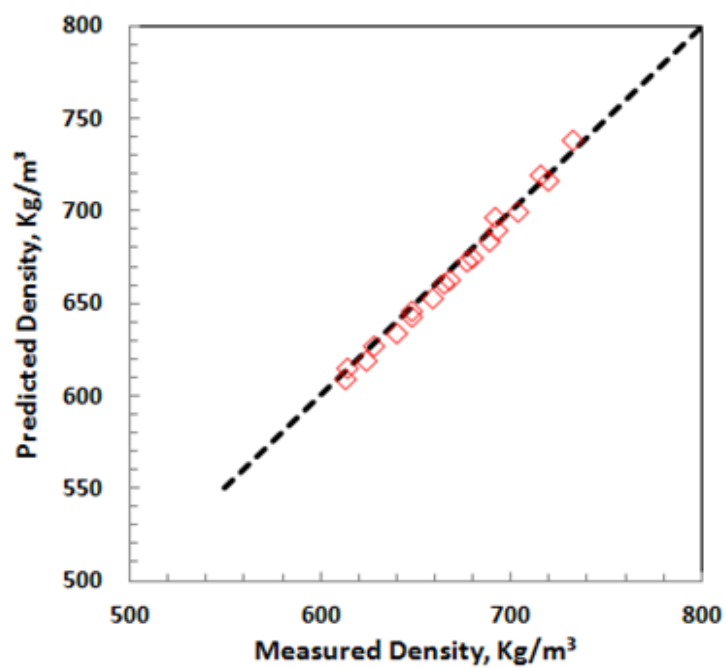


Figure 4–19. Predicted versus measured density for mixtures of ethane and *n*-octadecane (Nourizadeh *et al.*, 2012)

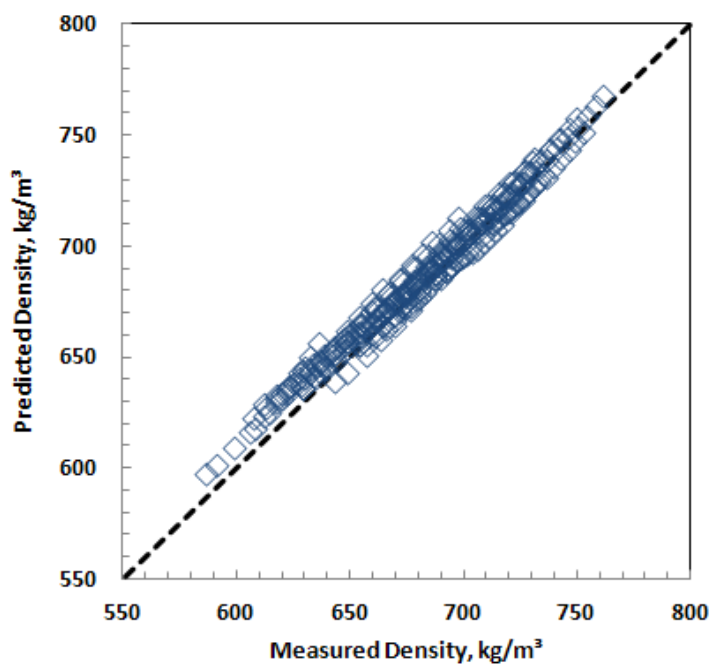


Figure 4–20. Predicted versus measured density for mixtures of methane and *n*-decane (data from NIST database, 2008).

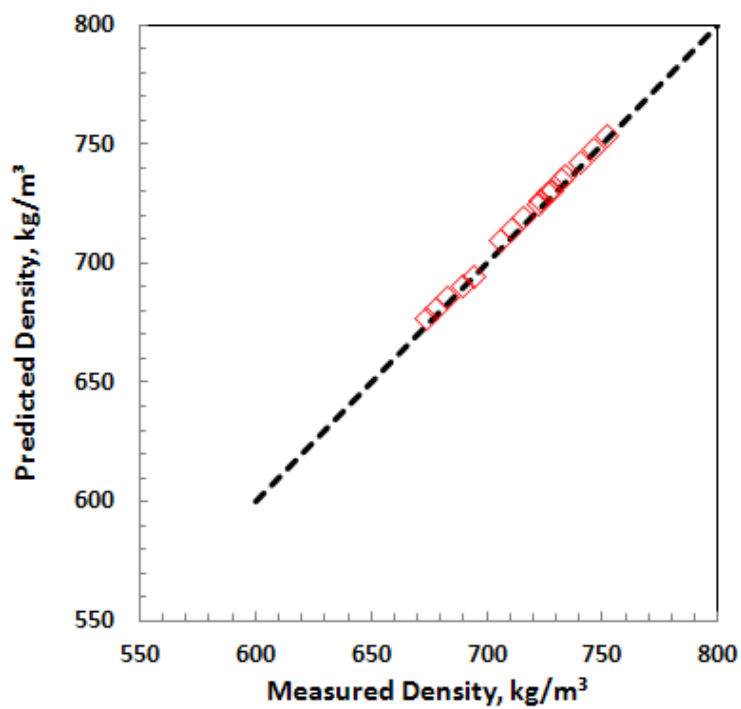


Figure 4–21. Predicted versus measured density for mixtures of methane and *n*-tetradecane (Nourizadeh *et al.*, 2012)

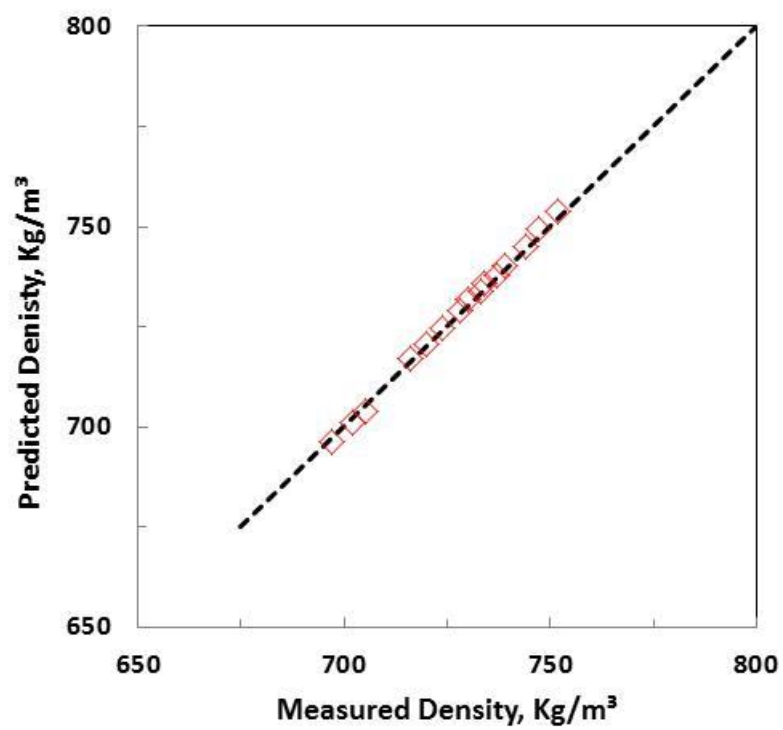


Figure 4–22. Predicted versus measured density for mixtures of methane and *n*-octadecane (Kariznovi *et al.*, 2012)

Table 4-5. AAD, AARD, MAD, and MARD of pure hydrocarbon mixtures.

Mixture	AAD (kg/m³)	AARD (%)	MAD (kg/m³)	MARD (%)
<i>n</i> -butane / <i>n</i> -decane	1.8	0.26	6.5	0.97
propane / <i>n</i> -decane	2.0	0.30	6.5	0.97
ethane / <i>n</i> -decane	5.4	0.75	8.3	0.96
ethane / <i>n</i> -tetradecane	3.5	0.53	7.5	1.15
ethane/ <i>n</i> -octadecane	3.8	0.57	6.3	0.95
methane / <i>n</i> -decane	6.2	0.93	19.5	3.06
methane / <i>n</i> -tetradecane	2.8	0.40	4.1	0.57
methane / <i>n</i> -octadecane	3.5	0.50	6.8	0.95
propane / toluene	2.5	0.33	6.9	0.99
propane / cyclooctane	2.4	0.32	7.1	0.95
methane / toluene	3.5	0.47	14.9	2.90

Dispersion plots for the densities of mixtures of propane/toluene, propane/cyclooctane, and methane/toluene are also shown in Figures 4-23 to 4-25, respectively. The AD, ARD, MAD, and MARD for the predicted densities of these mixtures are provided in Table 4-5. The results are similar to those obtained for mixtures of *n*-alkanes. Hence, the effective densities appear to be valid for any hydrocarbon mixtures. Again, there is little evidence of excess mixing volumes except perhaps for the mixtures of methane and toluene, Figure 4-25. Table 4-6 compares the effective density values for methane, ethane, propane, and *n*-butane with API density values (API, 1992).

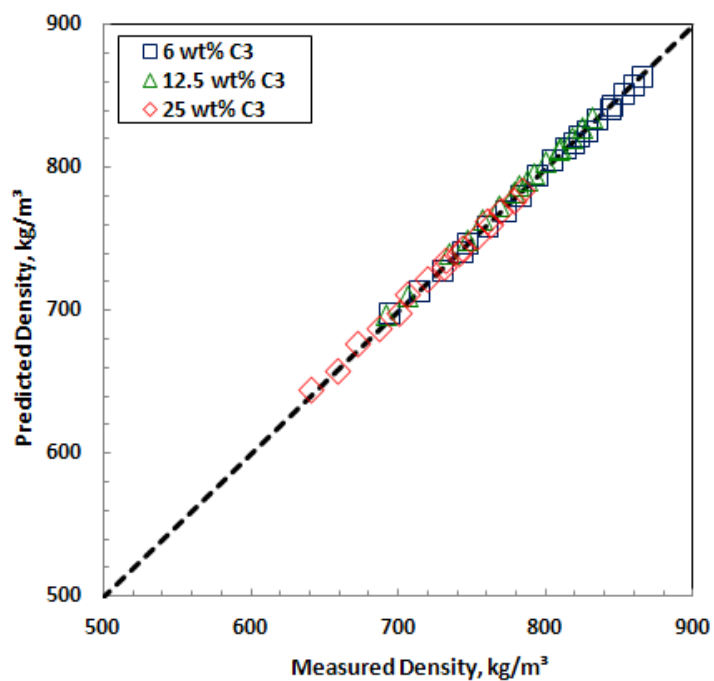


Figure 4–23. Predicted versus measured density for mixtures of propane and toluene.

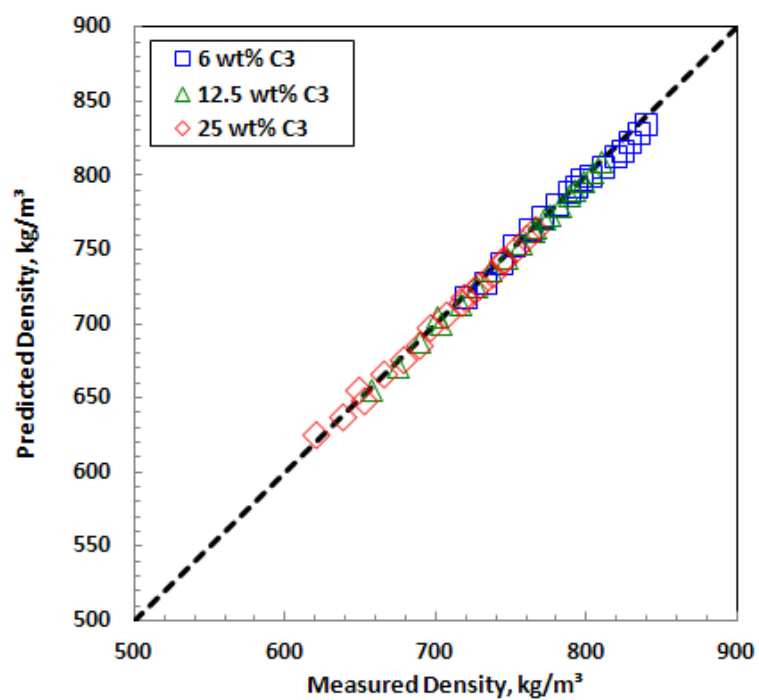


Figure 4–24. Predicted versus measured density for mixtures of propane and cyclooctane.

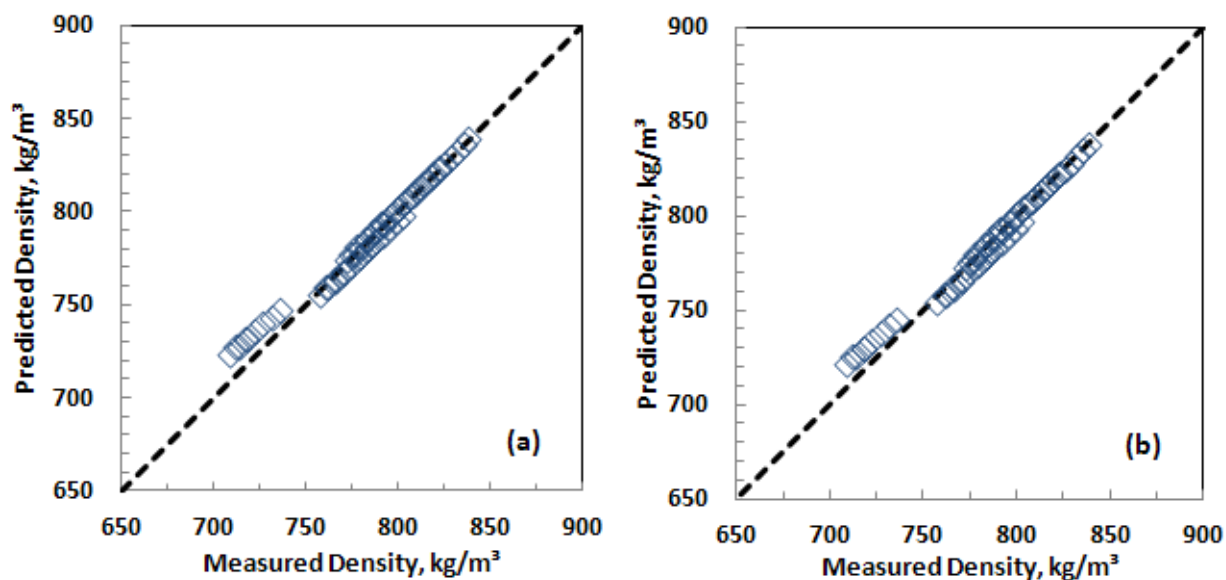


Figure 4–25. Predicted versus measured density for mixtures of methane (C_1) and toluene: a) regular solution mixing rule; b) excess volume mixing rule with $\beta_{ij} = -0.006$.

Table 4-6. Comparison between the effective liquid density of dissolved gas components with their API liquid density value at standard condition.

Compound	Liquid density @ 60 F and 1 atm (kg/m^3)	Effective density @ 60 F and 1 atm (kg/m^3)	ARD (%)
methane	299.7	330.5	10
ethane	355.9	465.7	31
propane	506.5	546.7	7.9
<i>n</i> -butane	583.4	600.6	3.0

4.3 Bitumen Density Correlation

Before considering the density of diluted bitumens, it is necessary to determine the density of the bitumens themselves. The measured densities are shown for Bitumens A and B in Figure 4-26 and 4-27, respectively, and are tabulated in Appendix B. In order to calculate mixture densities at conditions in between the measured bitumen values, the bitumen density data were correlated as follows:

$$\rho = \rho_0 \exp(c_0(P - 0.1)) \quad \text{Equation 4-8}$$

where P is the pressure in MPa, ρ_0 is the density at atmospheric pressure, and c_0 is the oil compressibility. The atmospheric density and oil compressibility were related to temperature as follows:

$$\rho_0 = A_B + B_B T \quad \text{Equation 4-9}$$

$$c_0 = C_B * \exp(D_B T) \quad \text{Equation 4-10}$$

where T is the temperature, and A_B , B_B , C_B , and D_B are fitting parameters. The fitted parameters for Bitumens A and B are provided in Table 4-7. The correlations fit the density data with an AAD of 0.32 for Bitumen A and 0.26 for Bitumen B and an AARD of 0.03% for both bitumen A and B (solid lines in Figures 4-26 and 4-27). The density of Bitumen B was approximately 2 kg/m³ greater than that of Bitumen A at any given temperature and pressure. The small difference in density may arise from small differences in the amount of light ends in each sample after their treatment to remove water and solids.

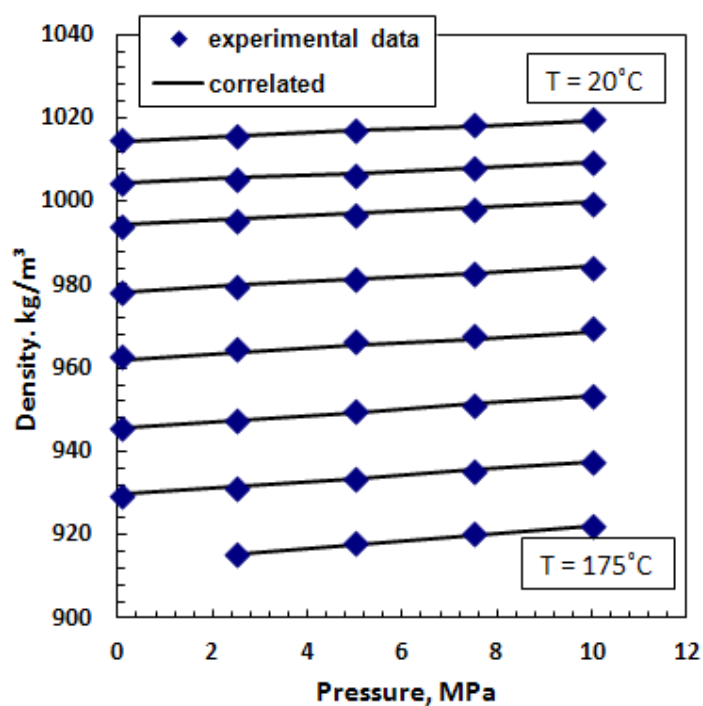


Figure 4–26. Measured and correlated density of Bitumen A.

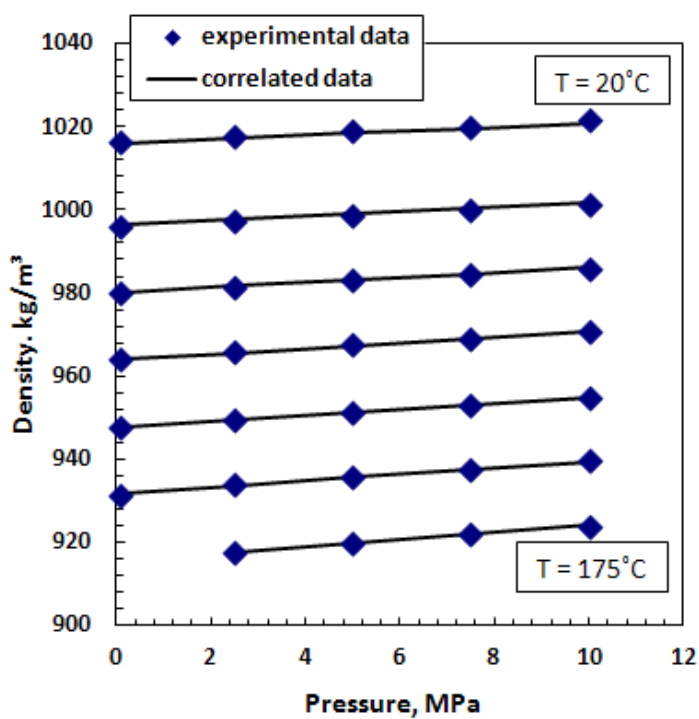


Figure 4–27. Measured and correlated density of Bitumen B.

Table 4-7. Fitted parameters for Bitumens A and B.

Bitumen	A_B (kg/m ³)	B_B (kg/m ³ K)	C_B (1/MPa x 10 ⁴)	D_B (1/K)
Bitumen A	1204.5	-0.6496	1.295	0.0045
Bitumen B	1205.4	-0.6470	1.488	0.0041

4.4 Diluted Bitumen Density

Table 4-8 summarizes the bitumen mixtures and conditions for which the density was measured. The data for propane diluted bitumen were collected in this work. The data for the other diluted bitumens were collected by Motahhari in the same lab (As part of another project with AER group, 2012). Note, Bituman A was used for the measurements with *n*-heptane and propane while Bitumen B was used for the measurements with ethane and *n*-butane.

Table 4-8. The composition, temperatures, and pressures of the diluted bitumens for which density data were collected.

Mixture	Composition (wt%)	Temperature Range (°C)	Pressure Range (MPa)	Source
Bitumen A / <i>n</i> -heptane	15, 30	20 - 175	0.1 – 10	Motahhari (2011)
Bitumen B / <i>n</i> -butane	7.3, 14.5	20 - 175	0.1- 10	Motahhari (2012)
Bitumen A / propane	5.5, 12, 16	20 - 150	1 – 10	This work
Bitumen B / ethane	5.2	20 - 150	2.5 - 12.5	Motahhari (2012)

Figures 4-28 to 4-31 are dispersion plots of the calculated versus measured density for bitumen diluted with *n*-heptane, *n*-butane, propane, and ethane, respectively. The density was calculated with the regular solution mixing rule (a) and the excess volume mixing rule (b). For heptane, butane, and propane the measured density was higher than the density calculated from the regular solution mixing rule. In other words, the mixtures shrank upon mixing (negative excess volume). There is a significant size difference between the solvent molecules and the majority of the molecules in the bitumen. The shrinkage is likely a consequence of different sized molecules packing more efficiently than similar sized molecules. The shrinkages observed for the dissolved gases were similar to that observed for the liquid mixture of heptane and bitumen. Even with the regular solution mixing rule, the average absolute deviations did not exceed 9 kg/m³, Table 4-9, only slightly outside the accuracy of the measured mixture densities (± 3 kg/m³ based on ± 0.5 wt% accuracy in the composition measurement). Hence, the effective liquid density correlations appear to be valid for diluted bitumens as well as mixtures of pure hydrocarbons.

The mixtures of ethane and bitumen appear to be regular solutions. However, the data may be anomalous given that mixtures of more dissimilar components are expected to be less ideal. It is possible that there is a composition error that skews the data or that the effective liquid density determined for liquid ethane is slightly too high. There is insufficient information to reach a definite conclusion at this time.

There also may be a systematic difference between Bitumen A and Bitumen B. Bitumen A appears to form less regular solutions with the *n*-alkanes than Bitumen B. Given that both bitumen samples were obtained from the same source, it seems unlikely that the physical behaviour of the two samples would differ. Rather, the differences may arise from non-representative sampling. For example, if the bitumen samples were not perfectly homogeneous, the subsamples used to measure the bitumen density may not be identical to the subsamples used to measure the diluted bitumen densities.

The density data were also fitted with the excess volume mixing rule and a single binary interaction parameter for each diluted bitumen system. The binary interaction parameters used to fit the data are provided in Table 4-9 along with the deviations for the regular solution mixing rule and excess volume mixing rule. The excess volume mixing rule fit the data almost within the precision of the individual density measurements ($\pm 0.4 \text{ kg/m}^3$ based on $\pm 0.5^\circ\text{C}$ temperature fluctuation).

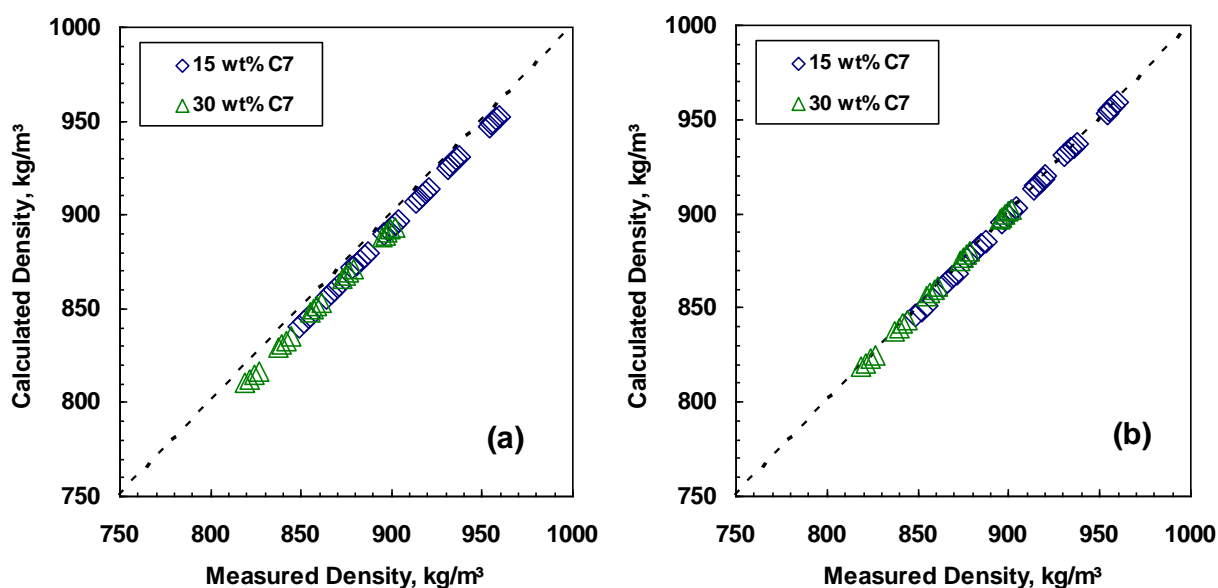


Figure 4-28. Calculated versus measured density for *n*-heptane (C7) diluted Bitumen A: a) regular solution mixing rule; b) excess volume mixing rule with $\beta_{ij} = +0.022$.

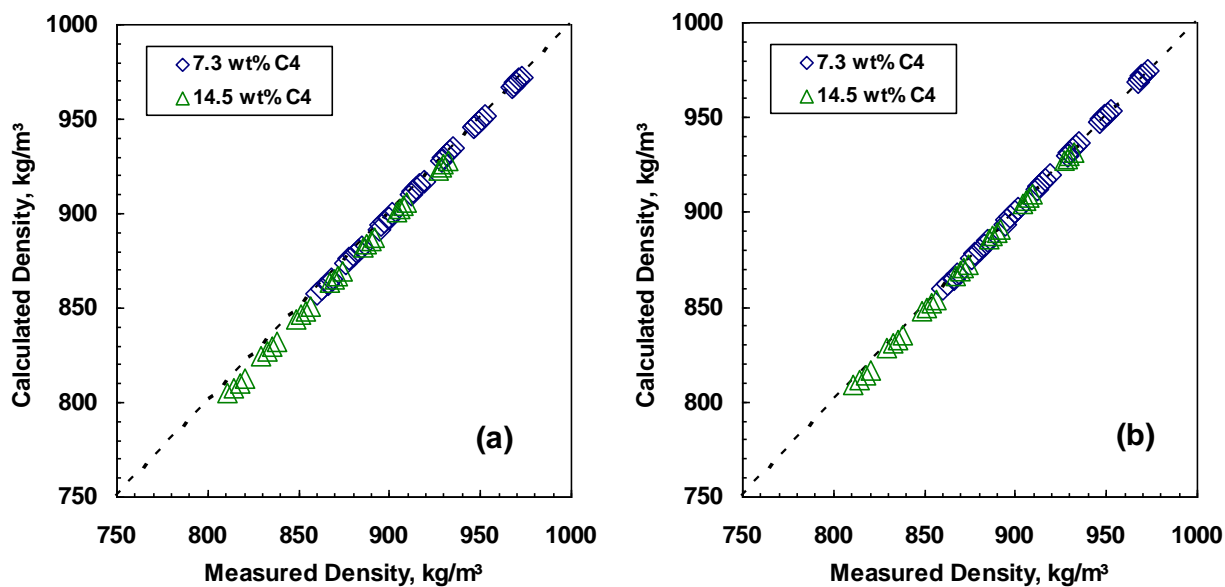


Figure 4–29. Calculated versus measured density for *n*-butane (C4) diluted Bitumen B: a) regular solution mixing rule; b) excess volume mixing rule with $\beta_{ij} = +0.013$.

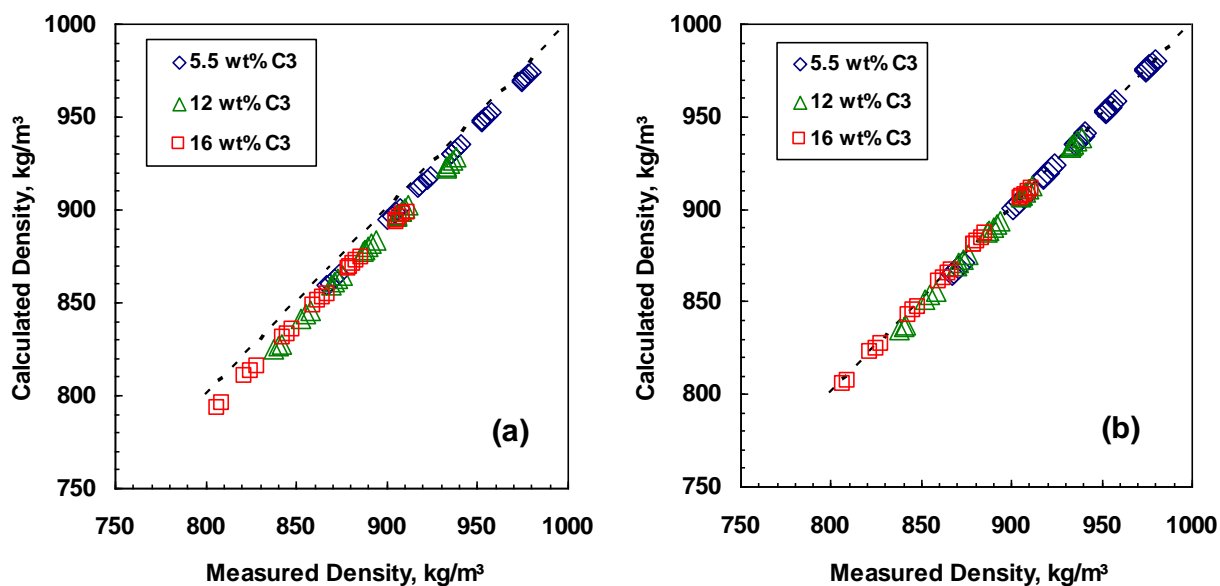


Figure 4–30. Calculated versus measured density for propane (C3) diluted Bitumen A: a) regular solution mixing rule; b) excess volume mixing rule with $\beta_{ij} = +0.040$.

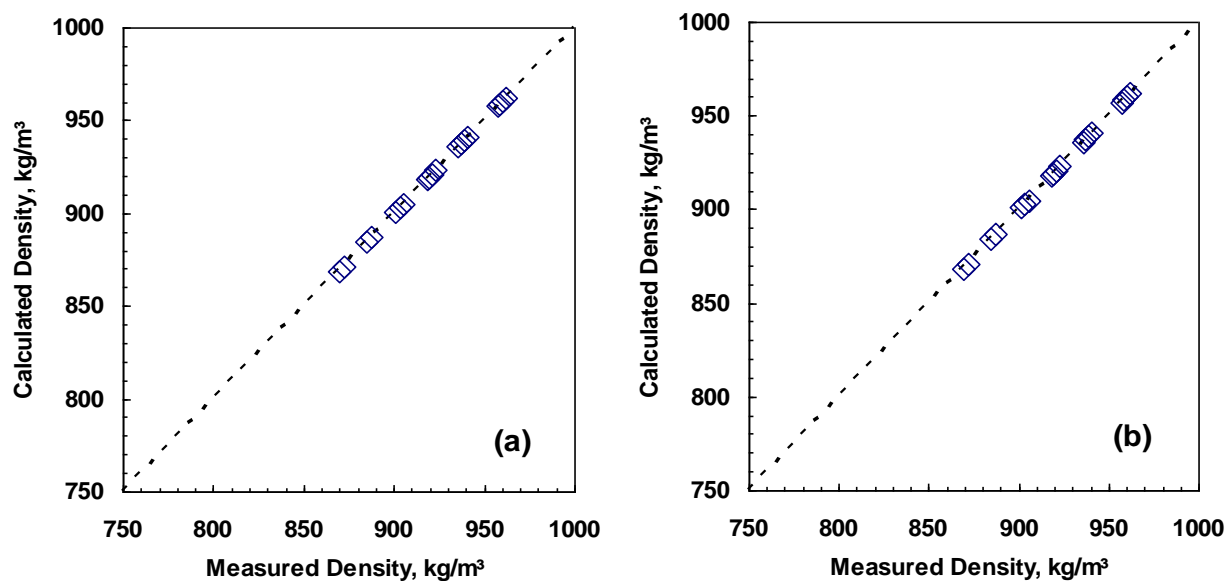


Figure 4–31. Calculated versus measured density for ethane (C2) diluted Bitumen A: a) regular solution mixing rule; b) excess volume mixing rule with $\beta_{ij} = -0.001$.

Table 4-9. AAD, AARD, MAD, and MARD of diluted bitumen mixtures.

Mixture	Regular Solution Mixing Rule		Excess Volume Mixing Rule		
	AAD (kg/m ³)	ARD (%)	β_{ij}	AAD (kg/m ³)	ARD (%)
Bitumen A + <i>n</i> -heptane	7.3	0.83	+0.022	1.1	0.13
Bitumen B + <i>n</i> -butane	2.8	0.33	+0.013	1.1	0.12
Bitumen A + propane	8.9	1.0	+0.040	0.6	0.07
Bitumen B + ethane	0.4	0.04	-0.001	0.4	0.04

Additional data were also available for *n*-decane diluted heavy oil (Kumar, 2012) and toluene diluted Bitumen A maltenes (Sanchez, 2012). The fitted β_{ij} for the

respective mixtures were -0.002 and 0.008. The data are provided in Appendix C. The β_{ij} values for these mixtures are in good agreement with the values found for mixtures of pure hydrocarbons, Figure 4-32.

The best fit values of β_{ij} for the diluted bitumens do not appear to follow a clear trend. For example, the β_{ij} values required to match each data point for each bitumen/solvent system were calculated and compared with the β_{ij} values determined for pure hydrocarbon mixtures, Figure 4-32. Although for each solvent, the β_{ij} values appear to increase as the normalized specific volume difference increases, the average β_{ij} values from solvent to solvent are scattered. For instance, the β_{ij} data for *n*-heptane and propane appear to fall on a linear extrapolation of the β_{ij} of the pure hydrocarbon mixtures (dashed line) whereas the data for *n*-butane and ethane deviate significantly from this trend.

To make density predictions for mixtures without density data, it is necessary to predict β_{ij} . One approach is to fit the β_{ij} to the normalized specific volume difference. The following quadratic extrapolation (solid line) provides a more optimized but still imperfect fit for all of the mixtures:

$$\beta_{ij} = -0.22 \left(\frac{dv}{v_{avg}} \right)^2 + 0.25 \left(\frac{dv}{v_{avg}} \right) - 0.045 \quad \text{Equation 4-11}$$

The quadratic extrapolation is plausible given that mixtures of an *n*-alkane with a non-hydrocarbon do show a maximum in the excess mixing volumes when plotted against carbon number of the *n*-alkane (see Figure 2-5). However, the correlation is inexact possibly because the calculated densities of the mixtures can be skewed by small errors in the effective liquid densities and bitumen densities.

The quadratic fit of the β_{ij} was used to calculate the density of the diluted bitumen mixtures. Figure 4-33 shows the measured and calculated densities of the diluted bitumens at 50°C (a) and 100°C (b). The AAD and AARD are less than 3.6 kg/m³

and 0.4%, respectively, at all temperatures, pressures, and compositions considered. In other words, using effective liquid densities and the excess volume mixing rule with the β_{ij} from Equation 4-11 provides a density prediction for diluted bitumens that is within 3.6 kg/m³ of the measured values. An alternative is to use an average constant β_{ij} of approximately 0.02. With a β_{ij} of 0.02, the AAD and AARD are less than 4.5 kg/m³ and 0.5%, respectively, at all temperatures, pressures, and compositions considered.

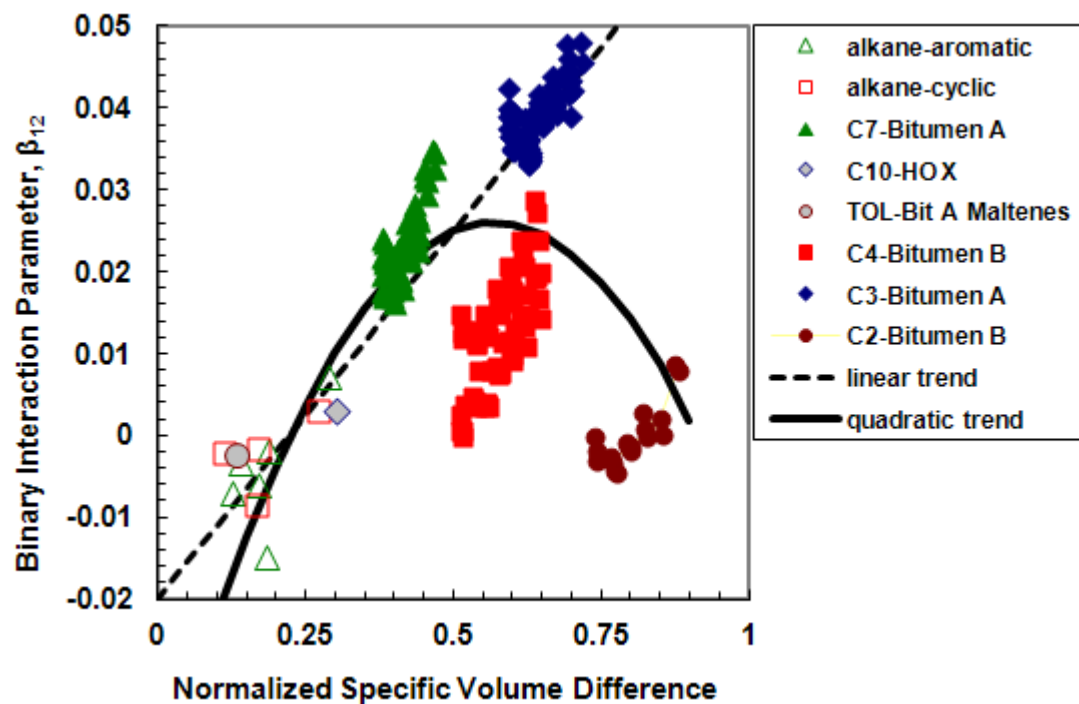


Figure 4–32. Comparison of binary interaction parameters for diluted bitumens and pure hydrocarbon mixtures.

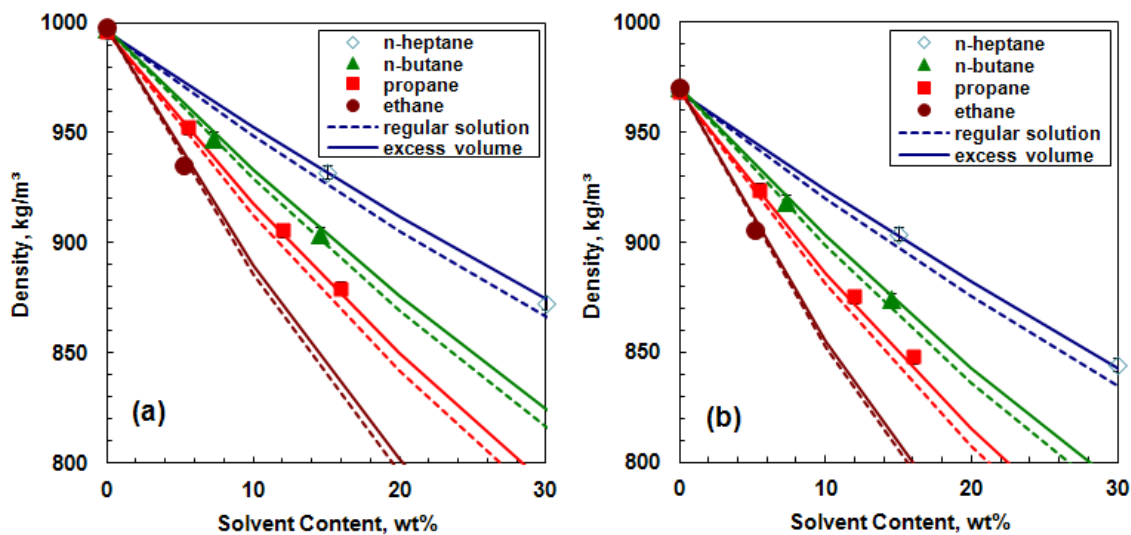


Figure 4–33. Density of bitumen diluted with *n*-alkanes at: a) 50°C and 2.5 MPa; b) 100°C and 10 MPa. Equation 4-11 was used to determine the β_{ij} for the excess volume mixing rule.

CHAPTER FIVE: CONCLUSION AND RECOMMENDATION

5.1 Summary

Density was measured for *n*-alkane binary mixtures at pressures from 10 to 40 MPa and temperatures from room temperature up to 175°C. The mixtures included: *n*-decane plus ethane, propane, and *n*-butane; toluene and propane; cyclooctane and propane. Density data were also collected for bitumen diluted with: ethane (Motahhari, 2012), propane, *n*-butane (Motahhari, 2012), and *n*-heptane at pressures from atmospheric up to 10 MPa.

A new density correlation was developed based on the effective density concept introduced by Tharanivasan *et al.*, (2011). To determine the effective densities of light *n*-alkanes, the molar volume data of higher *n*-alkanes (C₇ and up) were linearly extrapolated versus molecular weight. The calculated effective liquid molar volumes of the lower *n*-alkane were converted to mass density and then correlated to temperature and pressure. A criterion related to the critical temperature and pressure of the mixture was developed to define the range of validity for the correlation. The effective density correlation was then applied to predict the density of diluted bitumens.

5.2 Conclusions

The main conclusions from this thesis are presented below:

1. The density of hydrocarbon mixtures can be modeled, generally within experimental error, using a symmetric excess volume based mixing rule. The mixing rule includes a binary interaction parameter which can be determined by fitting experimental data. The binary interaction parameters for hydrocarbon pairs appear to correlate to the normalized molar volume difference between the two components.

2. A correlation was developed for the effective liquid density of dissolved gases. The effective density values were linearly pressure dependent and the model applied parameters which were linearly temperature dependent. The correlation when applied with a regular solution mixing rule, predicted the density of mixtures of pure hydrocarbons within measurement error. The correlation is applicable in the liquid region and is suitable for bitumen and solvent mixtures.
3. Shrinkage was observed when bitumen was diluted with an *n*-alkane; in other words, there is a negative excess volume for these mixtures. The shrinkage was typically less than 1%. Such shrinkage is typical when mixing hydrocarbons of different size and indicates a more efficient packing at the molecular level.
4. Binary interaction parameters were required to fit the density of diluted bitumens. The β_{ij} values for diluted bitumens did not follow a consistent trend. Nonetheless, they were correlated to the normalized difference in molar volume with a quadratic function. The mixture densities were predicted to within 3.6 kg/m³ using this correlation.

5.3 Recommendations

To improve the effective density model and to enhance its capability the following recommendations are made in terms of experimental data and modeling methods:

1. For pure hydrocarbon mixtures, data were collected for different types of mixtures involving light *n*-alkanes including *n*-alkane/*n*-alkane, *n*-alkane/aromatic, and *n*-alkane/cyclic pairs. It is recommended to evaluate *n*-alkane/branched alkane mixtures to extend the applicability of the model.

2. In this thesis, the only gases studied as solvents were hydrocarbons. However, other gases such as CO₂ and N₂ can be also applied in solvent-assisted heavy oil recovery techniques. These gases could be considered in future studies to extend the applicability of the effective density model.

3. Mixtures of ethane and bitumen appear to form regular solutions. However mixtures of more dissimilar components are expected to be less ideal. It is possible that there is a composition error or that the effective liquid density determined for liquid ethane is slightly too high. It is recommended to collect more data on the mixture of ethane diluted bitumen to validate the results presented in this thesis.

References

- Aalto, M., Keskinen, K. I., Aittamaa, J., and Liukkonen, S. (1996). An Improved Correlation for Compressed Liquid Densities of Hydrocarbon. Part 1. Pure Compounds. *Fluid Phase Equilibria* , 114, 1-19.
- Agrawala, M., Yarranton, H.W. (2001). An Asphaltene Association Model Analogous to Linear Polymerization, *Industrial and Engineering Chemistry*, 4664-4672.
- Alonso, M. C., Poveda Vilches, J. L., Sanchez-Pajares, R. G., and Delgado, J. N. (1983). Excess Volumes of (Tolunene + n-alkanes). *Chemical Thermodynamics* , 913-917.
- American Petroleum Institute Technical Data Book, Petroleum Refining, Refining Department, 5th Edition, New York, May 1992.
- Ashcroft, S., Isa, M. (1997). Effect of the Dissolved Gases on the Densities of Hydrocarbons, *Chemical and Engineering Data*, 1244-1248.
- Ashcroft, S., Bookers, D., and Turner, J. (1992). Volumetric Behaviour of Mixtures of Crude Oils and Light Hydrocarbons. *Journal of Institute of Energy* , 131-136.
- Assael, M. J., Dymond, J. H., and D., E. (1994). An Improved Representation for n-Alkane Liquid Densities. *International Journal of Thermophysics* , 155-164.
- Aucejo, A., Burguet, M. C., Munoz, R., and Marques, J. L. (1995). Densities, Viscosities, and Refractive Indices of Some n-Alkane Binary Liquid Systems at 298.15 K. *Chemical and Engineering Data* , 141-147.
- Audonnet, F., and Padua, A. A. (2004). Viscosity and Density of Mixtures of methane and n-decane from 298 to 393 K and up to 75 MPa. *Fluid Phase Equilibria*, 235-244.
- Badamchi-Zadeh, A., Yarranton, H. W., W.Y, a. S., and B.B, M. (2009). Phase Behaviour and Physical Property Measurements for VAPEX Solvents: Part I. Propane and Athabasca Bitumen . *Canadian Petroleum Technology* , 54-61.
- Badamchi-Zadeh, A., Yarranton, H., Maini, B., and Satyro, M. (2009). Phase Behaviour and Physical Property Measurements for VAPEX Solvents: Part II. Propane, Carbon Dioxide and Athabasca Bitumen . *Canadian Petroleum Technology* , 57-65.

Bergman, D. (1976). Prediction of the Phase Behavior of the Natural Gas. PhD Thesis, University of Michigan .

Boduszynski, M. (1987). Composition of Heavy Petroleum. 1. Molecular Weight, Hydrogen Deficiency, and Heteroatom Concentration as a Function of Atmospheric Equivalent Boiling Point up to 1400 OF (760 °C). *Energy and Fuels* , 2-11.

Boduszynski, M. (1988). Composition of Heavy Petroleum. 2. Molecular Characterization. *Energy and Fuels* , 597-613.

Briggs, P., Baron, R., and Fulleylove, R. (1988). Development of Heavy Oil Reservoirs. *Petroleum Technology* , 206-214.

brønsted, J. N., and Koefoed, J. (1946). *Det. Kgl. Danske Videnske Selsk. Mat. Fys. Medd.* , 22, 1-32.

Canada's Oil Sands—Opportunities and Challenges to 2015: An Update.. http://www.neb.gc.ca/clfnsi/rnrgynfmtn/nrgyrprt/lsnd/pprntsndchllngs20152006/qa_pprntsndchllngs20152006-eng.html, National Energy Board of Canada, 2007-06-30, 2007

Canet, X., Baylaucq, A., Boned, C. (2002). High-Pressure (up to 140 MPa) Dynamic Viscosity of the Methane + Decane System. *International Journal of Thermophysics*, 1469-1486.

Cavet, R. H. (1962). Physical Data for Distillation Calculation Vapor-Liquid Equilibria. 27th mid-year meeting of API, Division of Refining . San Francisco.

Chang, C., and Zhao, X. (1990). A new generalized equation for predicting volumes of compressed liquids. *Fluid Phase Equilibria* , 231-238.

Chevalier, J. L., Petrino, P. J., and Gaston-Bonhomme, Y. H. (1990). Viscosity and Density of Some Aliphatic, Cyclic, and Aromatic Hydrocarbons Binary Liquid Mixtures. *Chemical Engineering Data* , 206-212.

Chueh, P. L., and Prausnitz, J. M. (1969). A Generalized Correlation for the Compressibilities of Normal Liquids. *AIChE* , 471-472.

Cibulka, I., and Hnědkovský, L. (1996). Liquid Densities at Elevated Pressures of n-Alkanes from C5 to C16: A Critical Evaluation of Experimental Data. *Chemical and Engineering Data* , 657-668.

Cooper, E. F., and Asfour, A. A. (1991). Densities and Kinematic Viscosities of Some C6-C16 n-Alkane Binary Liquid Systems at 293.15 K. *Chemical Engineering Data* , 285-288.

Czerwiński, G. J., Tomasula, P., and Tassios, D. (1988). Vapor - liquid equilibria with the vdW - 711 equation of state. *Fluid Phase Equilibria* , 63-83.

de Sant'Anna, H., Ungerer, P., and de Hemptinne, J. (1999). Evaluation of an improved volume translation for the prediction of hydrocarbon volumetric properties. *Fluid Phase Equilibria* , 193-204.

Doolittle, A. (1964). Specific Volumes of n-Alkanes. *Chemical and Engineering Data* , 275-279.

Dymond, J. H., and Malhotra, R. (1987). Densities of n-Alkanes and Their Mixtures at Elevated Pressures. *International Journal of Thermophysics* , 541-555.

Dymond, J. H., and Robertson, J. (1982). (p,r,T) of some pure n-alkanes and binary mixtures of n-alkanes in the range 298 to 373 K and 0.1 to 500 MPa. *Chemical Thermodynamics* , 14, 51-59.

Dymond, J. H., Young, K. J., and D., I. J. (1980). Transport properties of nonelectrolyte liquid mixtures—II. Viscosity coefficients for the n-hexane + n-hexadecane system at temperatures from 25 to 100°C at pressures up to the freezing pressure or 500 MPa. *International Journal of Thermophysics* , 345-373.

Dymond, J., and Malhotra, R. (1988). The Tait Equation: 100 Years On. *International Journal of Thermophysics* , 941-951.

Erno, B., Christ, J., and Given, R. (1994). Equation Predicts Shrinkage of Heavy Oil/Condensate Blends. *Oil and Gas Journal* , 62-67.

Estrada, M. R., Iglesias-Silva, G. A., and Hall, K. R. (2006). Experimental Measurements and Prediction of Liquid Densities for n-alkane Mixtures. *Chemical Thermodynamics* , 38, 337-347.

Francis, A. (1959). Pressure-Temperature-Density Relations of Pure Liquids. *Chemical and Engineering Science* , 37-46.

Goates, J. R., B., O. J., and B., G. R. (1981). Excess Volumes of n-hexane + n-heptane, + n-octane, + n-nonane, and + n-decane at 283.15, 298.15, and 313.15 K. *Chemical Thermodynamics* , 907-913.

Goates, J. R., Ott, J. B., and B., M. J. (1977). Determination of excess volumes in cyclohexane+ benzene and+ n-hexane with a vibrating-tube densimeter. *Chemical Thermodynamics* , 9, 249-257.

Goates, J. R., Ott, J. B., and Grigg, R. B. (1979). Excess Volumes of Cyclo-hexane + n-hexane, + n-heptane, + n-octane, + n-nonane, + n-decane. *Chemical Thermodynamics*, 497-506.

Gomez-Ibanez, J. D., and Liu, T.-C. (1961). The Excess Volume of Cyclohexane and Some Normal Alkane. *Physical Chemistry*, 2148-2151.

Gray, M. (1994). *Upgrading Petroleum Residues and Heavy Oils*. New York: Marcel Dekker.

Gunn, R., and Yamada, T. (1971). A Corresponding State Correlation of Saturated Liquid Volumes. *AIChE*, 1341-1345.

Hepler, L. G., and Hsi, C. (1989). *AOSTRA Technical Handbook on Oil Sands, Bitumen and Heavy Oils*. Edmonton, AB, Canada: Alberta Oil Sands Technology and Research Authority.

Harnett, D. L., (1982). *Statistical Methods*, 3rd Edition, Addison-Wesley Publication Company.

Hankinson, R., and Thompson, G. (1979). A New Correlation for Saturated Densities of Liquids and Their Mixtures. *AIChE*, 659-663.

Huang, P. (1977). *Characterization and Thermodynamic Correlations for Undefined Hydrocarbon Mixtures*. PhD Thesis, The Pennsylvania State University .

Hutchings, R. S., and Van Hook, W. A. (1985). Excess Molar Volumes and deviations from congruence of some binary solutions of an n-alkane in another n-alkane. *Chemical Thermodynamics*, 523-529.

Jacobs, F., Donnelly, J. K., Stanislav, J., and SVrcek, W. (1980). Viscosity of Gas-saturated Bitumen . *Canadian Petroleum Technology* , 46-50.

Jhaveri, B. S., and Youngren, G. K. (1988). Three-Parameter Modification of the Peng-Robinson Equation of State To Improve Volumetric Predictions . *Society of Petroleum Engineers* , 1033-1040.

- Kariznovi, M., Nourizadeh, H., Abedi, J. (2011). Measurement and Modeling of Liquid Saturated Properties (Solubility, Density, and Viscosity) of (Ethane + n-Tetradecane) Binary Systems. *Chemical and Engineering Data*, 3669-3672.
- Kariznovi, M., Nourizadeh, H., Abedi, J. (2012). Measurement and Equation of State Prediction of Vapor-Liquid Equilibrium and Physical Properties for the System Methane + n-Octadecane. *Fluid Phase Equilibria*, 102-106.
- Kashiwagi, H., and Makita, T. (1982). Viscosity of twelve hydrocarbon liquids in the temperature range 298–348 K at pressures up to 110 MPa. *International Journal of Thermophysics* , 289-305.
- Kesler, M., and Lee, B. (1976). Improve Prediction of Enthalpy of Fractions. *Hydrocarbon Processing* , 55, 153-158.
- Knapstad, B., Skjolsvik, P. A., and Oye, H. A. (1990). Viscosity of the n-Decane - Methane System in the liquid phase. *Physical Chemistry* , 94, 1156-1165.
- Kokal, S. L., and Sayegh, S. G. (1995). Asphaltene: The Cholesterol of Petroleum.
- Kokal, S. L., and Sayegh, S. G. (1990). Gas-saturated bitumen density predictions using the volume-translated Peng-Robinson equation of state. *Chemical and Petroleum Technology* , 77-82.
- Lagourette, B., Boned, C., Saint-Guirons, H., Xans, P., and Zhou, H. (1992). Densimeter calibration method versus temperature and pressure. *Measurement Science and Technology* , 699-703.
- Lal, K., Tripathi, N., and Dubey, G. (2000). Densities, Viscosities, and Refractive Indices of Binary Liquid Mixtures of Hexane, Decane, Hexadecane, and Squalan with Benzene at 298.15 K. *Chemical Engineering Data* , 961-964.
- Lee, A. L., Gonzalez, M. H., and Eakin, B. E. (1966). Viscosity of Methane/n-Decane Mixtures. *Chemical and Engineerin Data* , 11, 281-287.
- Lee, I., and Kesler, M. (1975). A Generalized Thermodynamic Correlation Based on Three-Parameter Corresponding States. *AIChE* , 21, 510-527.
- Loria, H., Pereira-Almao, P., and Satyro, M. (2009). Prediction of Density and Viscosity of Bitumen Using the Peng-Robinson Equation of State . *Industrial and Engineering Chemistry Research* , 10129-10135.

Magoulas, K., and Tassios, D. (1990). Thermophysical properties of n-Alkanes from C1 to C20 and their prediction for higher ones. *Fluid Phase Equilibria* , 119-140.

Marra, R., Poettmann, F., and Thompson, R. (1988). Density of Crude Oil Saturated with CO₂. *Society of Petroleum Engineering* , 815-821.

Martin, J. (1979). Cubic Equations of State-Which? *Industrial and Engineering Chemistry Fundamentals* , 81-97.

Martin, J. (1959). *Thermodynamic and Transport Properties of Gases, Liquids, and Solids*. New York: American Society of Mechanical Engineers and Mc-Graw Hill.

McCain, W. (1990). *The Properties of Petroleum Fluids*. Tulsa, Oklahoma: PennWell Publishing Company.

Mehrotra, A. K., and Svrcek, W. Y. (1982). Viscosity, Density and Gas Solubility Data for Oil Sand Bitumens. Part I: Athabasca Bitumen Saturated with CO and C₂H₆. *AOSTRA JOURNAL RESEARCH* , 263-268.

Mehrotra, A. K., and Svrcek, W. Y. (1985). Viscosity, Density and Gas Solubility Data for Oil Sand Bitumens. Part II: Peace Rive Bitumen Saturated with N₂, CO, CH₄, CO₂ and C₂H₆. *AOSTRA JOURNAL OF RESEARCH* , 269-279.

Mehrotra, A. K., and Svrcek, W. Y. (1985). Viscosity, Density and Gas Solubility Data for Oil Sand Bitumens. Part III: Wabasca Bitumen Saturated with N₂, CO, CH₄, CO₂ and C₂H₆. *AOSTRA JOURNAL OF RESEARCH* , 83-93.

Mehrotra, A., and Svrcek, W. (1985). Bitumen Density and Gas Solubility Predictions Using the Peng-Robinson Equation of State. *AOSTRA Journal of Research* , 215-226.

Mehrotra, A., and Svrcek, W. (1988). Properties of Cold Lake Bitumen Saturated with Pure Gases and Gas Mixtures. *Canadian Journal of Chemical Engineering* , 656-665.

NIST Standard Reference Database; NIST/TRC Source Database; WinSource, Version 2008.

Nourizadeh, H., Kariznovi, M., Abedi, J. (2012). Experimental Measurement and Equation of State Modeling of Liquid Saturated Properties (Solubility, Density, and Viscosity) of (Ethane + n-Octadecane) Binary Systems. *Chemical and Engineering Data*, 137-141.

Nourizadeh, H., Kariznovi, M., Abedi, J. (2012). Vapor-liquid Equilibrium Measurement and Thermodynamic Modeling of Binary Systems (Methane + n-Tetradecane). *Fluid Phase Equilibria*, 96-101.

Oliveira, C., and Wakeham, W. (1992). The Viscosity of Five Liquid Hydrocarbons at Pressures Up to 250 MPa. *International Journal of Thermophysics* , 773-790.

Ortiz Gonzalez, D. (2009, April). Effect of Surfactants on Asphaltene Interfacial Films and Stability of Water-in-Oil Emulsions. PhD Thesis . Calgary, Alberta, Canada.

Péneloux, A., Rauzy, E., and Fréze, E. (1982). A consistent correction for Redlich-Kwong-Soave volumes. *Fluid Phase Equilibria* , 7-23.

Peng, D., and Robinson, D. (1976). A new two-constant equation of state. *Industrial and Engineering Chemistry Fundamental* , 59-64.

Racket, H. G. (1970). Equation of State for Saturated Liquids. *Chemical and Engineering Data*, 514-517.

Rea, H., Spencer, C., and Danner, R. (1973). Effect of pressure and temperature on the liquid densities of pure hydrocarbons. *Chemical and Engineering Data* , 227-230.

Redlich, O., and Kwong, J. (1949). An equation of state. Fugacities of gaseous solutions. *Chemical Reviews* , 233-244.

Reid, R., Prauznitz, J., and Poling, B. (1987). *The Properties of Gases and liquids* (4th Edition ed.). New York: McGraw-Hill.

Riazi, M. (2005). Characterization and properties of petroleum fractions. *Astm Intl*.

Robinson, E. (1983). Calculate Density of Spiked Crudes. *Hydrocarbon Processing* , 115-120.

Sarkar, M. (1984). Property Prediction-Gas Saturated Bitumen. Masters Thesis. Calgary, Alberta, Canada.

Schrodt, J., and Akel, R. (1989). Binary Liquid Viscosities and Their Estimation from Classical Solution Thermodynamics. *Chemical Engineering Data* , 8-13.

Shana'a, M., and Canfield, F. (1968). Liquid Density and Excess Volume of Light Hydrocarbon Mixtures at -165 C. *Transactions of the Faraday Society* , 2281-2286.

Soave, G. (1972). Equilibrium constants from a modified Redlich—Kwong equation of state. *Chemical Engineering Science* , 1197-1203.

Sóreide, I., Improved Phase Behavior Predictions of Petroleum Reservoir Fluids From a Cubic Equation of State, “Dr. Ing. Dissertation, Norwegian Inst. Of Technology, 1989

Speight, J. (2001). *Handbook of Petroleum Analysis*. Laramie, Wyoming: John Wiley and Sons.

Speight, J. (2007). *The Chemistry and Technology of Petroleum*. New York: Marcel Dekker Inc.

Spencer, C., and Danner, R. (1972). Improved Equation for Prediction of Saturated Liquid Density. *Chemical and Engineering Data*, 236-241.

Standing, M. B., and Katz, D. L. (1942). Density of Crude Oil Saturated with Natural Gas. 146.

Strausz, O., and Lown, E. M. (2003). *The Chemistry of Alberta Oil Sands Bitumens and Heavy Oils*. Calgary, AB, Canada: Alberta Energy Research Institute.

Strausz, O., Mojelsky, T., and Lown, E. (1992). The molecular structure of asphaltene: an unfolding story. *Fuel* , 1355-1363.

Svrcek, W. Y., and Mehrotra, A. (1982). Gas Solubility, Viscosity and density measurements for Athabasca Bitumen . *Canadian Petroleum Technology* , 31-38.

Tait, P. (1888). *Physics and Chemistry of the Voyage of HMS Challenger*.

Tharanivasan, A., Yarranton, H., and Taylor, S. (2011). Application of a Regular Solution-Based Model to Asphaltene Precipitation from Live Oils. *Energy and Fuel* , 25, 528-538.

Thomson, G., Brobst, K., and Hankinson, R. (1982). An Improved Correlation for Densities of Compressed Liquids and Liquid Mixtures. *AIChE* , 671-676.

Ungerer, P., and Batut, C. (1997). Prediction of the Volumetric Properties of Hydrocarbons with an Improved Volume Translation Method. *Oil and Gas Science and Technology* , 609-623.

Van der Waals, J. D. (1873) *Over de Continuïteit van den Gas-en Vloeistoftoestand*. Thesis, Leiden.

- VMG Sim Software, (2010). Virtual Material Group Ltd., Version 6.0. Calgary, AB, Canada
- Ward, S. H., and Clarke, K. (1950). Determination of Viscosity and Specific Gravities of the Oils in Samples of Athabasca Bituminous Sand. Edmonton, Alberta: Alberta Research Council.
- Watson, K. (1943). Thermodynamics of the Liquid State. Industrial and Engineering Chemistry , 398-406.
- Whitson, C. (1980). Charazterizing Hydrocarbon Plus Fractions . EUROPEC Conference. London.
- Witek, M., Goldon, A., Hofman, T., and Domanska, U. (1997). Denisties and Excess Volumes of Methyl 1,1-Dimethylpropyl Ether + Benzene or Cyclohexane or an Alkane (C6-C16) at 298.15 K. Chemical Engineering Data, 60-63.
- Wu, J., and Asfour, A. (1994). Densities and excess molar volumes of eight n-alkane binary systems at 293.15 and 298.15 K. Fluid Phase Equilibria , 305-315.
- Yarranton, H. W, Badamchi-Zadeh, A, Satyro, M. A., Maini, B.B (2008). Phase Behaviour and Physical Properties of Athabasca Bitumen, Propane and CO₂. Canadian International Petroleum Conference (pp. 1-7). Calgary: Petroleum Society.
- Yarranton, H., Alboudwarej, H., and Jakher, R. (2000). Investigation of Asphaltene Association with Vapor Pressure Osmometry and Interfacial Tension Measurements. Industrial and Engineering Chemistry , 2916-2924.
- Yen, L., and Woods, S. (1966). A Generalized Equation for Computer Calculation of Liquid Densities. AIChE, 95-99.

APPENDIX A – PURE HYDROCARBON MIXTURES DENSITY DATA

Table A-1. Measured densities for mixtures of 6 wt% ethane and 94 wt% *n*-decane.

Temperature (°C)	Pressure (MPa)	Measured Density (kg/m ³)
14.68	10	722.2
14.68	20	729.0
14.70	30	734.2
14.71	40	740.0
50.02	10	697.2
50.01	20	705.5
50.02	30	712.6
50.00	40	719.6
75.00	10	676.8
75.01	20	685.0
75.01	30	693.6
75.01	40	701.6
125.02	10	639.1
125.01	20	651.1
125.01	30	660.8
125.01	40	670.3
175.00	20	600.5
175.00	30	627.3
175.00	40	639.7

Table A-2. Measured densities for mixtures of 12.5 wt% ethane and 87.5 wt% *n*-decane.

Temperature (°C)	Pressure (MPa)	Measured Density (kg/m ³)
21.72	10	679.9
21.71	20	688.4
21.71	30	695.8
21.70	40	701.9
50.00	10	653.0
50.00	20	665.9
50.00	30	673.6
50.00	40	680.9
74.99	10	633.4
74.99	20	646.4
74.99	30	655.5
74.99	40	663.0
124.99	10	582.9
124.99	20	601.8
124.99	30	616.0
124.99	40	627.2
174.99	20	554.0
174.99	30	575.0
174.99	40	590.4

Table A-3. Measured densities for mixtures of 6 wt% propane and 94 wt% *n*-decane.

Temperature (°C)	Pressure (MPa)	Measured Density (kg/m ³)
18.31	10	721.3
18.31	20	728.1
18.32	30	734.0
18.33	40	741.1
49.99	10	699.0
49.99	20	708.0
49.99	30	715.4
49.99	40	722.9
75.02	10	679.7
75.00	20	689.4
75.00	30	698.0
75.01	40	706.0
124.96	10	641.3
124.97	20	653.7
124.98	30	665.0
124.98	40	674.6
175.02	10	599.9
175.02	20	617.0
175.02	30	631.2
175.03	40	643.4

Table A-4. Measured densities for mixtures of 12.5 wt% propane and 87.5 wt% *n*-decane.

Temperature (°C)	Pressure (MPa)	Measured Density (kg/m ³)
19.24	10	706.2
19.24	20	713.1
19.22	30	721.1
19.20	40	727.4
49.98	10	685.2
49.98	20	695.1
49.98	30	702.7
49.98	40	710.6
74.98	10	664.5
74.98	20	675.2
74.98	30	684.1
74.97	40	692.2
124.97	10	624.0
124.98	20	637.9
124.99	30	649.9
124.99	40	660.0
175.00	10	579.8
175.01	20	599.5
175.01	30	615.2
175.01	40	628.1

Table A-5. Measured densities for mixtures of 25 wt% propane and 75 wt% *n*-decane.

Temperature (°C)	Pressure (MPa)	Measured Density (kg/m ³)
19.26	10	673.2
19.27	20	681.6
19.28	30	689.3
19.29	40	698.6
50.00	10	652.7
50.00	20	663.8
50.00	30	672.7
50.01	40	681.2
75.02	10	628.8
75.01	20	641.1
75.00	30	651.7
75.00	40	661.4
124.98	10	582.1
125.00	20	599.8
125.01	30	614.5
125.01	40	626.5
174.99	10	530.4
175.01	20	557.1
175.01	30	576.8
175.00	40	592.2

Table A-6. Measured densities for mixtures of 6 wt% propane and 94 wt% toluene.

Temperature (°C)	Pressure (MPa)	Measured Density (kg/m ³)
20.09	10	844.8
20.11	20	852.4
20.14	30	859.3
20.16	40	865.6
49.99	10	818.6
49.98	20	827.5
49.99	30	835.2
49.99	40	843.2
75.02	10	794.3
75.02	20	804.6
75.03	30	813.6
75.03	40	822.2
125.00	10	746.5
125.01	20	760.5
125.01	30	772.4
125.01	40	782.7
175.02	10	694.0
175.00	20	713.9
175.01	30	729.8
175.01	40	743.2

Table A-7. Measured densities for mixtures of 12.5 wt% propane and 87.5 wt% toluene.

Temperature (°C)	Pressure (MPa)	Measured Density (kg/m ³)
20.3	10	809.3
20.31	20	817.4
20.31	30	824.9
20.31	40	831.4
50.00	10	782.2
50.00	20	791.7
50.00	30	800.0
50.01	40	808.4
75.01	10	757.2
75.01	20	767.8
75.00	30	777.9
75.00	40	786.9
125.01	10	704.9
125.02	20	721.1
125.02	30	734.6
125.02	40	746.2
175.01	10	648.6
175.01	20	672.5
175.02	30	690.9
175.02	40	705.8

Table A-8. Measured densities for mixtures of 25 wt% propane and 75 wt% toluene.

Temperature (°C)	Pressure (MPa)	Measured Density (kg/m ³)
20.12	10	760.6
20.14	20	769.7
20.16	30	777.8
20.18	40	784.3
49.95	10	731.7
49.95	20	743.5
49.96	30	753.0
49.96	40	762.3
75.01	10	706.2
75.02	20	719.6
75.02	30	730.9
75.02	40	740.9
125.01	10	651.3
124.97	20	671.9
124.99	30	687.3
124.99	40	700.1
175.01	10	589.7
175.00	20	619.8
175.00	30	641.1
175.00	40	658.2

Table A-9. Measured densities for mixtures of 6 wt% propane and 94 wt% cyclooctane.

Temperature (°C)	Pressure (MPa)	Measured Density (kg/m ³)
20.18	10	823.2
20.18	20	828.8
20.18	30	834.0
20.18	40	839.6
50.02	10	792.8
50.02	20	802.3
50.02	30	810.7
50.02	40	818.6
75.02	10	770.7
75.02	20	779.7
75.02	30	788.6
75.02	40	797.2
125.02	10	733.3
125.02	20	743.0
125.01	30	752.1
125.01	40	762.7
175.00	10	692.7
175.00	20	707.3
175.00	30	719.7
175.00	40	755.2

Table A-10. Measured densities for mixtures of 12.5 wt% propane and 87.5 wt% cyclooctane.

Temperature (°C)	Pressure (MPa)	Measured Density (kg/m ³)
20.41	10	791.4
20.41	20	797.9
20.42	30	804.0
20.42	40	809.8
49.99	10	766.0
49.99	20	774.8
49.99	30	781.9
49.99	40	788.9
74.99	10	746.4
74.99	20	756.0
74.99	30	764.1
74.99	40	771.7
124.97	10	703.4
124.97	20	716.1
124.97	30	726.9
124.97	40	736.3
175.03	10	657.2
175.02	20	674.8
175.02	30	688.9
175.01	40	701.1

Table A-11. Measured densities for mixtures of 25 wt% propane and 75 wt% cyclooctane.

Temperature (°C)	Pressure (MPa)	Measured Density (kg/m ³)
20.85	10	744.1
20.85	20	753.3
20.85	30	759.5
20.85	40	765.8
50.03	10	718.5
50.03	20	728.8
50.02	30	736.9
50.02	40	745.1
74.99	10	695.6
74.99	20	707.2
74.99	30	716.8
74.99	40	725.8
125.00	10	649.1
125.00	20	664.9
125.00	30	678.1
124.99	40	689.1
175.02	10	595.5
175.02	20	619.8
175.03	30	638.1
175.03	40	652.7

Table A-12. Measured densities for mixtures of 6 wt% *n*-butane and 94 wt% *n*-decane.

Temperature (°C)	Pressure (MPa)	Measured Density (kg/m ³)
18.46	10	726.3
18.47	20	732.8
18.47	30	738.9
18.48	40	743.9
50.00	10	703.5
50.00	20	712.3
50.00	30	719.4
50.00	40	726.9
75.00	10	684.4
75.00	20	694.1
75.00	30	702.4
75.00	40	710.1
124.98	10	646.5
124.98	20	659.0
124.98	30	669.9
124.98	40	679.1
175.00	10	606.3
175.00	20	623.0
175.00	30	636.8
175.00	40	648.6

Table A-13. Measured densities for mixtures of 12.5 wt% *n*-butane and 87.5 wt% *n*-decane.

Temperature (°C)	Pressure (MPa)	Measured Density (kg/m ³)
18.36	10	715.6
18.36	20	721.4
18.36	30	728.4
18.37	40	733.0
50.01	10	692.8
50.01	20	701.1
50.01	30	708.6
50.01	40	716.3
74.98	10	672.9
74.98	20	682.6
74.98	30	691.3
74.98	40	699.3
125.00	10	633.9
125.00	20	646.5
125.00	30	658.1
125.00	40	667.6
175.01	10	591.3
175.01	20	609.3
175.00	30	624.1
175.00	40	636.9

Table A-14. Measured densities for mixtures of 25 wt% *n*-butane and 75 wt% *n*-decane.

Temperature (°C)	Pressure (MPa)	Measured Density (kg/m ³)
18.96	10	696.0
18.97	20	704.2
18.97	30	711.0
18.98	40	717.4
50.02	10	669.5
50.02	20	681.2
50.02	30	689.8
50.02	40	698.3
75.00	10	649.1
74.98	20	662.1
74.99	30	672.3
75.00	40	681.0
125.00	10	607.2
125.00	20	625.7
124.99	30	638.9
124.99	40	649.2
174.99	10	567.4
175.00	20	589.5
175.00	30	607.1
175.00	40	620.7

APPENDIX B – DEAD BITUMENS DENSITY DATA

Table B-1. Measured densities for dead bitumen A.

Temperature (°C)	Pressure (MPa)	Measured Density (kg/m ³)
19.4	0.1	1014.924
19.4	2.5	1015.911
19.4	5	1017.028
19.4	7.5	1018.455
19.4	10	1019.955
35	0.1	1004.325
35	2.5	1005.159
35	5	1006.375
35	7.5	1007.893
35	10	1009.370
50	0.1	994.200
50	2.5	995.326
50	5	996.709
50	7.5	998.237
50	10	999.514
75	0.1	978.323
75	2.5	979.719
75	5	981.288
75	7.5	982.680
75	10	984.261
100	0.1	962.882
100	2.5	964.522
100	5	966.242
100	7.5	967.852
100	10	969.528
125	0.1	945.677
125	2.5	947.602
125	5	949.528
125	7.5	951.067
125	10	953.123

Table B-1: *Continued*

Temperature (°C)	Pressure (MPa)	Measured Density (kg/m ³)
150	0.1	929.152
150	2.5	931.338
150	5	933.351
150	7.5	935.386
150	10	937.319
175	2.5	915.516
175	5	917.846
175	7.5	920.247
175	10	922.220

Table B-2. Measured densities for dead bitumen B.

Temperature (°C)	Pressure (MPa)	Measured Density (kg/m ³)
19.7	0.1	1016.3
19.7	2.5	1017.6
19.7	5	1018.9
19.7	7.5	1020.1
19.7	10	1021.6
50	0.1	995.9
50	2.5	997.3
50	5	998.6
50	7.5	999.9
50	10	1001.3
75	0.1	979.9
75	2.5	981.5
75	5	983.0
75	7.5	984.3
75	10	985.9
100	0.1	964.0
100	2.5	965.8
100	5	967.5
100	7.5	969.1
100	10	970.6
125	0.1	947.6
125	2.5	949.6
125	5	951.4
125	7.5	953.0
125	10	954.9
150	0.1	931.3
150	2.5	933.7
150	5	935.8
150	7.5	937.6
150	10	939.5
175	2.5	917.6
175	5	919.9
175	7.5	922.0
175	10	923.9

APPENDIX C – ADDITIONAL DENSITY DATA

Table C-1. Measured densities of *n*-decane diluted Heavy Oil at 23 °C. (Kumar, 2012)

<i>n</i> -decane Mass Fraction (wt%)	Measured Density (kg/m ³)
0	983.0
15	934.8
25	904.3
30	889.1
35	876.5
100	726.0

Table C-2. Measured densities of toluene diluted Bitumen A Maltene. (Sanchez, 2012)

Maltene Mass Fraction (wt%)	Measured Density (kg/m ³)
0.969	985.2
0.843	966.3
0.624	940.2
0.461	917.9
0.418	912.1
0.321	901.4
0.226	892.6
0.129	880.5
0.023	869.4
0.006	867.6
0.002	867.2
0.001	867.0

APPENDIX D - ERROR ANALYSIS

D.1. Accuracy Estimation for Mixture Compositions

The composition of the hydrocarbon mixtures were calculated from the volume displacements of each phase as follows:

$$w_1 = \frac{\rho_1 V_1}{\rho_1 V_1 + \rho_2 V_2} \quad \text{Equation D-1}$$

where V is volume, ρ is density, and 1 and 2 indicate the first and second fluid displaced.

The accuracy of the densities is affected by the accuracy of the measured pressure and temperature as well as the accuracy of the original density data. The accuracy of the original density data is in the order of 0.5 kg/m^3 (NIST Standard Database, version 2008). The temperature was constant to within $\pm 0.01 \text{ }^\circ\text{C}$ and therefore had negligible effect on the density. The accuracy of the pressure gauge used for the displacements was $\pm 100 \text{ kPa}$ which could lead to a density error of 1 kg/m^3 . Overall, the potential error in the densities is 1.5 kg/m^3 .

The first volume displacement is the difference between the estimated dead volume and the fluid displacement. The largest source of error by far is the dead volume with a potential error of $\pm 0.5 \text{ cm}^3$. The second volume is simply the volume of displaced fluid. The error in the pump displacement is $\pm 0.01 \text{ cm}^3$.

The compositions were calculated assuming the maximum and minimum errors in each volume and density. The maximum errors are reported in Table D1. Note, the diluted bitumen compositions were based on gravimetric measurements and the maximum errors were approximately 0.2 wt\% (Motahhari (2012), As part of another project in AER lab).

Table D-1. Composition accuracy of pure hydrocarbon mixtures

Mixture	Composition (wt%)	Variation (\pm)
C ₂ /C ₁₀	6.00	0.20
C ₂ /C ₁₀	12.50	0.21
C ₃ /C ₁₀	6.00	0.29
C ₃ /C ₁₀	12.50	0.26
C ₃ /C ₁₀	25.00	0.26
C ₄ /C ₁₀	6.00	0.29
C ₄ /C ₁₀	12.50	0.29
C ₄ /C ₁₀	25.00	0.28
C ₃ /Tol	6.00	0.26
C ₃ /Tol	12.50	0.26
C ₃ /Tol	25.00	0.25
C ₃ /Cyclooctane	6.00	0.26
C ₃ /Cyclooctane	12.50	0.26
C ₃ /Cyclooctane	25.00	0.25

D.2. Repeatability of Density Data

Totals of 44 and 48 repeat measurements were performed for the hydrocarbon mixtures and diluted bitumens, respectively. The data are presented in Table D-1 and D-2, respectively. The standard deviations of the hydrocarbon mixture and the diluted bitumen data were 0.33 and 0.18 kg/m³, respectively. The 90% confidence interval of the pure hydrocarbon systems and diluted bitumen were ± 0.54 and ± 0.29 , respectively. Details are provided below.

First, the mean and standard deviation for each pair of measurements were calculated.

The mean is defined as:

$$\bar{x} = \frac{1}{n} \sum_{i=1}^n x_i \quad \text{Equation D-2}$$

where \bar{x} is the mean, n is the number of repeat measurements, and x_i is a measured value.

The sample standard deviation, s , defined as:

$$s = \sqrt{\frac{1}{n-1} \sum_{i=1}^n (x_i - \bar{x})^2} \quad \text{Equation D-3}$$

It was assumed that the sources of error for each hydrocarbon mixture were the same and the average sample deviation was calculated from the variances of each measurement pair using Equation D-3. The same procedure was followed for the diluted bitumens.

To calculate the confidence interval for a single measurement, x , it was assumed that the errors followed a normal distribution. The characteristic parameter of the normal distribution, Z , is defined as:

$$Z = \frac{\sqrt{n}}{s} |x - \bar{x}| \quad \text{Equation D-4}$$

The confidence interval is then given by:

$$x - Z_{\alpha/2} \frac{s}{\sqrt{n}} \leq \bar{x} \leq x + Z_{\alpha/2} \frac{s}{\sqrt{n}} \quad \text{Equation D-5}$$

where α is the probability a measurement falls outside the confidence interval.

A confidence interval of 90% was utilized in all the error analyzes corresponding to $\alpha/2 = 0.05$ and giving $Z = 1.645$ on the cumulative normal distribution table (Harnett, 1982). For a single measurement and a 90% confidence interval, Equation D-5 becomes:

$$\bar{x} - 1.645s \leq \mu \leq \bar{x} + 1.645s \quad \text{Equation D-6}$$

Table D-2. Error Analysis of Pure Hydrocarbon Mixtures.

Mixture	T (°C)	P (MPa)	Solvent Content (wt%)	ρ (1st Pass) kg/m ³	ρ (2nd Pass) kg/m ³	ρ (avg) kg/m ³	Variance
C ₂ /C ₁₀	125	10	6.0	639.1	639.4	639.3	0.01
C ₂ /C ₁₀	125	20	6.0	651.1	651.1	651.1	0.00
C ₂ /C ₁₀	125	30	6.0	660.8	660.7	660.7	0.00
C ₂ /C ₁₀	125	40	6.0	670.3	670.3	670.3	0.00
C ₂ /C ₁₀	125	10	12.5	582.9	581.3	582.1	0.67
C ₂ /C ₁₀	125	20	12.5	601.8	600.2	601.0	0.66
C ₂ /C ₁₀	125	30	12.5	616.0	615.5	615.8	0.05
C ₂ /C ₁₀	125	40	12.5	627.2	626.3	626.7	0.19
C ₃ /C ₁₀	75	10	6.0	679.7	679.4	679.6	0.02
C ₃ /C ₁₀	75	20	6.0	689.4	689.4	689.4	0.00
C ₃ /C ₁₀	75	30	6.0	698.0	698.0	698.0	0.00
C ₃ /C ₁₀	75	40	6.0	706.0	705.9	706.0	0.00
C ₃ /C ₁₀	75	10	12.5	664.5	663.4	664.0	0.30
C ₃ /C ₁₀	75	20	12.5	675.2	675.3	675.2	0.00
C ₃ /C ₁₀	75	30	12.5	684.1	684.3	684.2	0.02
C ₃ /C ₁₀	75	40	12.5	692.2	692.2	692.2	0.00
C ₃ /C ₁₀	75	10	25.0	628.8	630.3	629.5	0.54
C ₃ /C ₁₀	75	20	25.0	641.1	641.3	641.2	0.01
C ₃ /C ₁₀	75	30	25.0	651.7	652.8	652.3	0.27
C ₃ /C ₁₀	75	40	25.0	661.4	663.0	662.2	0.65
C ₃ /C ₁₀	50	10	6.0	818.6	818.3	818.5	0.02

Table D-2. *Continued.*

Mixture	T (°C)	P (MPa)	Solvent Content (wt%)	ρ (1st Pass) kg/m ³	ρ (2nd Pass) kg/m ³	ρ (avg) kg/m ³	Variance
C ₃ /C ₁₀	50	20	6.0	827.5	827.8	827.7	0.02
C ₃ /C ₁₀	50	30	6.0	835.2	835.6	835.4	0.03
C ₃ /C ₁₀	50	40	6.0	843.2	843.6	843.4	0.03
C ₃ /C ₁₀	75	10	12.5	757.2	757.4	757.3	0.01
C ₃ /C ₁₀	75	20	12.5	767.8	768.1	768.0	0.02
C ₃ /C ₁₀	75	30	12.5	777.9	777.9	777.9	0.00
C ₃ /C ₁₀	75	40	12.5	786.9	786.8	786.9	0.00
C ₃ /C ₁₀	125	10	25.0	651.3	653.1	652.2	0.85
C ₃ /C ₁₀	125	20	25.0	671.9	672.2	672.1	0.02
C ₃ /C ₁₀	125	30	25.0	687.3	687.7	687.5	0.06
C ₃ /C ₁₀	125	40	25.0	700.1	700.1	700.1	0.00
C ₄ /C ₁₀	125	10	6.0	646.5	646.2	646.4	0.02
C ₄ /C ₁₀	125	20	6.0	659.0	659.3	659.1	0.02
C ₄ /C ₁₀	125	30	6.0	669.9	670.2	670.0	0.03
C ₄ /C ₁₀	125	40	6.0	679.1	678.8	678.9	0.02
C ₄ /C ₁₀	125	10	12.5	633.9	633.8	633.8	0.00
C ₄ /C ₁₀	125	20	12.5	646.5	646.3	646.4	0.00
C ₄ /C ₁₀	125	30	12.5	658.1	658.1	658.1	0.00
C ₄ /C ₁₀	125	40	12.5	667.6	667.5	667.6	0.00
C ₄ /C ₁₀	175	10	25.0	567.4	567.3	567.4	0.01
C ₄ /C ₁₀	175	20	25.0	589.5	589.3	589.4	0.00
C ₄ /C ₁₀	175	30	25.0	607.1	607.0	607.0	0.01
C ₄ /C ₁₀	175	40	25.0	620.7	620.5	620.6	0.01

Table D-3. Error Analysis of Diluted Bitumen Mixtures.

Mixture	T (°C)	P (MPa)	Solvent Content (wt%)	ρ (1st Pass) kg/m ³	ρ (2nd Pass) kg/m ³	ρ (avg) kg/m ³	Variance
Bit/C ₇	50	0.1	15.00	930.4	930.8	930.6	0.04
Bit/C ₇	50	2.5	15.00	931.8	932.2	932.0	0.04
Bit/C ₇	50	5	15.00	933.5	933.9	933.7	0.03
Bit/C ₇	50	7.5	15.00	935.2	935.6	935.4	0.05
Bit/C ₇	50	10	15.00	936.9	937.2	937.1	0.02
Bit/C ₇	75	0.1	15.00	913.8	913.3	913.5	0.06
Bit/C ₇	75	2.5	15.00	915.5	915.0	915.2	0.06
Bit/C ₇	75	5	15.00	917.4	917.0	917.2	0.06
Bit/C ₇	75	7.5	15.00	919.1	918.6	918.9	0.07
Bit/C ₇	75	10	15.00	920.9	920.3	920.6	0.09
Bit/C ₇	100	0.1	15.00	896.5	895.9	896.2	0.08
Bit/C ₇	100	2.5	15.00	898.4	898.0	898.2	0.05
Bit/C ₇	100	5	15.00	900.4	899.8	900.1	0.07
Bit/C ₇	100	7.5	15.00	902.4	901.8	902.1	0.09
Bit/C ₇	100	10	15.00	904.3	904.0	904.2	0.04
Bit/C ₇	125	0.1	15.00	878.3	878.2	878.3	0.00
Bit/C ₇	125	2.5	15.00	880.6	880.6	880.6	0.00
Bit/C ₇	125	5	15.00	882.9	882.8	882.9	0.00
Bit/C ₇	125	7.5	15.00	885.0	884.9	885.0	0.00
Bit/C ₇	125	10	15.00	887.3	887.3	887.3	0.00
Bit/C ₇	150	2.5	15.00	863.5	863.6	863.6	0.00
Bit/C ₇	150	5	15.00	866.1	866.3	866.2	0.01
Bit/C ₇	150	7.5	15.00	868.6	868.7	868.6	0.00
Bit/C ₇	150	10	15.00	871.0	871.1	871.0	0.01
Bit/C ₇	50	2.5	30.00	872.8	872.9	872.9	0.00
Bit/C ₇	50	5	30.00	874.7	874.9	874.8	0.01
Bit/C ₇	50	7.5	30.00	876.6	876.7	876.6	0.00
Bit/C ₇	50	10	30.00	878.6	878.6	878.6	0.00
Bit/C ₇	75	2.5	30.00	854.8	855.1	854.9	0.02

Table D-3. Continued.

Mixture	T (°C)	P (MPa)	Solvent Content (wt%)	ρ (1st Pass) kg/m ³	ρ (2nd Pass) kg/m ³	ρ (avg) kg/m ³	Variance
Bit/C ₇	75	5	30.00	857.0	857.3	857.1	0.03
Bit/C ₇	75	7.5	30.00	858.9	859.1	859.0	0.02
Bit/C ₇	75	10	30.00	861.0	861.1	861.1	0.01
Bit/C ₇	100	2.5	30.00	837.3	837.2	837.2	0.00
Bit/C ₇	100	5	30.00	839.5	839.5	839.5	0.00
Bit/C ₇	100	7.5	30.00	841.8	841.7	841.7	0.01
Bit/C ₇	100	10	30.00	844.3	844.2	844.2	0.01
Bit/C ₇	125	2.5	30.00	818.9	818.5	818.7	0.03
Bit/C ₇	125	5	30.00	821.5	821.3	821.4	0.01
Bit/C ₇	125	7.5	30.00	824.2	823.8	824.0	0.03
Bit/C ₇	125	10	30.00	826.8	826.5	826.7	0.02
Bit/C ₄	50	2.5	7.25	947.5	947.0	947.2	0.08
Bit/C ₄	50	5	7.25	949.1	948.5	948.8	0.08
Bit/C ₄	50	7.5	7.25	950.8	950.2	950.5	0.08
Bit/C ₄	50	10	7.25	952.4	951.8	952.1	0.09
Bit/C ₄	75	2.5	7.25	929.9	929.6	929.7	0.01
Bit/C ₄	75	5	7.25	931.6	931.5	931.6	0.01
Bit/C ₄	75	7.5	7.25	933.4	933.1	933.2	0.02
Bit/C ₄	75	10	7.25	935.0	934.7	934.9	0.02